

# FINAL REPORT

An Assessment of Aquifer/Well Flow Dynamics:  
Identification of Parameters Key to Passive Sampling and  
Application of Downhole Sensor Technologies

SERDP Project ER-1704

December 2014

Sanford Britt  
**ProHydro, Inc.**

James Martin-Hayden  
**University of Toledo**

Mitchell A. Plummer  
**Idaho National Laboratory**

*Distribution Statement A*

*This document has been cleared for public release*





## Table of Contents

List of Tables

List of Figures

List of Acronyms

Definitions

List of Keywords

**1.0 Abstract**

**2.0 Objective**

**3.0 Background**

**4.0 Materials and Methods**

**4.1 Conceptual Model Development**

**4.2 Physical Laboratory Experiments**

*4.2.1 2D Physical Modeling*

*4.2.2 3D Planar Laser-Induced Fluorescence Tomography*

*4.2.3 3D Physical Modeling*

*4.2.4 3D Flow Field*

*4.2.5 Fracture Borehole Model*

**4.3 Analytical and Numerical Modeling**

*4.3.1 Analytical Modeling Approach and Methods*

*4.3.2 Numerical Modeling Approach*

*4.3.3 Numerical Modeling Methods*

*4.3.2.1 2D Tank Replica Model*

*4.3.2.1 Thermal Convection Model*

**4.4 Field Experiments**

*4.4.1 Multilevel Passive Sampling*

*4.4.2 Tracer Tests*

*4.4.3 Installation of New Wells*

*4.4.4 Purge Dynamics Testing*

*4.4.5 Pour Testing*

## **5.0 Results and Discussion**

### **5.1 Field Investigation**

*5.1.1 Stratification Analysis*

*5.1.2 Purge Curve Analysis*

*5.1.3 Sample Pouring Tests*

*5.1.3.1 Fill Method*

*5.1.3.2 Fill Rate*

*5.1.3.3 Variability*

*5.1.3.4 Discussion*

### **5.2 Analytical and Numerical Models of Monitoring Well Pumping**

*5.2.1 Flow Distortions During Ambient Conditions*

### **5.3 Physical Modeling**

*5.3.1 2D and 3D Physical Models*

*5.3.2 Fracture Borehole Model*

*5.3.3 Planar Laser-Induced Fluorescence (PLIF) Tomographic Imaging*

### **5.4 Physical and Numerical Modeling**

*5.4.1 Non-Thermal Density Driven Flow*

*5.4.2 Thermal Convection in a Well*

## **6.0 Conclusions and Implications**

### **Literature Cited**

### **Appendix A Supporting Data**

### **Appendix B List of Scientific / Technical Publications**

### **Appendix C Laboratory Reports**

## List of Tables

**Table 1** Snap Sampler Deployment Positions

**Table 2** Sensor Deployment Positions

**Table 3** New Well Construction Details

**Table 4** Samples Collected During Purge Testing

**Table 5** Comparison of Open Well vs. Baffle Separator Samples

**Table 6** Pour Tests: Summary of the Pour-Test Study Results.

**Table 7** Pour Tests: Summary of the Statistical Analyses Comparing the Different Fill Methods

**Table 8** Pour Tests: Summary of the Statistical Analyses Comparing the Different Fill Rates

**Table 9** Pour Tests: Pooled %RSD Value for each Fill Method and Flow Rate.

## List of Figures

- Figure 1** Sand Tank Apparatus used in Britt's (2005) Tracer Experiments
- Figure 2** Sand Tank Apparatus for Laser-Induced Fluorescence (LIF) Scanning
- Figure 3** Photo and Schematic of LIF Imaging Equipment
- Figure 4** Physical Model of "Half Well"
- Figure 5** Geometry of the Fracture Borehole Model
- Figure 6** 2D Horizontal Flow to a Well
- Figure 7** Illustration of a Device for Measuring the Critical Rayleigh Number
- Figure 8** Critical Gradient for the Onset of Convection
- Figure 9** Schematic of Finite Element Model of Britt's (2005) Tank Model
- Figure 10** Model Domain Geometry and Boundary Conditions for Quasi-2D Models
- Figure 11** Model Domain Geometry and Boundary Conditions for Axisymmetric Models
- Figure 12** Field Site Location
- Figure 13** In-Well Flow/Mixing Inhibitor Device ("Baffle")
- Figure 14** Field Site Well Location Map
- Figure 15** Construction Detail for New Wells
- Figure 16** Downhole Equipment Arrangement
- Figure 17** Flow Paths During Active Pumping
- Figure 18** Photos of Bottle Filling Methods
- Figure 19** Locations of New Wells
- Figure 20** Examples of Purge Curves for TCE in MW-29 and 1,1-DCE in MW-27
- Figure 21** Examples of Purge Curves for TCE cis-1,2-DCE in MW-24
- Figure 22** Simulated Well with Dyed Water Entering Above Pump Intake

**Figure 23** Simulated Well With Dyed Water Entering Above Pump Intake, Flow Rate Reduced

**Figure 24** Purge Curve Data Illustrate Small and Slow Changes in Parameter Readings

**Figure 25** Concentrations of Selected Compounds Through 5 Well Volumes Purged

**Figure 26** Purge Sampling Results with Tube Well Samples

**Figure 27** Tube Well and Baffled PDB Samples

**Figure 28** Groundwater Velocity Distribution and Stream Lines

**Figure 29** Physical and Numerical Models of the Diffuse Annulus

**Figure 30** Pumping Curves

**Figure 31** Concentration Distribution within the Monitoring Well

**Figure 32** Results of Numerical Simulation of Pumping

**Figure 33** Ambient Flow Regime Surrounding a Well and Induced Vertical Flow

**Figure 34** Physical Model of Half Well and Full 3D Well

**Figure 35** Transition from Thermal Stability to Thermal Instability

**Figure 36** Temperature Fluctuations Indicating Thermal Convection

**Figure 37** Relative Concentration Changes due to Pumping at the Well Bottom.

**Figure 38** Fracture Borehole Model Flow–Field/Well Interactions

**Figure 39** Lower Density Contrast Borehole Flow Experiment

**Figure 40** PLIF Imagery

**Figure 41** Schematic of the Finite Element Model

**Figure 42** Isopleths of Total Water Potential

**Figure 43** Simulated Solute Transport in a Numerical Replication of Britt's 2005 Experiment

**Figure 44** In-Well Flow Inhibitor

**Figure 45** Results of a Preliminary Dye Tracer Experiment Conducted at INL

**Figure 46** Results Horizontally-Oriented Dye Tracer Experiment Conducted at INL

**Figure 47** Results of a Numerical Simulation of Britt's (2005) Experiment

**Figure 48** Simulations Designed to Examine How the Vertical Extent of Convective Mixing

**Figure 49** Schematic Diagram and Results of a 2D Axisymmetric Model

**Figure 50** Temperatures Measured in a Shallow Unscreened Well

## List of Acronyms

**2D models:** Mathematical models that assume a uniform velocity in one coordinate plane

**3D models:** Mathematical and physical models in which flow is allowed to vary in three dimensions

**ASTM:** American Society for Testing and Materials

**DCA:** Dichloroethane

**DCE:** Dichloroethene

**DMLS:** Discrete multi-level sampler

**DNAPL:** Dense non-aqueous phase liquids, i.e., more dense than 1.00g/cc

**EC:** Electrical conductivity

**EC<sub>o</sub>:** Reference electrical conductivity

**C:** Solute concentration

**C<sub>o</sub>:** Reference concentration

**cosh:** Hyperbolic cosine

**ITRC:** Interstate Technical and Regulatory Council

**LIF:** Laser-induced fluorescence

**LNAPL:** Light non-aqueous phase liquids, i.e., less dense than 1.00g/cc

**LTM:** Long term monitoring

**MIP:** Membrane interface probe

**NAPL:** Non-aqueous phase liquids

**N<sub>wv</sub>:** Number of well volumes pumped, or the volume pumped divided by the volume of water within the screened section of the monitoring well

**ORP:** Oxygen reduction potential

**PCE:** Tetrachloroethene

**PDB:** Polyethylene diffusion bag

**PLIF:** Planar laser-induced fluorescence

**pH:** negative log of the hydrogen ion concentration

**Pz:** Level of the pumping well relative to the bottom of the well

**QA/QC:** Quality assurance / quality control

**SERDP:** Strategic Environmental Research and Development Program

**SON:** Statement of need

**sech:** Hyperbolic secant

**sinh:** Hyperbolic sine

**tanh:** Hyperbolic tangent

**TCE:** Trichloroethene

**USEPA:** United States Environmental Protection Agency

**USGS:** United States Geological Survey

**VC:** Vinyl chloride

**VOA vial:** Volatile organic analysis vial or a small container used to store and transport water sample to be analyzed for volatile organic solutes.

**VOC:** Volatile organic compounds, or compounds that volatilize easily from non-aqueous or aqueous phase.

**Vr:** Volume of pre-pumping well water remaining

**Vw:** Volume of water within the screened section of the monitoring well

**WV:** A well volume, or the volume of water within the screened section of the monitoring well.

## Definitions

**Ambient gradients:** hydraulic gradients in the formation surrounding the well.

**Axisymmetric:** Models in which flow velocities and concentrations are independent of angle about a central axis.

**Flow-weighted average concentration:** Solute concentrations within a monitoring well that are an average, weighted according to the flow rate entering the well.

**In situ sensors:** In-well transducers that convert aqueous chemical attributes into electrical signals.

**Low-flow purging:** purging performed with a pump discharge typically less than 1 Liter per minute.

**Natural gradient flow-through:** Process of groundwater flowing through a well driven by the hydraulic gradients in the formation surrounding the well.

**Naturally purged:** Process by which water within a monitoring well is continuously replaced with in-flowing groundwater.

**Passive sampling:** Non-purge sampling or no-purge sampling; sampling that does not require removal of water from the well prior to sampling.

**Physical model:** A small-scale reproduction of a physical environment; in this report: a tank of sand with a small-scale monitoring well.

**Traditional groundwater sampling methods:** Groundwater sampling methods that involve pumping or bailing before the sample is collected

## List of Keywords

COMSOL  
Convection  
Groundwater sampling  
Long-term monitoring  
Low flow sampling  
Multi-level sampling  
No-purge sampling  
Navier-Stokes  
Numerical modeling  
Passive sampling  
Purging  
Rayleigh  
Sand tank  
Stratification  
Vertical flow  
Well purging

## **Acknowledgements**

Acknowledgement goes to the Strategic Environmental Research and Development Program (SERDP) for funding this project and to Dr. Andrea Leeson Environmental Restoration Program Director and her staff for support and assistance during the course of the project. Field and Laboratory work was conducted by the authors with assistance of Tommie Hall of the US Army Corps ERDC-CRREL. The Los Angeles field site was made available by Mr. Joseph Kennedy. Staff at CRREL, INL, UT and ProHydro are also acknowledged for supporting work.

## **1.0 Abstract**

Long-term monitoring (LTM) costs make up a substantial percentage of environmental restoration budgets for both government agencies and the private sector. A major portion of LTM costs are costs associated with groundwater sampling and analysis. One promising cost-saving strategy is the replacement of traditional groundwater sampling approaches by a combination of passive sampling devices and *in situ* sensors. However, regulatory and operational acceptance of changes in groundwater sampling methodologies is conditional on both laboratory and field validation of the methods and an in-depth understanding of the way such methods represent groundwater chemistry.

**Objective.** The project objective for ER-1704 was to develop a fuller understanding and description of how contaminant concentrations measured in a well—using either passive sampling devices or *in situ* sensors—relate to contaminant concentrations in the surrounding formation. ER-1704 research has elucidated several key factors in the relationship between solute concentrations in wells and in the surrounding formation, thus providing additional scientific basis for cost effective application of alternative sampling and monitoring strategies. Solid scientific basis for non-purge groundwater monitoring is imperative for gaining user and regulatory acceptance of the alternate techniques. Defining the measurable attributes of aquifer/well conditions that either suggest likelihood or imply limits to well mixing phenomena were primary objectives of the work.

**Methods.** Physical and numerical modeling efforts were completed to illustrate the relationship between solutes in groundwater and those found in wells. Physical mixing processes that occur during ambient flow in aquifers and during active pumping activities were explored to show how potentially stratified contaminants may manifest in open well screens. Complex flow patterns driven by flow velocity changes, very small density contrasts, and temperature contrasts were identified as possible sources of well convection and mixing. Specifically, the modeling explored:

- 2D and 3D physical tank models. Dye tracer testing was conducted to illustrate flow in and around models wells.
- Analytical models. Models of well flow patterns were used to resolve well flushing during purging.
- Axisymmetric Numerical Models. Pumping models were constructed to simulate pumping flow to a well, allowing variations in adjacent hydraulic properties and contaminant distribution to be easily tested.
- Numerical Bore Model. In-well density convection phenomena were explored using a closed bore well model.

- Numerical Section Model. 2D mass and energy transport models were constructed to test inflow phenomena, density-driven convection, and the effects of in-well flow limiting devices.

Physical field testing was completed to test and illustrate contaminant fluctuations and differentials in field conditions. As such, these tests were less well-controlled and near-well flow conditions were only inferentially known until experimental data was generated. This approach is much more similar to practitioner conditions where collected data drives interpretation.

- Multilevel passive sampling. Multilevel sampling was conducted using two approaches: 1) open well sampling; 2) isolated zone sampling.
- Well Installation. New wells were installed with special design configurations to explore the relationship between contaminant concentrations inside and outside the well during ambient flow and during pumping.
- Purge Dynamics Testing. Special purging protocols tested how pumping rate, consistency of flow rate, changes in flow rate prior to sampling, and duration of pumping affects pump discharge concentrations, relative to concentrations measured in the well.
- Bottle Filling Test. An outdoor field test of methods that are commonly used to fill VOA vials was conducted. This test was conducted to assess the degree to which field sample handling affects analytical results.

### **Findings.**

1. Passive sampling (or remote passive sensing) in unpumped wells. Wells tend to redistribute adjacent aquifer contaminant heterogeneity. Homogenization often occurs, but the degree of mixing varies from well to well. Redistributive effects are highly sensitive to very small density contrasts in the inflowing fluid. Because of these density-driven effects, when aquifer contaminant chemistry is stratified, solute distribution in a well may not match that in the adjacent formation. Often times, the passive sample closely matches the flow-weighted-average of inflowing water. This condition is not perfect, however, and concentration distributions vary from well to well. There are many factors affecting contaminant distribution in an unpumped well that are not readily known without exhaustive testing. Pumping dynamics are also complex, meaning that differences from pumped comparators do not always clarify which method is “correct” in such circumstances. Contaminant position in the aquifer relative to the passive sampling device position in the well is usually not known, and understanding of that aquifer-contaminant geometry may not be improved by multilevel passive sampling in an open bore. Isolated zone sampling can improve determination of aquifer contaminant stratification, but the degree of improvement is variable and well-dependent. As a general replacement for purge sampling, passive sampling or passive sensing do yield similar results in most cases. Where results are different, and information is desired,

causes can often be found through more thorough multiple-sample-testing during purging, multilevel passive sampling within the well, or a combination of the two.

2. Pumping dynamics. Aquifer contaminant position relative to the pump intake position is rarely known, but knowledge may be improved by collecting multiple samples during purging. Contaminant position in the aquifer relative to the pump position in the well drives concentration stability during pumping. Volume of water removed from the well is a more reliable predictor of contaminant concentration stability than measurement of traditional “purge parameters” such as temperature pH, EC, ORP and DO; yet concurrently, large volumes removed do not always assure contaminant concentration stability. Some contaminants of interest stabilize faster than others, depending on the specific well, suggesting that unique contaminant distribution heterogeneity and chemical-specific biological activity can influence the stability of contaminant concentrations during purging.
3. Physical, Numerical, and Analytic Models. Good matches between simulation results, experimental data, and theoretical analysis of flow and transport support our hypothesis that redistributive effects by vertical mixing is common. Physical model experiments show that small heterogeneities exert strong influence on flow in the open bore of a model well. Horizontal laminar flow across the model bore could not be reproduced except under conditions in which density variations are much less than would be expected in the field. Density contrasts equivalent to as little as 10 parts per billion of dissolved solids are enough to cause near complete vertical redistribution in simulated wells. Thermal convective behavior induced by shallow seasonal thermal changes and deeper geothermal gradients may also either promote or inhibit well mixing effects.

**Overall Conclusions and Technical Transfer.** Contaminant redistributive effects in wells are nearly always present. Complete mixing appears to be very common; however, it is not universal. There is a continual balance between inflowing contaminant stratification (where present) and factors driving in-well mixing. Findings here imply common and very small drivers are responsible for slow but vigorous mixing relative to the residence time of water flowing through a typical well screen. Therefore, a tendency toward homogenization is anticipated to be common in field conditions. Most wells should experience strong redistribution effects, but some wells may maintain stratification or perhaps re-stratify differently from the surrounding formation. Ongoing technical transfer of these findings will promote better understanding in the environmental community that wells often represent a mixed flow-weighted average of the adjacent formation chemistry. This better understanding will yield cost savings in both short-term and long-term timeframes by accelerating the approval process for non-purge alternative sampling strategies, including passive sampling and *in situ* sensor technologies.

## **2.0 Objective**

Regulatory acceptance of *in situ* groundwater monitoring tools, as replacements for traditional groundwater sampling methods, is conditional on confidence in and an in-depth understanding of how such tools provide accurate measurements of groundwater chemistry. Providing this confidence and understanding was a principal objective of SERDP Statement of Need (SON) 09-05. The ER-1704 project plan incorporated efforts designed to explain the mechanics of ambient groundwater flow in and around monitoring wells and during active sampling. Efforts during the project have yielded promising results that help explain these mechanics. Deeper understanding and technical transfer of that understanding is essential for regulatory acceptance of these alternative approaches to long-term monitoring (LTM) for groundwater.

Considerable inertia still exists within the groundwater sampling community with regard to a perceived need to purge groundwater wells prior to sampling them. While this inertia has been overcome to a degree by efforts of the project team members in their work with the Interstate Technical and Regulatory Council (ITRC) Passive Sampler Team, American Society for Testing and Methods (ASTM), and other groups, there is substantial work to be done to allow passive methods to be widely and fully accepted where appropriate. Since *in situ* sensor technology is also by definition passive, application of *in situ* sensors also implicitly requires acceptance of passive sampling techniques. Our approach focused on the enhanced understanding of representativeness of passive sampling methodologies. This approach is designed to provide a basis for avoiding the “purge, sample, analyze” standard protocol that is largely followed today.

Accordingly, ER-1704 project work was designed to develop a fuller understanding and description of how contaminant concentrations measured in a well relate to contaminant concentrations in the surrounding formation. Specifically, the project addresses the following questions:

1. How does the relationship between solute concentrations in the well and in the surrounding formation depend on geochemical conditions, subsurface heterogeneity, well construction, sampling methodology and other primary controls on solute transport in the subsurface?
2. Several lines of evidence now indicate that rapid vertical mixing occurs in wells even under ambient (non-pumping) flow conditions. Which mechanism(s) cause this enhanced mixing?
3. Can results from previous studies, combined with experimental studies and modeling studies performed for the proposed project, be used to develop a comprehensive conceptual model of well behavior, and thus be used as a guide to developing a reliable predictive model for new subsurface monitoring methods?
4. Based on an improved understanding of well behavior, what adaptations might be made to existing sampling methods to provide more and/or more accurate information about subsurface conditions?

To meet the technical objectives of this project, we proposed a technical approach that included the following components.

- (1) Formulation of a comprehensive conceptual model for flow and transport into and around a well which incorporates all relevant physical properties and processes.
- (2) Laboratory experiments in 2D and 3D sand-tank physical models, focused on providing experimental data allowing for numerical model development and calibration. In this objective we expanded on the work done by (Britt 2005) through a combination of 2D and 3D experiments that:
  - specifically address the mechanisms that lead to rapid vertical mixing in a well,
  - explore how a range of heterogeneities, both physical and geochemical, affect concentrations in the well,
  - explore how different pumping rates, and changes in pumping rate, affect concentration distribution in the well,
  - examine how non-equilibrium chemistry, combined with other transient effects (e.g. pumping effects) relate to concentrations measured in the well, and
  - expand previous physical model studies, which essentially simulated a 2D flow problem, to examine 3D behavior around a well, in order to extend conclusions based on the 2D studies to actual well behavior.
- (3) Application of numerical models of flow and solute transport in and around a well to simulate the experiments conducted in component 2. These models are based on the conceptual model developed in component 1. The numerical models will enhance our understanding of the experimentally observed phenomena, as well as establish and sharpen our ability to accurately predict flow and transport into and around a well. This work builds on previous results of physical and numerical modeling by other scientists (e.g. Martin-Hayden 2000a, Varljen et al. 2006) to arrive at a comprehensive predictive model which accounts for the effects of the primary controls on contaminant concentration. The focus of this component will be on incorporating, based on a sound conceptual model, the effects of in-well behavior (stratification and mixing) and geochemical processes in these previously developed 3D models.
- (4) Field experiments using different sampling methods focuses on field testing and validation of the predictive capabilities of the numerical models. The field work includes experiments using both passive and active sampling methods to evaluate the field-based predictive capability of our models. Multiple downhole sampling approaches are utilized to isolate differences found between methods. These methods include open-well interval sampling, after Parsons (2003); baffle isolation zone testing, after Britt and Calabria (2008); purge dynamics testing, after Martin-Hayden and Britt (2006); and other methods described below.

### **3.0 Background**

A brief overview of well sampling approaches with respect to well flow dynamics is provided here (adapted and updated from Britt (2005)). Some of the unknowns identified therein were investigated in the (2005) study, and in the present investigation in response to the SERDP SON.

Purging monitoring wells in order to collect representative samples has been conventional procedure for upwards of 25 years (e.g. USEPA, 1977, USGS, 1980). Over much of that period, some level of controversy has continued over how best to purge wells, or whether it is necessary to purge wells at all (Robin and Gillham, 1987; Powell and Puls, 1993, Newell et al., 2000). Many studies have identified how anomalous or otherwise unrepresentative results may be generated from traditional purge and sampling techniques (e.g. Robbins, 1989, Gibs and Imbrigiotta, 1990; Reilly and Gibs, 1993; Conant et al., 1995; Church and Granato, 1996, Martin-Hayden and Robbins, 1997, Reilly and LeBlanc, 1998, Hutchins and Acree, 2000, Elci, et al., 2001 and 2003). Common situations shown by these and other studies have caused investigators to question what traditional purge-and-sample ground water monitoring results represent. Low-flow purge techniques (e.g. Puls and Barcelona, 1996) were developed and widely adopted to address some of the problems (e.g. falsely elevated metals concentrations), with the added benefit of reducing purge-water waste. No-purge techniques are also being explored and are being adopted where applicable (Vroblesky, 2001, Parker and Clark, 2002; Parker and Mulherin, 2007, Parsons Engineering Science, 2003; ITRC, 2004, 2006, 2007). These alternative techniques can solve some problems like elevated turbidity and VOC loss caused by bailer agitation or high pump rates, but they do not solve problems with vertical flow (Elci, et al., 2001 and 2003), pumping-induced variability (Martin-Hayden, 2000a and 2000b; Gibs, et al., 2000, Martin-Hayden and Britt 2006), or well convection (Martin-Hayden and Britt 2006; Vroblesky et al. 2007). Other techniques involve installing multichannel tubing wells (Einarson and Cherry, 2002); short-screen direct push wells (Kram, et al., 2001); or they involve installation of devices such as the Discrete Multi-Level Sampler within existing longer screen wells (Puls and Paul, 1997), or installation of baffle-type devices (Vroblesky et al. 2007, Britt 2008). These techniques are effective but may require a long term commitment to relatively expensive multi-interval sampling.

Contaminant transport interpretation and cleanup decision-making directly relies on accurate data and a clear understanding of what the data represent. Misdirection from anomalous data should clearly be avoided. Church and Granato (1996), Reilly, et al. (1989), and Elci, et al. (2001) show the mechanics of sampling bias and misdirection caused by vertical well bore flow. However, current work by this author and colleagues includes feasibility assessment of long-screen well rehabilitation by physically limiting

vertical flow within wellbores as a partial solution to vertical ambient flow (Britt and Calabria 2008).

Other sources of misdirection from sampling data include partial penetration (Robbins, 1989; Martin-Hayden and Robbins, 1997; and Chaing et al., 1995) and lithologic heterogeneity (Gibs et al., 1993). Anderson and others (1992) showed how DNAPL fingers and pools result in very strong dissolved contaminant stratification in an aquifer. Well screen dilution and redistribution of strong contamination stratification could clearly misdirect an investigator attempting to delineate contaminant distribution and transport. But very short multi-interval wells can also miss vertically limited, highly contaminated, zones. Just as the environmental industry is moving toward continuous geologic logging and chemical mapping of boreholes (e.g. GeoVis, MIP [membrane interface probe]) rather than collecting soil samples once every five feet, ground water data should similarly be collected over entire intervals. Of course, this is limited by geology, and wells should not cross significant lithologic boundaries, but if one doesn't know where contaminants are moving within a defined aquifer zone, one should sample and characterize the entire interval. Ground water monitoring system design must incorporate solutions for these conflicting problems to generate the most useful sampling data.

To alleviate concerns about these conflicting problems with representativeness, multi-level sampling within existing wells (Puls and Paul, 1997; Vroblesky and Peters, 2000; Parsons Engineering Science, 2003; Britt, 2006; Britt, 2008; Britt and Calabria, 2008) and sampling multi-interval well installations (Einarson and Cherry, 2002, and Kram, et al., 2001) can certainly help, as long as sufficient effort is made to understand what the results indicate, and one can afford to generate consistent comparison data.

Notwithstanding the interest of multi level sampling, *the practical long-term objective for most sampling programs is to be able to efficiently collect a single representative sample from each well.* The working hypothesis for the (2005) study was that under simple scenarios, contaminant mixing and dilution can and does occur in monitoring wells under natural flow-through conditions. The flow-through aspect of this hypothesis is no longer considered contentious—as ASTM observes in its 2002 standard practice document for low-flow purging:

“Low-flow purging...is based on the observations of many researchers that water moving through the formation also moves through the well screen. Thus, the water in the well screen is representative of the formation surrounding the screen.” (ASTM, 2002)

If flow-through and mixing creates a flow-weighted average concentration in the screen interval of a well, it is arguable that wells are “naturally purged.” Simple tracer

dissipation tests (see Robin and Gillham, 1987) could determine whether individual wells are “naturally purged” or not. Consequently, *naturally purged wells could allow collection of the ideal sample—a single, inexpensive, representative sample collected directly from the screen interval of the well.*

## **4.0 Materials and Methods**

This project was designed to evaluate whether naturally purged wells can provide an “ideal sample,” and to explore in more detail the dynamics of how measured contaminant concentrations vary as a function of parameters such as hydrogeologic conditions, geochemistry, well type, sampling method, contaminant type and concentration. Physical experiments included quasi 2-dimensional models of near well environments. Both porous media and simulated fracture media were physically modeled. Numerical models are explained in greater detail as they are more innovative and unique from a materials and methods perspective. The physical models are somewhat intuitive therefore not explained in great detail here beyond dimensions of the experiments. Britt (2005) and Martin Hayden and Wolfe (2000) described similar physical “sand tank” models in more detail. Methods for this approach follow below.

### **4.1 Conceptual Model Development**

Existing conceptual models for flow and transport around wells assume Darcian flow to and through the well, which, in turn, implies laminar flow to and through the well screen. However, prior to the experiments in this project, field data (Britt and Calabria 2008) and experimental data (Britt 2005) suggested that laminar flow through the well does *not* hold in tested laboratory conditions and limited testing in field conditions. In this component modifications and enhancement to existing conceptual models were developed necessary to reconcile observations with theory. This aspect of the research was an iterative effort, led by the results from experimental laboratory tests using 2D and 3D physical models, analytical and numerical modelling, and field tests.

### **4.2 Physical Laboratory Experiments**

Previous experiments (Britt 2005, Figure 1) demonstrated that under ambient conditions, vertical mixing in wells is much more rapid than previously anticipated. Further, the horizontal flow assumption could not be replicated. Laboratory experiments for this project follow up that work, by examining the same effect under different conditions, and determining how well construction affects the rate of vertical mixing. In addition, the following issues related to well behavior under different sampling conditions in different environments are explored.

- Fractured media transport and flow mixing in a model well
- Pumping flow dynamics testing to establish comparison criteria to traditional sampling

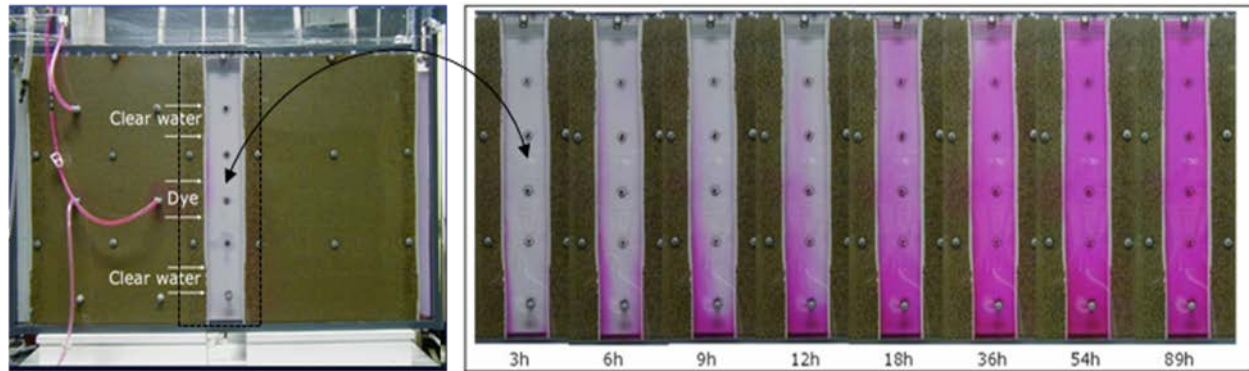


Figure 1. Sand tank apparatus (A) used in Britt's (2005) dye tracer experiments in a quasi- 2D horizontal flow field and (B) a time lapse sequence of images illustrating rapid vertical movement of dye relative to horizontal movement. Dye was injected in the sand to the left of the well and entered the well as illustrated in panel A. Times beneath time lapse images denote hours from time that dye was first observed in the well. Dye solution in this experiment was very slightly denser than the ambient flow solution.

#### 4.2.1 2D Physical Modeling

Quasi-two-dimensional<sup>1</sup> physical models were developed to examine a range of physical processes for which the 3D flow regime around the well is considered subordinate to questions about the interaction of the formation with the slow moving water in the well. For these experiments, a “model well” is defined as the open portion of the physical system that comprises the overall physical model. This is in contrast to the aquifer portion of the model, which may be filled with porous media, or a simulated fracture system. The “model well” is designed to replicate field conditions of an open section of a well or borehole within an aquifer.

- Effect of well construction on internal mixing
- Fractured media transport and flow mixing in a model well
- Strong hydraulic conductivity contrast flow testing in a model well
- Flow dynamics testing to establish comparison criteria to traditional sampling

Physical models were constructed to allow rapid change out of filter and well screen material to accommodate different testing scenarios. Tests were conducted with sufficient replications to satisfy the investigatory team that the observed phenomena are repeatable and reliable for predictive purposes. Observations were recorded using time-lapse photography, data logging, 3D planar-laser-induced fluorescence tomography, and other methods depending on the specific experiment.

Individual test runs under a variety of scenarios illustrate an in-well mixing effect similar to Britt's 2005 results, with additional details and causality defined during the trials. Attempts were

<sup>1</sup> i.e. the model is designed to produce a condition in which flow and transport is largely restricted to two dimensions

made to find scenarios and conditions that did not replicate the previously observed mixing phenomena. The purpose of this phase of the investigation is to add to the predictive capability and *identification of conditions contrary to the baseline flow-weighted averaging effect, and ultimately the project goal—delineation of when a single passive sample / sensor approach will and will not satisfactorily provide a representation of a well screen interval.*

#### 4.2.2 3D planar-laser-induced fluorescence tomography

We employed laser-induced fluorescence tomography to obtain a 3D description of the migration of the dye within the well and to develop a means of directly measuring dye concentrations at concentrations difficult to detect visibly. Figure 2 and 3 illustrate the tank configuration and apparatus. A 100 mW 532-nm wavelength laser was aimed at a cylindrical lens to produce a laser sheet which was then collimated via a parabolic mirror and directed into the top of the well section of the sand tank model. A pivoting dielectric mirror was used to translate the laser sheet through the well and images of fluoresced dye from a sequence of planes are collected via digital video. The laser plane translation rate was set so as to traverse the well column in approximately one second, so that each video effectively represents a 3D snapshot of dye position within the well. The individual frames of the 1-s video scans were then converted to 3D data using Matlab image processing functions, and the results used to examine dye behavior during transport into and through the well.

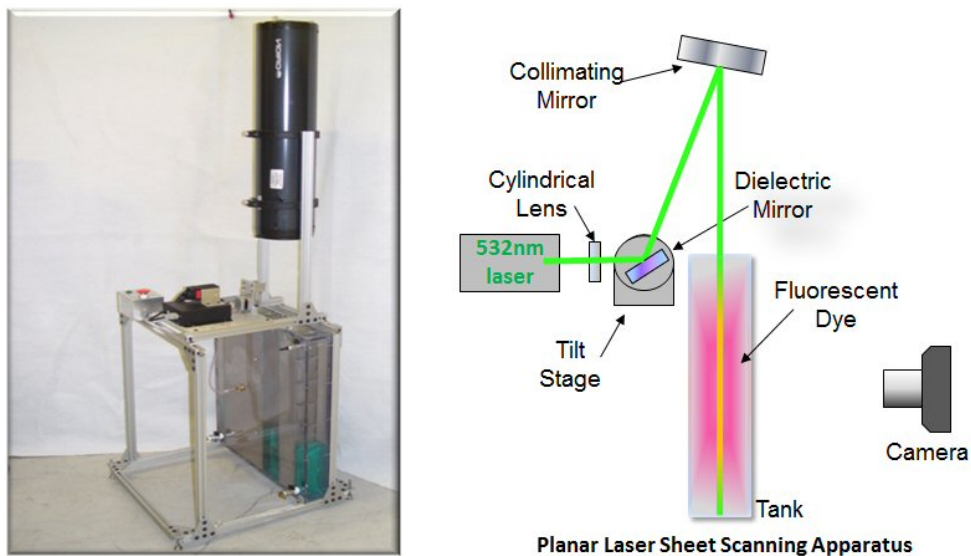


Figure 2. Photograph of INL's sand tank, (A) before filling, and (B) a close-up of a portion of the tank during one of the dye injection experiments, illustrating aquifer arrangement and dye movement in the well section of the tank

### 4.2.3 3D Physical Modeling

Three-dimensional physical models were developed to further investigate the 2D modeling findings in a 3D context. There are ongoing questions regarding the transferability of 2D experimental work to three dimensions, and from there to field conditions. Conversely, the 3D models also allow field findings to be further explored under controlled laboratory conditions. Testing the 2D findings with 3D physical modeling and field experiments are critical to ultimate acceptance of the findings by the environmental community.

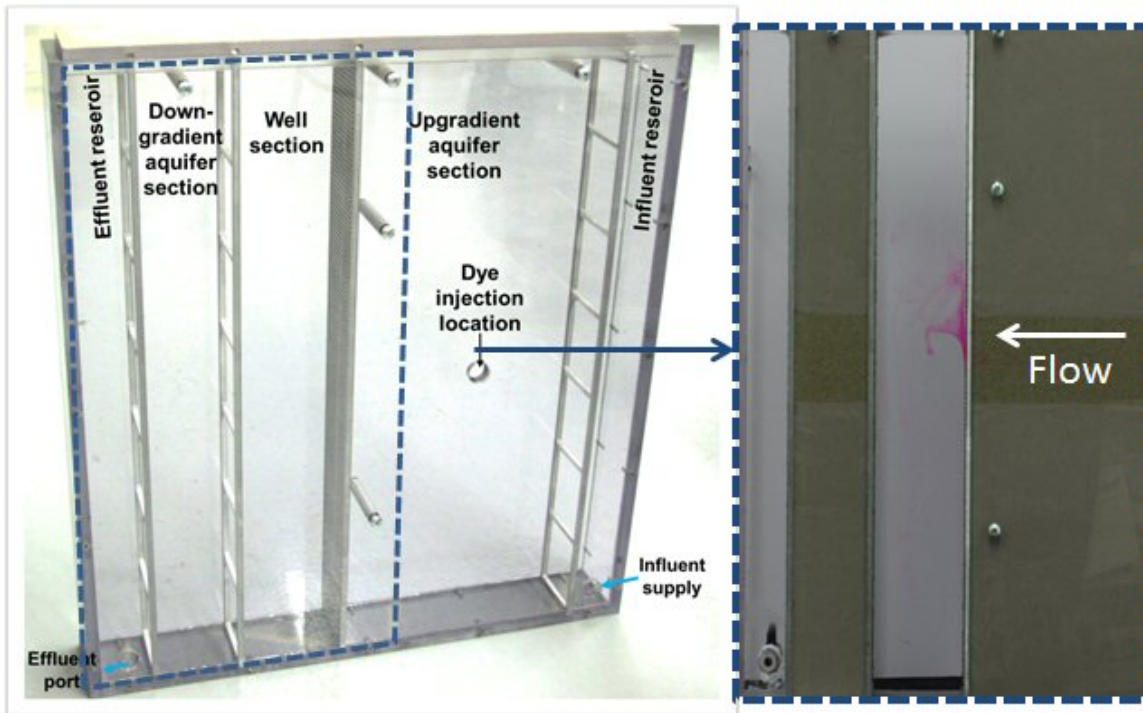


Figure 3. Photograph and schematic of the planar-laser-induced fluorescence tomographic imaging apparatus developed to examine dye transport into INL's replication of Britt's 2D sand tank model.

There are different ways to approach 3D physical model construction. Models can be small-scale representations of individual wells in cross section, or larger scale fully three dimensional configurations. There are advantages and disadvantages of each. A cross section of a well allows direct viewing and time-lapse photography of tracer dyes during well-bore flow/mixing and evaluation of downgradient "shadow" effects due to that in-well mixing, while fully three dimensional models allow more robust analyses of 3D flow fields within and around the well in the absence of transparent face-plate effects.

The 3D physical model was constructed to include both the "Half Well" configuration and the "Full 3D Well" in order to submit both to the same hydraulic, solutal and thermal conditions. Figure 4 shows the two configurations: the Half Well preserves ability to visually track solute movement along the centerline of flow approaching the well, within the well and down-gradient

of the well while the Full 3D Well allows visualization from the top and bottom of the well (through the transparent bottom of the tank).

#### 4.2.4 3D Flow Field

In order to provide easy observations of dye concentration throughout their physical model, Britt (2005) designed a sand tank model that approximates a flow system where the well is a continuous barrier to flow in a plan view of the system. Martin-Hayden and Wolfe (2000) designed physical model of a monitoring well cross section in order to track flow regimes and mixing within the well bore. The physical model in this study was designed to combine the visualization of flow through (of Britt 2005) and quasi-3D flow visualization (of Martin-Hayden 2000b). The first series of tests in the Half Well (Figure 4), represent a cross-sectional half of a 3-D flow field around a well in order to directly observe the flow regime and mixing within and adjacent to the well through the transparent face-plate. These tests were extended to the Full 3D

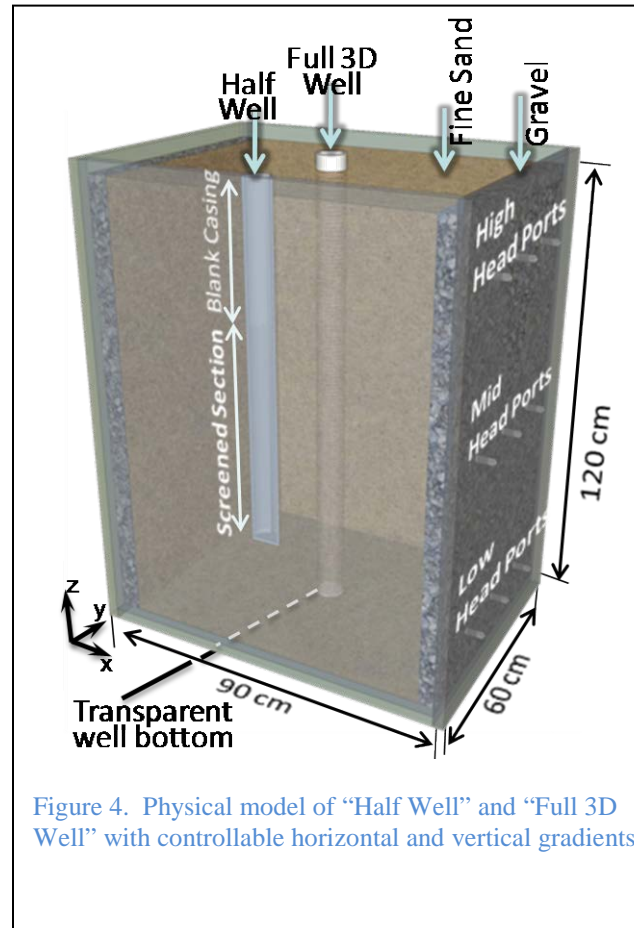


Figure 4. Physical model of “Half Well” and “Full 3D Well” with controllable horizontal and vertical gradients.

Well by using resistivity logging and in-well sensors to observe tracer movement. These models are used to test differences in behavior between the 2D and 3D physical models, so that conclusions based on the 2D model studies can be appropriately generalized to the 3D case.

#### 4.2.5 Fracture Borehole Model

Flow and mixing within fractured rock boreholes are expected to involve various processes that distinguish them from monitoring wells in granular media. In order to investigate these processes a physical model of a borehole within a fractured medium was constructed (Figure 5). The borehole model consists of a 47mm ID polycarbonate tube intersected by two fractures each consisting of a space between two 340mm x 300mm plates of 12.5mm thick polycarbonate. That fracture aperture is maintained with a rubber gasket around the edges that can be adjusted between 0.5mm and 0.8mm using a set of bolts around the perimeter of the plates. A hydraulic gradient and uniform flow is introduced by means of constant head reservoirs at either end of the fracture. Dye is introduced at the low-head side of the fracture and is imaged using a DSLR camera. The lower fracture, 250mm from the bottom of the borehole, is horizontal and the top fracture, 570mm from the bottom, is inclined at a 27° angle. The borehole extended another

370mm above the top fracture to represent the blank casing or the unfractured top portion of the borehole.

Imaging the dye passing from the fracture into the borehole allows visualization of the mixing as the water enters the well and quantification of the mixing within the well. The zone down gradient of the borehole represented the shadow zone indicating the influence of that mixing on the groundwater in the fracture. The grid beneath the transparent fracture is used to map the flow regime as groundwater converges on the borehole (capture zone) and as well water diverges from the borehole on the down-gradient side (shadow zone). The capture zones and shadow zones for each fracture are expected to change in geometry and size depending on the head difference between the fractures. The head difference between the fractures is also expected to control the characteristic of mixing and transport within the well. When density driven flow dominates the flow within the well, that mixing will determine the distribution of solutes in the well. When borehole flow overcomes density mixing the borehole flow regime will dominate transport. Submerging the fracture model in a bath of water maintained a uniform and constant temperature

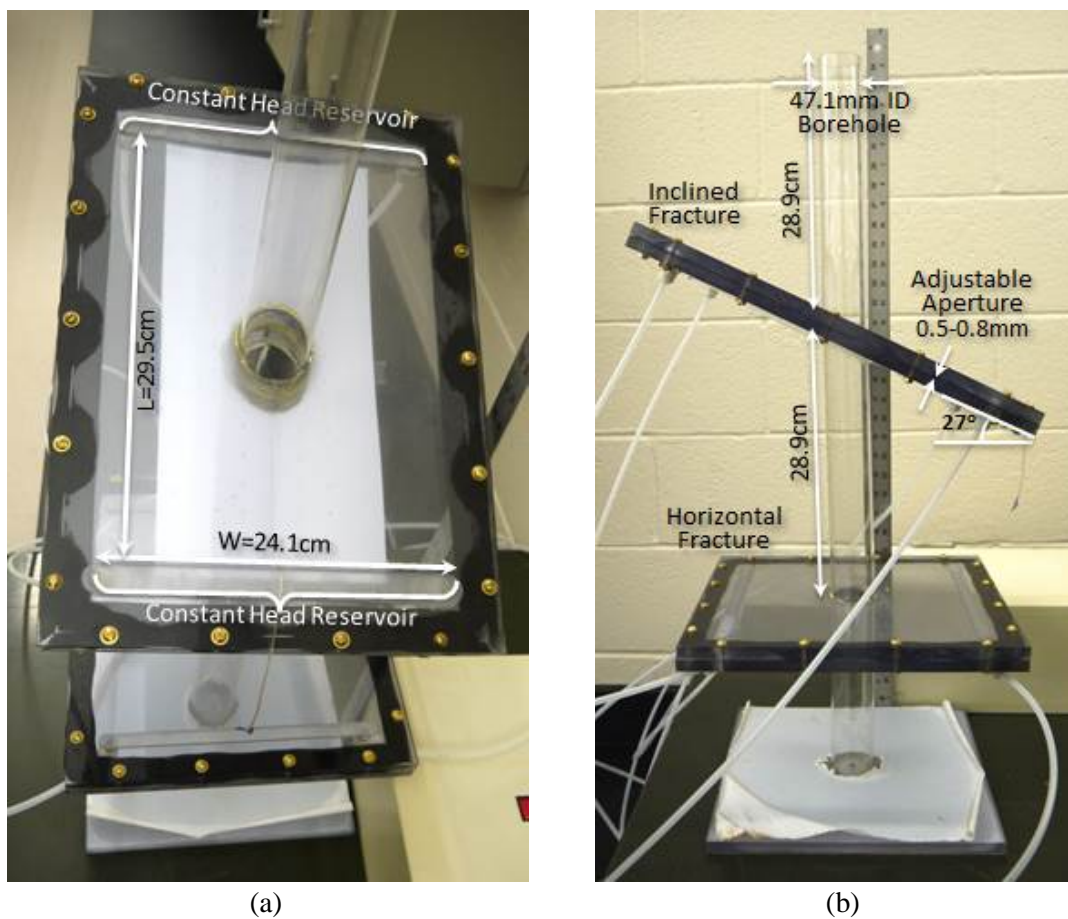


Figure 5: Geometry of the fracture borehole model, (a) downward oblique view of the top angled fracture, (b) a side view of the fracture model showing the vertical borehole, the angled top fracture and the horizontal bottom fracture.

as a means of controlling thermal convection and density mixing.

To visualize the capture zone and the shadow zone a head difference of 4.2mm was applied to the 0.50mm aperture top fracture resulting in a 0.10ml/s volumetric flow rate through the 241mm wide fracture and a velocity of 0.83mm/s. Dye was distributed uniformly within the constant head reservoir and tracked as it traversed the fracture and entered the borehole. Initial runs did not control for temperature or density differences between the fracture and the borehole. These temperature and density contrasts allow the characteristics of density mixing to be observed.

### 4.3 Analytical and Numerical Modeling

#### 4.3.1 Analytical Modeling Approach and Methods

Analytical models of wellbore hydrodynamics provide a rapid and flexible method of investigating fundamental aspects of wellbore flow during pumping. Analytical models also allow the results to be generalized in order to provide design criteria for pumping and sampling (Martin-Hayden 2000b). Previous models assumed inviscid flow, *i.e.*, Darcian flow, within the wellbore. These models provide estimates of travel time within the wellbore and relationships between the groundwater concentration distributions and concentration variation during pumping. In this study more complex analytical and numerical models are developed to account for Poiseuille (viscous pipe) flow and investigate the influences of viscosity on flow paths, travel time and concentration distributions. The velocity distributions within the screen section of the well are then compared to various mechanisms of wellbore mixing, *i.e.*, thermal and solutal convection as well as advection-diffusion/dispersion.

The analytical modeling began with investigations of wellbore flow during pumping. The distribution of groundwater entering the screen was modeled as an advective front forming an annulus of groundwater displacing a shrinking cylinder of pre-pumping well water. If the groundwater and well water are heterogeneous in concentration, and the well is unmixed or partially mixed during pumping, the distribution of groundwater and well water is used to characterize the heterogeneity of well water concentration during pumping. The travel-time calculations show how the concentrations at the pump intake will change with time (*i.e.*, “pumping curves”) and can be used to characterize variation of the pumped concentration. These pumping curves were generated for uniform groundwater concentrations and heterogeneous concentrations with the pump intake at various positions within the screened interval in order to simulate a variety of conditions during pumping.

When a screened monitoring well is not pumped (between sampling episodes, if sampled with a passive method or monitored with an *in situ* sensor) it acts as a highly conductive conduit that is very sensitive to wellbore mixing and vertical flow. The concentrations carried to the well depend on the surrounding flow regime established by the interaction of the well with the ambient hydraulic gradients, vertical as well as horizontal gradients. The redistribution of

concentration within the well depends on the vertical flow in addition to the mechanisms driving mixing. Vertical flow and various factors driving convection will work either in concert or in opposition to redistribute groundwater within the well. In this study, modeling of the conductive well bore and the surrounding formation showed the flow regime carrying groundwater to the well, vertical flow within the well and the distribution of well water discharge creating the shadow of altered and redistributed water.

#### 4.3.2 Numerical Modeling Approach

Numerical modeling studies have been conducted to examine how solute distribution in a well is influenced by low-flow pumping and by thermal and solutal convection effects and to examine the possible influence of well-screen geometry on in-well solute transport. Many previous studies of groundwater flow and solute transport that have included in-well transport effects have investigated flow under pumping conditions in which flow is dominated by the pumping-induced forced convection (Reilly and Gibs, 1993; Chiang et al., 1995; Elci et al. 2001; Varljen, 2006). Under those conditions, flow in the well can be approximated by solutions that use Darcy's law to describe conservation of momentum. That assumption may be invalid, however, when in-well velocities due to pumping are of the same order of magnitude as flow rates imposed by other forces, such as thermal or solutal convection. Development and use of *in situ* monitoring devices would normally require monitoring in-well concentrations without purging or pumping. Under those conditions thermal or solutal convection effects may exert significant influence on in-well solute transport. As such, an accurate understanding of that potential influence is required to understand how in-well solute monitoring would reflect solute distribution in the surrounding formation. Navier-Stokes equations for fluid flow are needed to describe flow and transport in the well under these conditions. However, even where flow is dominated by pumping, there are circumstances where application of Darcy's law may yield inaccurate results. One such example is the displacement of initial well water during well purging, for which Darcy's law provides an incorrect assumed stream-tube flow distribution and, therefore, an inaccurate description of purging behavior during pumping.

To more accurately describe in-well flow and transport behavior and to incorporate potential buoyancy effects, we simulated flow and transport using the 3D finite element analysis program COMSOL Multiphysics. The Multiphysics package allows solution of fully coupled fluid flow, solute transport and thermal energy transport on a finite-element domain, with fluid flow governed by Darcy's law, the Brinkman equations or Navier-Stokes equations for weakly compressible flows. The software provides convenient pre- and post-processing tools, and for problems involving solution of different governing equations, the solutions are coupled at the boundaries between the combined solution domains.

#### 4.3.2 Numerical Modeling Methods

It is commonly assumed that laminar flow through a well forces the solute distribution inside a well to mirror that outside the well. This would suggest that in cases where solute is confined to

certain strata in a hydrogeologic profile, that same vertical distribution would be reflected in a monitoring well. To test that conceptual model of flow through a well, Britt (2005) constructed a 2D sand tank that incorporated a vertical well section in a horizontal flow-dominated system (Figure 6). The well consisted of a 10-cm diameter included a coarse sand pack and divided two porous medium domains in which horizontal flow was controlled by constant head tanks on either end of the apparatus. A dye, mixed with water to yield a solution density  $\pm 0.00001x$  that of water, was injected just upstream of the well to examine solution behavior as the dye migrated laterally toward and into the well. In all experiments the dye was observed to migrate vertically in the well much faster than horizontally. While the horizontal rate of dye movement was well approximated by the volumetric flux, the vertical rate was on the order of 30 times faster. INL conducted experiments that essentially replicated Britt's apparatus, at similar horizontal velocities and up to an order of magnitude greater than the 2005 study.

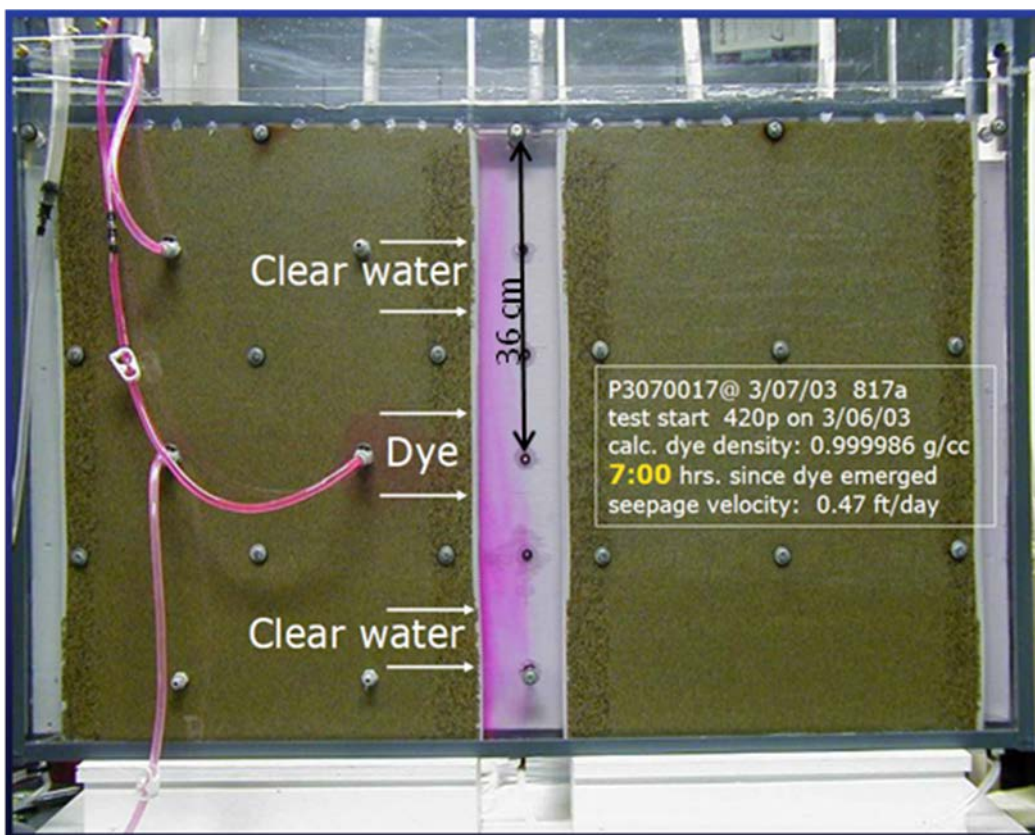


Figure 6. The quasi-2D horizontal flow to a well apparatus of Britt (2005), used to examine solute transport through a well under ambient horizontal flow. Far left and right columns provided constant head boundaries while sealed upper and lower surfaces result in a confined hydraulic system. Dye was injected at the marked port and migrated to the well at a velocity of  $\sim 0.47$  ft per day, with limited dispersion approximately denoted by indicators on the edge of the visible plume in the sand. Dye distribution illustrates rapid vertical movement

Britt's (2005) experiments demonstrated that slight density differences did yield different vertical distribution of solutes in the well. To estimate the sensitivity of a well to density-driven mixing effects, we use dimensionless parameters that compare the forces driving buoyancy-

driven mixing to those forces that attenuate that effect. Effects that attenuate flow due to a net buoyant force include viscosity and diffusivity, and the Rayleigh number is the dimensionless parameter that expresses the balance between those effects. The form of the Rayleigh number and the value at which natural convection begins varies with the geometry of a particular system. For flow in a vertical tube separating two solutions of differing density (Figure ), the Rayleigh number, Ra, is

$$Ra = \frac{gR^4}{\mu D} \left( -\beta \frac{dc}{dz} \right)$$

where g is gravitational acceleration, R is radius of the tube, μ is kinematic viscosity, D is the diffusion coefficient, β is the fractional volumetric expansion coefficient, and dc/dz is the concentration maintained by the reservoirs on each end (Cussler,1997). Taylor (1954) determined that the critical Rayleigh number for the onset of natural convection for the configuration shown in Figure is 68. Thus, for a 10-cm

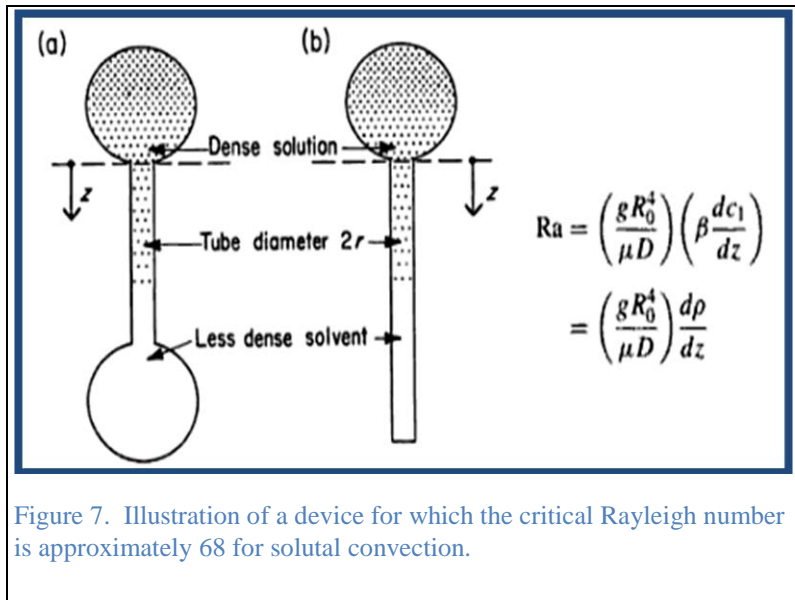


Figure 7. Illustration of a device for which the critical Rayleigh number is approximately 68 for solutal convection.

diameter tube, the critical concentration gradient for solute driven convection is approximately 0.4 μg/(L m). In dilute solutions, the volumetric expansion coefficient associated with slight increases in solute concentration is approximately 1E-3 L/kg, so the relative density difference represented by this concentration gradient is approximately 4E-10 m<sup>-1</sup>.

Thermal gradients can, of course, also drive convective flow, but because heat can also diffuse into the well and surrounding medium the critical Rayleigh number depends on the ratio of the thermal conductivity of the fluid in a tube to that of the surrounding medium. Zhukhovitskii and Gershuni (1976) show that the critical Rayleigh number for thermal convection in a tube can be calculated from the expression:

$$Ra = \frac{96}{5(1 + 7\lambda)} \left[ 3(33 + 103\lambda) - \sqrt{3(2567 + 14794\lambda + 26927\lambda^2)} \right],$$

where λ is the ratio of the thermal conductivities inside and outside the tube. When the thermal conductivity of the fluid is much greater than the surrounding medium, this equation yields a critical Rayleigh number of 68, identical to the solutal convection case. For conditions more

typical of the saturated zone, the critical Rayleigh number is approximately 149 (Berthold and Borner, 2008). Using the latter number to estimate when natural convection would dominate transport by diffusion in, again, a 5-cm diameter well, we see that a thermal gradient of 0.0035 K/m would be sufficient, which is approximately an order of magnitude lower than typical geothermal gradients. The fractional expansion coefficient for water at 10°C is approximately  $8.8\text{E-}5 \text{ K}^{-1}$ , so the critical gradient reflects a relative density difference of approximately  $3\text{E-}7 \text{ m}^{-1}$ . This is approximately three orders of magnitude larger than necessary to produce solutal convection because the dissipative effect of thermal diffusivity is approximately that much larger than typical solutal diffusion coefficients (Figure 8).

Because the Rayleigh number is proportional to the fourth power of tube radius, the critical gradient describing the onset of convection has the non-linear dependence on radius shown in Figure 8.

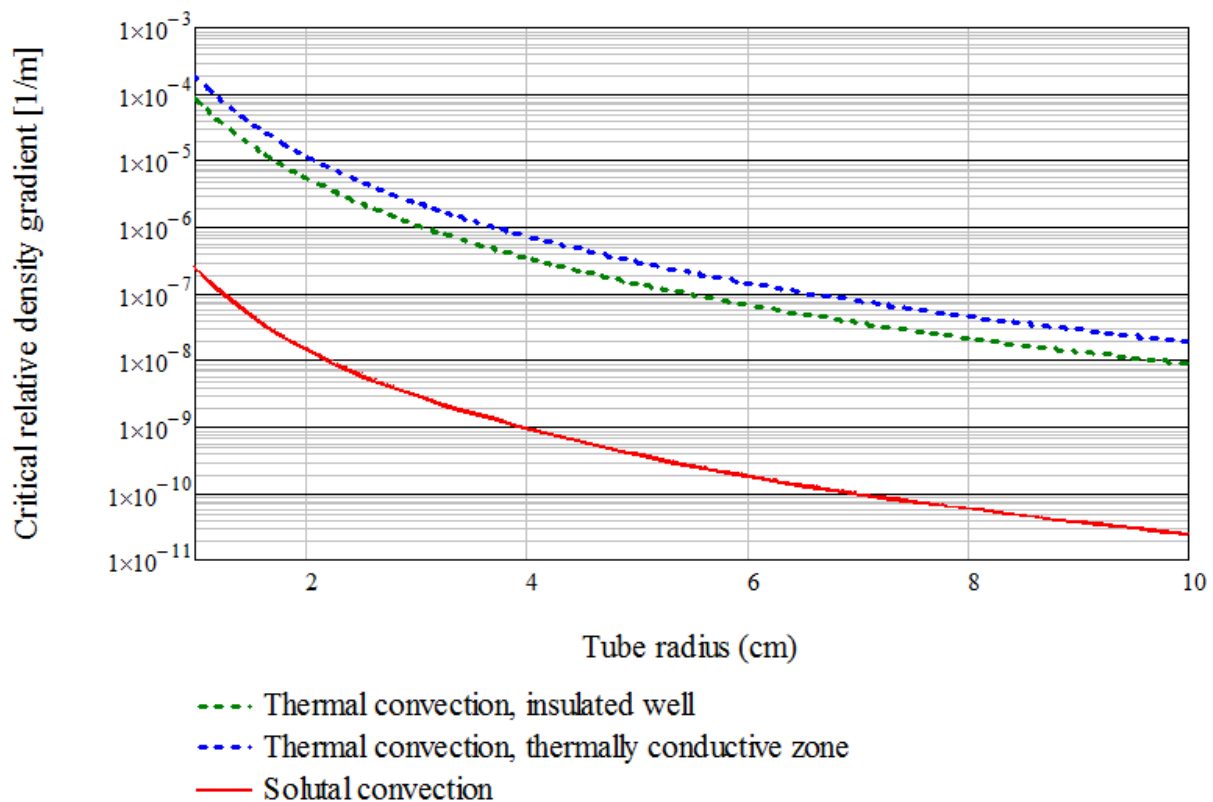


Figure 8. Critical gradient for the onset of convection in a tube, for thermal and solutal convection, as a function of tube radius.

The Rayleigh number analysis defines when free convection will dominate diffusion in thermal energy or solute transport but it does not predict the scale of the convective cells that develop or the rate of mixing induced by convection (Gretener, 1967). This information is needed to predict the effect of natural convection on solute distribution in a well, particularly where forced

convection in the horizontal or vertical direction may also influence solute movement. Parametric analysis of geometrically described flows adds some insight for particular scenarios. For flow in a cylinder, for example, the first convective flow regime expected to occur is flow down one half of the cylinder with a compensating upward flow along the opposite half of the cylinder (Donaldson, 1961). Axisymmetric flow, with one flow direction along the center of the cylinder and the oppositely directed flow in an annular ring surrounding it, does not occur until higher Rayleigh numbers. To examine the details of convective flow behavior, we use numerical simulation, solving the equations for open water flow (Navier-Stokes) in domains representing wells and applying Darcy's law in porous media. Heat transport and solute transport are calculated by coupling the advection-dispersion equation to the local flow equation, which may vary between domains.

Numerical simulations of solute transport were conducted using several different domains, depending on the problem of interest. To examine solute transport and heat transport in an experimental apparatus like that of Britt (2005), we developed models that essentially reproduced the 2-D geometry and boundary conditions of that experiment (Figures 9, 10A), or used a similar geometry with slightly taller aspect (*e.g.* Figure 10B), to examine vertical movements of greater extent. In these and other models, flow in the well section was described using Navier-Stokes equations, while flow in the surrounding porous media domains was described using Darcy's law. Solute transport and heat transport were described using advection-dispersion models and – in cases without forced convection – density-based buoyant forces included using a Boussinesq approximation.

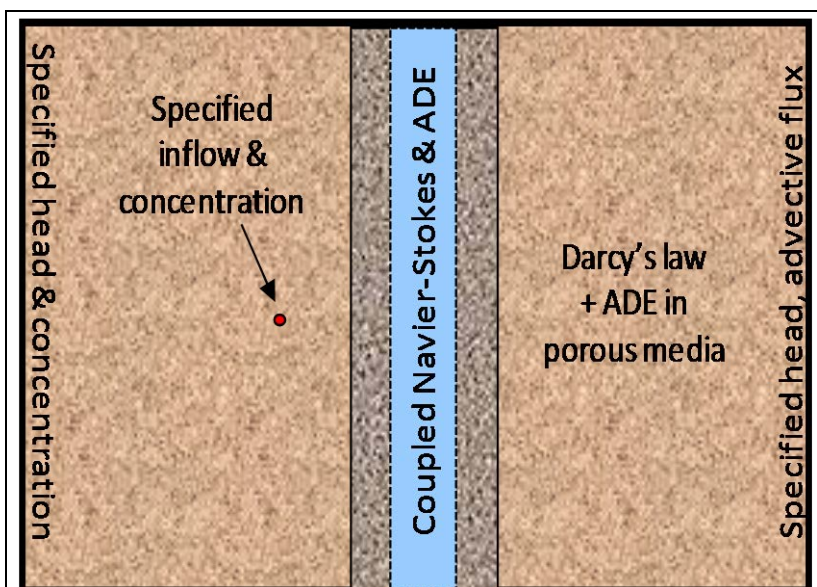


Figure 9. Schematic of the finite element model used to simulate Britt's (2005) experiment that displayed strong vertical mixing with relative density gradients less than  $1E-5$ .

To examine solute transport under pumping conditions, we simulated flow and transport in a 1-m by 10-cm radius well, surrounded by a 10-cm zone of porous media (Figure 11A), using an axisymmetric domain. Pumping in that model was represented as a specified flux, concentration outflow boundary along the bottom of the well section.

The effect of time-varying temperature gradients on flow in a well were also investigated with a 1-m tall well section in an axi-symmetric model domain (Figure 11B), but with an extended aquifer surrounding the well to allow more accurate description of the transient heat exchange between the well and the aquifer.

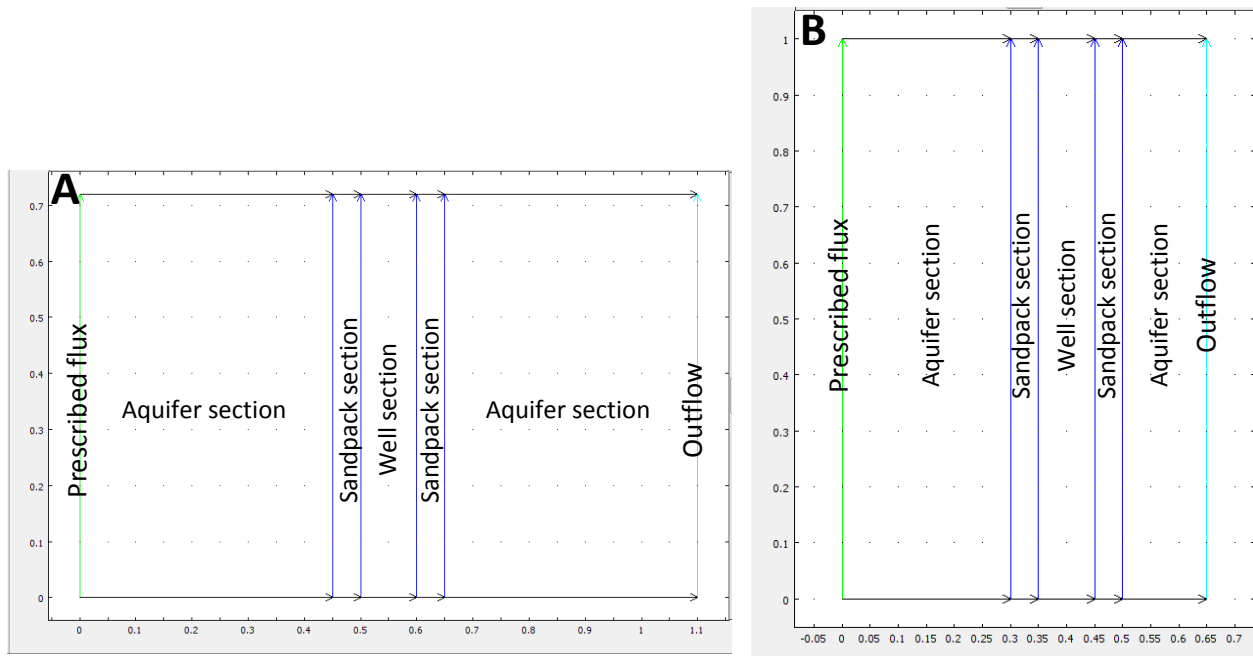


Figure 10. Model domain geometry (distances in meters) and boundary conditions for simulations of Britt's 2005 laboratory experiment (A) and similar scenarios with greater vertical extent (B).

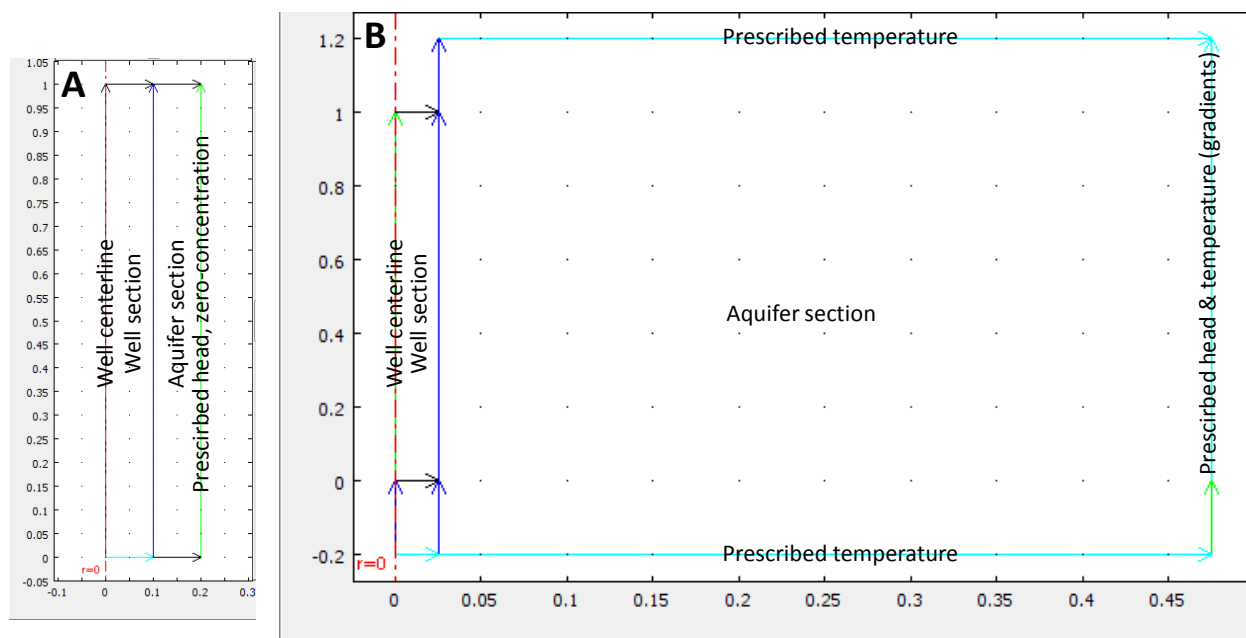


Figure 11. Model domain geometry (distances in meters) and boundary conditions for simulations of solute transport in a well with extraction from any point along the screen (A) and free convection behavior in a well under constant or time-varying temperature gradients induced by seasonal temperature fluctuations (B).

#### 4.4 Field Experiments

Field experimentation is a key factor in establishing the predictive capability of the physical and numerical modeling. Many aspects of the experimental laboratory work require field validation. Additional field experimentation to test in-well mixing effects, as well as effects of purge rate, purge rate change, density effects and other parameters were needed to establish the dynamics of variability associated simply with the way traditional samples are collected.

A field site for the study was selected and approval for its use was obtained from the private site owner and the local oversight agency (the California Department of Toxic Substances Control). The field site is the former Angeles Chemical Facility located at 8915 Sorenson Avenue in Santa Fe Springs, California (Figure 12). The site has a wide range of volatile organic compound contamination, including petroleum hydrocarbons, chlorinated solvents, ketones, and 1,4-dioxane. Contaminant concentrations range from below detection level to NAPL-indicating concentrations. Hydrogeologically, the site has a range of flow regimes from nearly stagnant, poor-yield, and highly heterogeneous, to high flow, high-yield, and low-heterogeneity. Wells include short to moderate length screens 5-15 feet, of 2-inch and 4-inch construction. The site is less than 2 acres in total area. A Remedial Investigation Report prepared for the site by the

California Department of Toxic Substances Control was available to guide the site work. Details of the site geology and investigation derived data are included in that report.

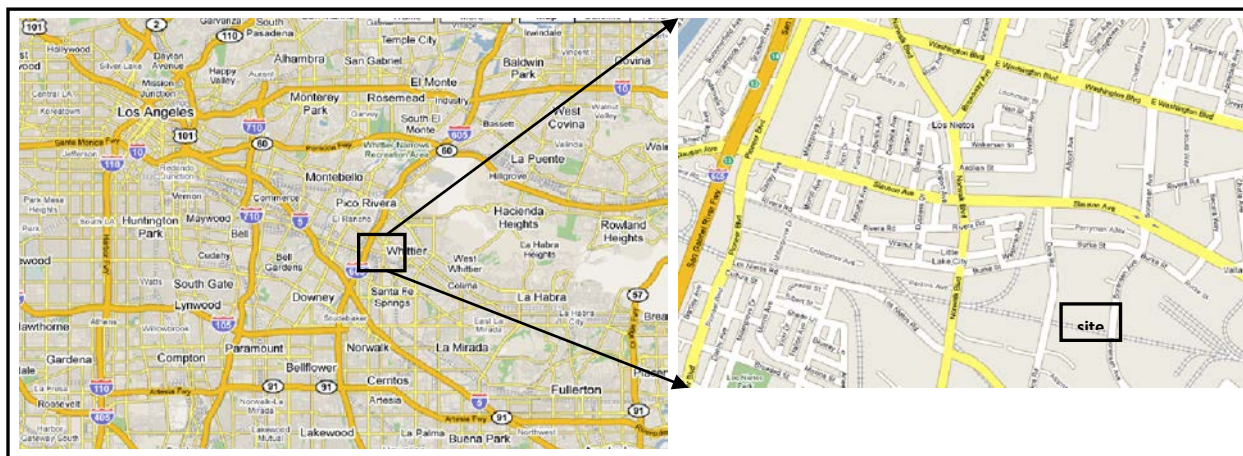


Figure 12. Site Location near Los Angeles, California

Historically, several individual wells at the site have been sampled at intervals to identify contaminant stratification. Many were suitable candidates for active and passive sampling approaches to illustrate laboratory experimental findings. During the first field season we conducted the following tests:

- Multilevel passive sampling. Multilevel sampling utilizing existing site wells was conducted using two approaches: 1) open well sampling with several stacked passive sampling devices deployed in each open well to assess ambient stratification; 2) isolated zone sampling utilizing stacked passive samplers deployed in each well with baffle isolation devices to limit ambient mixing between zones.
- Tracer Tests. After the passive samplers were removed from the existing test wells, several wells were outfitted with sensor devices for tracer testing. The tracer (deionized water) was placed in the wells to measure flow through via tracer dissipation.
- Well Installation. Based on passive sampling results and tracer tests, new wells were installed in locations where contaminant stratification was identified. Short screen wells along with tube well ports within the well filter pack were incorporated into the well installation. Sampling to explore the relationship between inside and outside the well during ambient flow and during pumping was used to illustrate small-scale vertical heterogeneity.
- Purge Dynamics Testing. Low flow purging and volume-based purging comparisons included protocols to test how pumping rate, consistency of flow rate, changes in flow rate prior to sampling, and duration of pumping affects pump discharge concentrations, relative to concentrations measured in the well. Physical testing of flow dynamics within individual test wells was accomplished through high resolution temperature, ORP, and conductivity tools, and other physical methods to define physical conditions and dynamics downhole. These physical experiments were done in conjunction with chemical testing to illustrate flow patterns.

- **Bottle Filling Test.** In Addition to the passive sampling and purge curve sampling analysis, a single outdoor field test of methods that are commonly used to fill VOA vials was conducted. This test was conducted to assess the degree to which field sample handling affects analytical results.

#### 4.4.1 Multilevel Passive Sampling

Eight existing wells at the site were sampled at multiple levels within the saturated screen interval. The intent of the initial sampling episode was to determine current levels of contaminant stratification in local geographic areas of the selected wells. Stratification information was used to select locations for new well installations required to accommodate equipment for the field program. Two modes of passive sampling were employed for the initial sampling phase. One mode included passive sampling in the open well, while the second mode included zone isolation between sampling devices. Snap Samplers were selected for the passive sampling. Of the available passive samplers, the Snap Sampler is the only device that collects an undisturbed whole-water sample of the ambient flow-through present in the well at the time of sampling. Multiple-interval samples are achievable, and installation of zone separation baffles is relatively easy to accomplish using this device (Figure 13). The following wells were selected for preliminary interval monitoring: MW-9, MW-14, MW-15, MW-16, MW-17, MW-20, MW-21, and MW-24. Figure 14 shows locations of these wells.



Figure 13. In well flow inhibitor used by ProHydro, Inc. to limit vertical solute migration in a well.

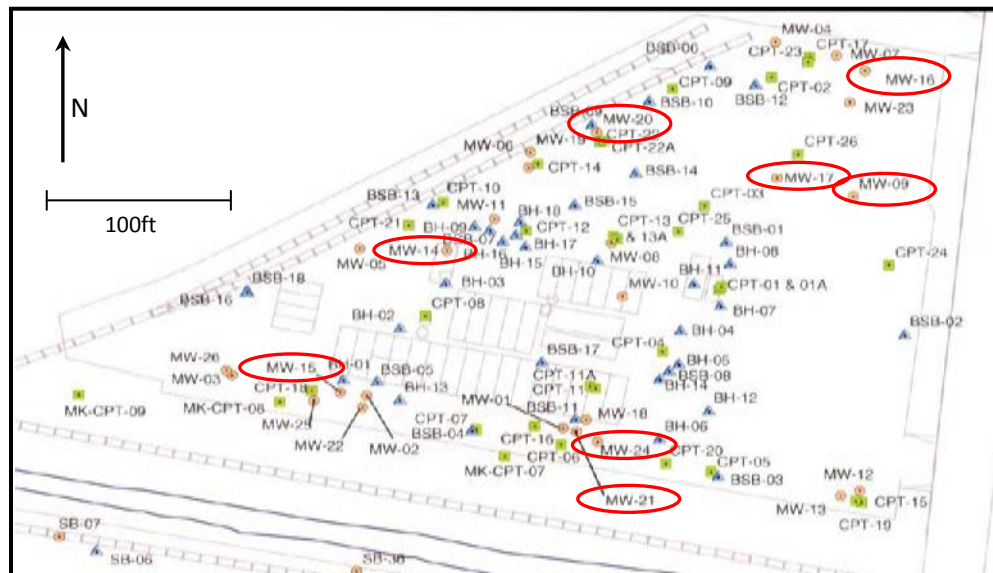


Figure 14. Well Location Map

A total of 26 sets of samplers were deployed in the selected wells. Each well was outfitted with 2 to 4 sets of Snap Samplers activated with pneumatic trigger systems. Pneumatic trigger lines were fixed at each well head to assure they remain in a fixed position during sampler equilibration. Trigger lines were measured/length-corrected in the field to accommodate discrepancies from available well construction information. Deployment was completed according to the depth intervals shown in Table 1. Because up to four zones were monitored in 10-foot well screens, and two zones monitored in the 5 foot saturated screens, a maximum of only two Snap Samplers were deployed with the actuator in any single 2.5-ft interval. Most samples consisted of (2) 40 ml VOA vial Snap Samplers. For duplicate samples, Matrix Spikes, and Matrix Spike Duplicate samples, samples were collected using either 125ml or 350ml Snap Sampler bottles. For these QA/QC samples, each sample was poured into standard laboratory-supplied VOA vials. By collecting the QA/QC samples in this manner, the replicates are true replicates rather than a combination of Snap VOAs and lab VOAs. This also eliminated concerns with spatial variability or collection and handling methods. In this initial installation, Snap Samplers were deployed with isolation baffles separating each sampling zone.

**Table 1, Snap Sampler Deployment Positions**

| Well                             | MW-9      | MW-14   | MW-15   | MW-16   | MW-17   | MW-20   | MW-21   | MW-24   |
|----------------------------------|-----------|---------|---------|---------|---------|---------|---------|---------|
| <b>TOC Elevation</b>             | 149.16    | 149.71  | 150.6   | 148.32  | 149.03  | 149.14  | 150.02  | 149.9   |
| <b>screen interval (bgs)</b>     | 30.5-45.5 | 55 - 65 | 54 - 64 | 29 - 46 | 56 - 66 | 57 - 67 | 53 - 63 | 67 - 77 |
| <b>Well diameter (in)</b>        | 4         | 2       | 2       | 2       | 2       | 2       | 2       | 4       |
| <b>Depth to Water (ft) 03/09</b> | 40.31     | 54.2    | 55.64   | 39.9    | 52.2    | 52.95   | 54.16   | 53.94   |
| <b>Sample zone</b>               |           |         |         |         |         |         |         |         |
| <b>Zone 1</b>                    | 41        | 56      | 57      | 41      | 57      | 58      | 55.5    | 68      |
| <b>Zone 2</b>                    | 43.5      | 58.5    | 59.5    | 43.5    | 59.5    | 60.5    | 58      | 70.5    |
| <b>Zone 3</b>                    |           | 61      | 62      |         | 62      | 63      | 61.5    | 73      |
| <b>Zone 4</b>                    |           | 63.5    |         |         | 64.5    | 65.5    |         | 75.5    |

Following an approximate two-week equilibration period, Snap Samplers were triggered and retrieved (1st week of June 2009). Upon completion of initial sampling activities at each well, each isolation baffle was removed prior to redeployment. The purpose of the second sampling event, and for removing the baffles, is to test the difference in ambient stratification the open well. Samplers were deployed and again allowed to equilibrate within the wells for approximately two weeks. After the second sampling event equilibration period, Snap Samplers were triggered, retrieved and prepared for laboratory submittal.

Later in the field program (2011), a second multilevel field testing program was conducted. The second phase included deployment of polyethylene diffusion bag samplers at 1 foot intervals in two wells. The two wells were installed with multilevel sampling ports (“tube wells”) described in more detail below. The PDBs were isolated from each other using plastic baffle devices designed to limit in well mixing effects. The purpose of these test was to compare the outside tube well samples to isolated passive devices located inside the well.

#### 4.4.2 Tracer Tests

After removal of all of the sampling equipment from the first passive sampler deployment in 2009, the eight existing test wells were tested for natural flushing using a tracer. Downhole logging sensors were deployed in two depths (in each well) to collect tracer dissipation data. Table 2 provides the sensor deployment depths for all the sensors. The tracer deionized water and was emplaced using a tremie to introduce minimal agitation, yet promote thorough mixing of the tracer in the well screen column. Minimally sufficient tracer was applied to allow measurement without significant disruption of either the flow regime or long term aquifer chemistry. Recovery of well chemistry to the pre-tracer condition was recorded with the logging sensors. Sensors measured temperature, pH, oxidation-reduction potential, electrical conductivity and chloride. Data was collected for up to two weeks, depending on field schedule. Measurements were logged at 15 minute intervals over the course of deployment period to allow

sufficiently frequent measurement of tracer dissipation. Flushing rate was determined from this tracer approach.

**Table 2, Sensor Deployment Positions**

| Well                             | MW-9      | MW-14   | MW-15   | MW-16   | MW-17   | MW-20   | MW-21   | MW-24   |
|----------------------------------|-----------|---------|---------|---------|---------|---------|---------|---------|
| <b>TOC Elevation</b>             | 149.16    | 149.71  | 150.6   | 148.32  | 149.03  | 149.14  | 150.02  | 149.9   |
| <b>screen interval (bgs)</b>     | 30.5-45.5 | 55 - 65 | 54 - 64 | 29 - 46 | 56 - 66 | 57 - 67 | 53 - 63 | 67 - 77 |
| <b>Well diameter (in)</b>        | 4         | 2       | 2       | 2       | 2       | 2       | 2       | 4       |
| <b>Depth to Water (ft) 03/09</b> | 40.31     | 54.2    | 55.64   | 39.9    | 52.2    | 52.95   | 54.16   | 53.94   |
| <b>Sensor zone</b>               |           |         |         |         |         |         |         |         |
| <b>Zone 1</b>                    | 41        | 57.5    | 57      | 41      | 58.5    | 60.5    | 56      | 70.5    |
| <b>Zone 2</b>                    | 43.5      | 62.5    | 61      | 43.5    | 63.5    | 65.5    | 60      | 75.5    |

#### 4.4.3 Installation of New Wells

The drilling program was designed to accommodate sampling requirements of the active pump-sampling phase of the investigation. Most of the on-site wells are 2-inch diameter and would not accommodate all of the equipment required to run the purging dynamics tests. Additionally, the testing program required sampling ports located outside the wells, in the annular space between the well and the borehole wall. Therefore three new wells were installed to satisfy those requirements.

The new wells are 4-inches in diameter, with multilevel sampling ports installed outside the well casings (Table 3). New well locations and specific design criteria were based on results of the initial well sampling and tracer testing described above. Figure 15 illustrates the construction detail. Wells were installed by standard methods, and developed thoroughly by surging, bailing and pumping to achieve high quality sample access points. During development, sustainable flow rates for the wells were determined.

**Table 3, New Well Construction Details**

| Well                         | MW-27                              | MW-28                              | MW-29      |
|------------------------------|------------------------------------|------------------------------------|------------|
| <b>Depth (ft)</b>            | 65                                 | 62.5                               | 46         |
| <b>Well Diameter (in)</b>    | 4                                  | 4                                  | 4          |
| <b>Diameter of hole (in)</b> | 18/12                              | 18/12                              | 12         |
| <b>Screen interval (ft)</b>  | 55-65                              | 52.5 – 62.5                        | 41-46      |
| <b>Tube well depths (ft)</b> | 55.5-56.5; 58-59; 60.5-61.5; 63-64 | 53-54; 55.5-56.5; 58-59; 60.5-61.5 | 42, 45     |
| <b>Material screened</b>     | medium-coarse clean sand           | medium-coarse clean sand           | silty sand |

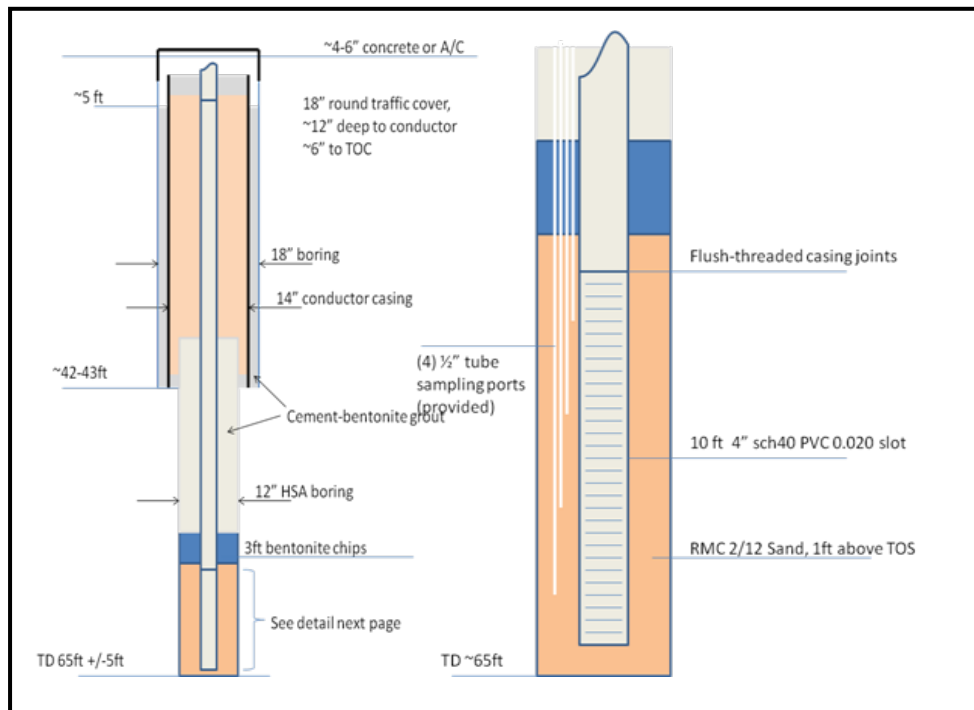


Figure 15. Construction Detail for New Wells

After the wells were installed and developed, the wells were instrumented with sensors and outfitted with Grundfos RediFlo2 pump or bladder pump equipment and Snap Samplers in anticipation of purge sampling work. The multi-parameter sensors were capable of measuring and recording pressure (depth of submergence), electrical conductivity, temperature, oxidation-reduction potential, chloride ion and pH. The RediFlo2 is an electric submersible pump capable of adjustable flow rates as low as approximately 100ml/minute up to several liters per minute. The bladder pump used in MW-29 (a low recharge well) was capable of flow rates as low as 50ml per minute up to approximately 250ml per minute. Equipment installed in the wells was left to stabilize for one week to one month in advance of sampling. The stabilization period is designed to allow the well itself, and the equipment installed to chemically equilibrate with the surrounding formation water. Previous research (Parker and Ranney 1997, 1998, 2000, 2003) shows that new plastics can sorb contaminants and thus could bias results if not equilibrated. Pre-deployment of the sensors, pumps, samplers will limit potential bias from new materials in the equipment. Figure 16 graphically represents the arrangement of equipment to be deployed in the test wells for the purge dynamics testing.

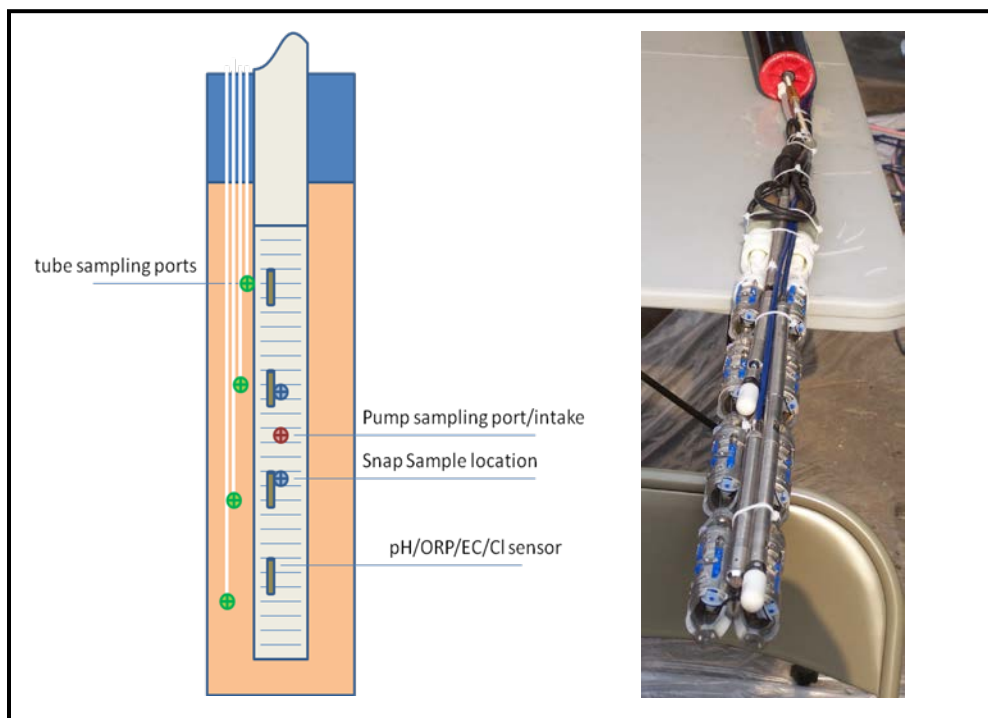


Figure 16. Downhole Equipment Illustration and Photo.

The tube sampling ports were placed on the upgradient side of the well during installation. By installing the wells and equipment well in advance of sampling, natural flow-through is allowed to establish a dynamic equilibrium between the equipment and flowing formation water.

#### 4.4.4 Purge Dynamics Testing

Several tests were completed during the purge testing phase. Low flow purging (defined as any flow rate less than approximately 1000ml per minutes that generates less than 0.3ft of drawdown) was conducted, with multiple VOC samples collected along the “purge” curve. These tests were designed to test how flow rate, flow rate changes, and variable contaminant concentrations along the well screen influencing aggregate concentrations pumped from the well, and other changes observed during the course of purging. Multiple in-well sensors measured water-quality parameters (pH, ORP, EC, Cl) of the inflowing water, chemistry as well as these parameters were measured in the pumped discharge water as well. Before purging and toward the end of a purge cycle, two sets of Snap Samplers were triggered to compare water flowing to the pump from above and below the pump intake, before and after purging. Tube wells located at depths along the screen interval, just outside the well screen were used to collect samples of water moving to the well at the end of the purge cycle. Figure 17 illustrates flow paths of water entering the well during pumping.

Varljen, *et al.* (2006) simulated steady state pumping scenarios numerically at steady state, with similar graphic representations. Varljen posited that since steady-state inflow came from the whole screen zone, the discharge is basically by definition a flow weighted average. Martin-

Hayden (2000a) provided an analytic solution for inflowing contaminant concentrations over time, which made a case for strong influence on pump discharge by inflowing contaminant position relative to the pump position and to time of purging. The experiments in this project, with instrumented sampling wells, were designed to help clarify how the variability of various factors (aquifer permeability, contaminant concentrations, pump location, extraction rate, and time) influence what pump discharge “represents.”

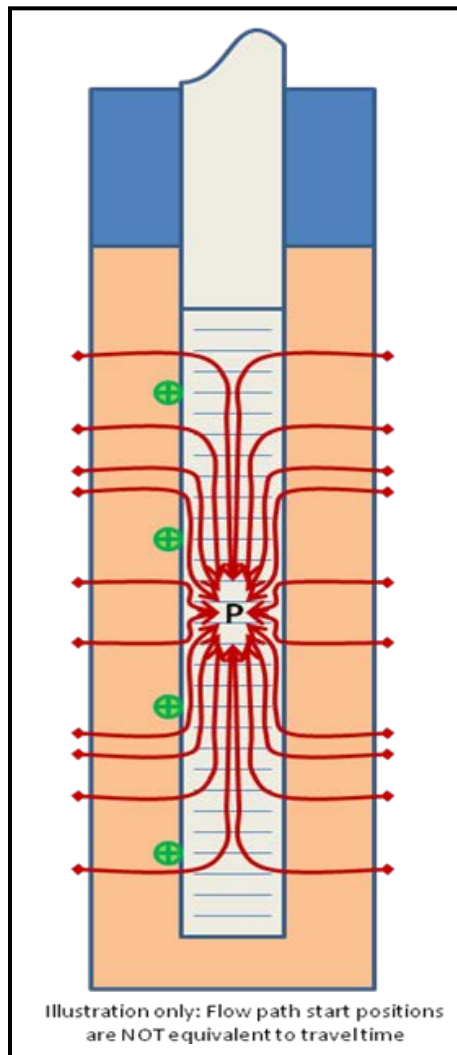


Figure 17. Flow Paths During Active Pumping

As described above, the 3 new test wells were instrumented with sensors, Snap Samplers and a purge pump several days to a month in advance of purge sampling. The Snap Samplers were deployed just above and below the pump intake position. Sensors were deployed at the same 2 positions as the Snap Samplers and at third interval (above) and fourth interval (below) the Snap Samplers. The sensor positions were approximately the same as the tube well sampling ports.

This positioning was designed to collect data on water flow/chemistry ahead of purge sampling activities, and to document changes as purge sampling progresses.

Four-inch well(s) have a nominal inside diameter of 10cm and a length of 305cm. One fully saturated well casing volume is therefore:

$$1WV = (10\text{cm}/2)^2 \times 3.14 \times 305\text{cm}$$

$$1WV = 23.9 \times 10^3 \text{ cm}^3, \text{ or } 23.9 \text{ liters}$$

For 2-inch (5cm) wells:

$$1WV = (5\text{cm}/2)^2 \times 3.14 \times 305\text{cm}$$

$$1WV = 6.25 \times 10^3 \text{ cm}^3, \text{ or } 6.0 \text{ liters}$$

#### Purge sample protocol

- Start sensor parameter logging at 1 minute intervals approximately 1 hour before pump start (continue for duration of all testing activities).
- Activate first set of Snap Samplers to close.
- Start pumping 100-1000mL/minute as determined during well development for steady drawdown.
- Collect VOC samples from the pump discharge at a rate of approximately 6 samples per well volume, or one per 4 liters for 5 well volumes.
- For wells with a flow rate change test, increase purge rate to a rate that will increase drawdown approximately 2-3x that of the lower rate, as determined during well development.
- For wells with a flow rate change test, reduce flow back to initial rate, to allow water level to rise during purging; collect VOC samples every 1 minute for 10 minutes, followed by samples every 5 minutes for 20 more minutes.
- Collect annular space sampling port samples (“tube well samples”) during the increased flow rate purging episode.
- Snap the second set of Snap Samples, turn off pump, & recover Snap Samplers from the well.

Table 4 includes a listing of the wells, flow rates, times of purging, volumes purged and number and type of samples collected during the tests conducted during the trial. Appendix A contains

the details of the sampling events and samples collected during the purge intervals. Analytical results will be described in greater detail in the Results section.

**Table 4, Samples Collected During Purge Testing**

| Well (diameter) | Date    | Flow Rate ml/min | Minutes purged | Total Volume/well volumes purged | Number of Samples | Snap Samples | Tube Samples | Duplicate and/or MS/MSD |
|-----------------|---------|------------------|----------------|----------------------------------|-------------------|--------------|--------------|-------------------------|
| MW-24 (4")      | 8/24/09 | 840              | 158            | 213/9                            | 42                | 4            | N/A          | n                       |
| MW-28 (4")      | 8/25/09 | 900              | 98             | 92/4                             | 33                | 4            | 2            | y(2)                    |
| MW-29 (4")      | 9/1/09  | 90               | 492            | 44/5                             | 26                | 4            | 1            | y(2)                    |
| MW-27 (4")      | 9/2/09  | 1200             | 100            | 120/6                            | 32                | 4            | 3            | y(1)                    |
| MW-15 (2")      | 3/16/10 | 100              | 91             | 9/4.5                            | 30                | 2            | N/A          | y(1)                    |
| MW-27 (4")      | 3/16/10 | 340              | 98             | 70/5                             | 30                | 4            | 0            | n                       |
| MW-16 (2")      | 3/17/10 | 105              | 122            | 13/5                             | 30                | 2            | N/A          | y(1)                    |
| MW-28 (4")      | 3/17/10 | 165              | 226            | 37/5                             | 33                | 4            | 0            | n                       |
| MW-24 (4")      | 8/16/10 | 370              | 302            | 112/4.7                          | 33                | 4            | N/A          | n                       |

#### 4.4.5 Pour Testing

A single outdoor field test of methods that are commonly used to fill VOA vials was conducted to assess the degree to which field sample handling affects analytical results. Three different fill rates and three different fill methods were used. The fill rates for the tests were 50 ml per minute, 250 ml per minute, and 1 L per minute. The fill methods included a vertical “top pour” approach where water sample was allowed to free-fall from 2 cm above the top of the vial to the bottom of the vial; a “side pour” method where the vial was held at a 30 to 45 degree angle to allow the discharge to flow smoothly down the side of the vial; and a “bottom fill” method where the discharge tube was placed at the bottom of the VOA vial and then slowly retracted while keeping the end of the tubing slightly submerged during the filling process (Figure 18). There were six replicates for each combination of fill rate and fill method. Sampling was first conducted at 50 mL/min; then at 250 mL/min; and last at 1 L/min. It took approximately 50 seconds to fill a vial at the lowest flow rate, approximately 15 seconds at 250-mL/min rate, and approximately 3 seconds at 1 L/min. For each flow rate, the sampling order was reversed with each set of samples (i.e. a set of samples consisted of a top-pour sample, a side-pour sample, and a bottom-fill sample).

Analytes in the test solution included benzene; chloroform; 1,1-dichloroethane (11DCA); 1,2-dichloroethane (12DCA); 1,1-dichloroethene (11DCE); cis-1,2-dichloroethene (cDCE); tetrachloroethene (PCE); toluene; 1,1,1-trichloroethane (111TCA); trichloroethene (TCE); trichlorofluoromethane (TCFMA); vinyl chloride (VC); and 1,4-dioxane. Sample handling,

processing, and analyses were conducted as described previously. Additional information on the methods used can be found in Parker and Britt (2012).

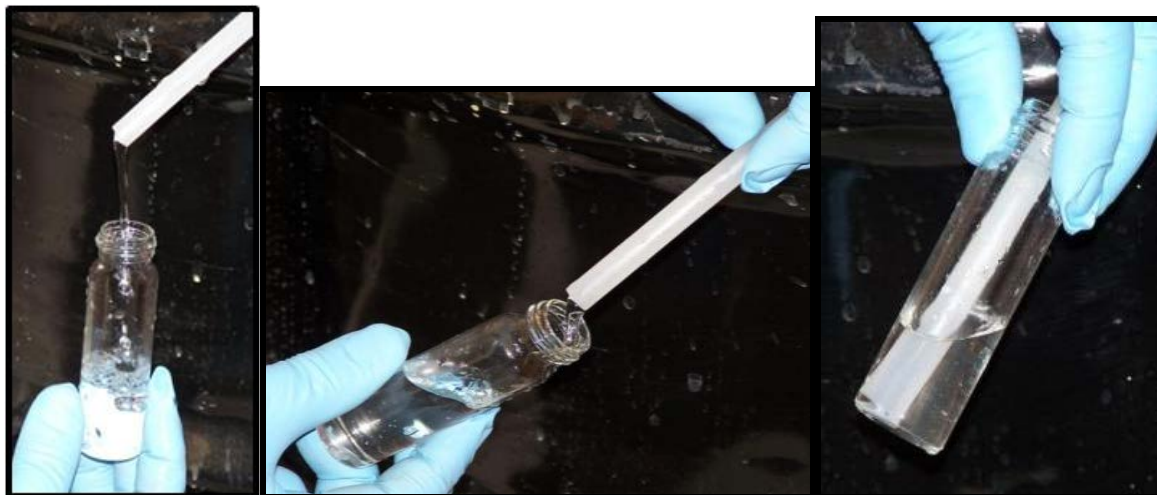


Figure 18. Photos of top-pour, side-pour, and bottom-fill methods, respectively.

For each of the twelve analytes found in the test solution, the concentration for a given fill method and fill rate was divided by the mean concentration of that analyte. The normalized values were then pooled into one data set. This provided us with a data set with 233 values for each pour method or fill method (or 699 total values). SigmaStat (3.1) software (by Systat Software Inc.) was used for the following statistical analyses. A two-way Analysis of Variance (ANOVA) was conducted to determine if either the pour method or the flow rate had an effect on analyte concentrations for the entire suite of analytes. The Holm-Sidak method for a pair-wise multiple comparison test (Systat Software, Inc. 2004) was used to determine which flow rates and fill methods differed from each other.

## **5.0 Results and Discussion**

### **5.1 Field Investigation**

Several phases of the field investigation yielded results that satisfied the goals of the physical field testing program. Initial multilevel sampling provided information that allowed selection of appropriate locations for test well installation at the field site. New wells largely functioned as anticipated and allowed collection of active and passive sampling data to inform our research questions.

Results from three primary focus areas for the field investigation are presented here: 1) multilevel passive sampling and sensing for stratification analysis, 2) purge sampling with multiple sample collection for “purge curve” analysis, and 3) ancillary testing for greater understanding sample collection variability.

#### *5.1.1 Stratification Testing Results*

Results from stratification testing of the existing wells indicated a stronger degree of stratification during the phase of sampling where baffle mixing inhibitors were deployed between passive samplers. Table 5 illustrates results for several constituents in the isolated vs un-isolated sampling. Consistent with previous work by the investigators, there were differences in degrees of stratification with the alternate deployment configurations. Somewhat surprisingly, in some cases, the stratification effect inverted using the zone separation method and was chemical-specific. However, not all examples showed substantial differentials.

**TABLE 5, Comparison of Open Well vs. Baffle Separator Samples**

| <b>Well/Chemical</b> | <b>BAFFLE maximum difference ratio*</b> | <b>NO BAFFLE maximum difference ratio</b> | <b>Stratification Measurement Improvement**</b> |
|----------------------|---|---|---|
| MW9 (2 zones)        |   |   |   |
| Benzene              | -1.6                                    | -1.1                                      | 45%   |
| 11DCA                | 1.7                                     | -1.2                                      | <b>reverse</b>                                  |
| 11DCE                | 1.1                                     | -1.1                                      | <b>Reverse</b>                                  |
| cis-1,2DCE           | 1.1                                     | 1   | 10%   |
| PCE                  | -3.3                                    | 1.7                                       | <b>Reverse</b>                                  |
| TCE                  | -1.4                                    | 1.1                                       | <b>Reverse</b>                                  |
| VC                   | 3.7                                     | -3.6                                      | <b>reverse</b>                                  |
| MW14 (3 zones)       |   |   |   |
| Benzene              | 21                                      | 14  | 50%   |
| 11DCA                | 144                                     | 36  | 300%  |
| 11DCE                | 28                                      | 7.6                                       | 268%  |
| cis-1,2DCE           | 21                                      | 9.2                                       | 128%  |
| PCE                  | -6.0                                    | -4.8                                      | 25%   |

| Well/Chemical  | BAFFLE maximum difference ratio* | NO BAFFLE maximum difference ratio | Stratification Measurement Improvement** |
|----------------|----------------------------------|------------------------------------|--|
| TCE            | -1.6                             | -2.5                               | -36%                                     |
| VC             | 129                              | 10                                 | 1190%                                    |
| MW17 (4 zones) |                                  |                                    |  |
| Benzene        | --                               | --                                 |  |
| 11DCA          | 2.0                              | 1.2                                | 67%                                      |
| 11DCE          | -1.3                             | 1.5                                | <b>reverse</b>                           |
| cis-1,2DCE     | 1.2                              | -1.1                               | <b>reverse</b>                           |
| PCE            | --                               | --                                 |  |
| TCE            | -1.4                             | -1.2                               | 17%                                      |
| VC             | --                               | --                                 |  |
| MW21 (3 zones) |                                  |                                    |  |
| Benzene        | --                               | --                                 |  |
| 11DCA          | 3.8                              | 7.1                                | -46%                                     |
| 11DCE          | 2.5                              | 1.7                                | 47%                                      |
| cis-1,2DCE     | 3.3                              | 2.7                                | 22%                                      |
| PCE            | 1.9                              | -1.3                               | <b>reverse</b>                           |
| TCE            | 1.4                              | -1.3                               | <b>reverse</b>                           |
| VC             | 6.5                              | 5.1                                | 27%                                      |
| MW24 (4 zones) |                                  |                                    |  |
| Benzene        | --                               | --                                 |  |
| 11DCA          | 1.5                              | 1.3                                | 15%                                      |
| 11DCE          | -2.0                             | -1.1                               | 82%                                      |
| cis-1,2DCE     | 1.2                              | 1.1                                | 9%                                       |
| PCE            | -1.4                             | 1.3                                | <b>reverse</b>                           |
| TCE            | -1.9                             | -1.3                               | 46%                                      |
| VC             | --                               | --                                 |  |

\* difference between highest and lowest concentration, negative denotes concentrations are higher at the bottom of the well

\*\* positive percentage is greater stratification present with zone isolation; negative percentage is lesser stratification, reverse denotes stratification direction changed with and without zone isolation

These preliminary stratification data were used to select locations where stratification was relatively strong for installation of new wells. Three locations were selected. Figure 19 shows the locations relative to the existing stratification test wells. As described in the Materials and Methods section, these wells were constructed to allow multiple sampling approaches with a variety of downhole sensors and sampling equipment.

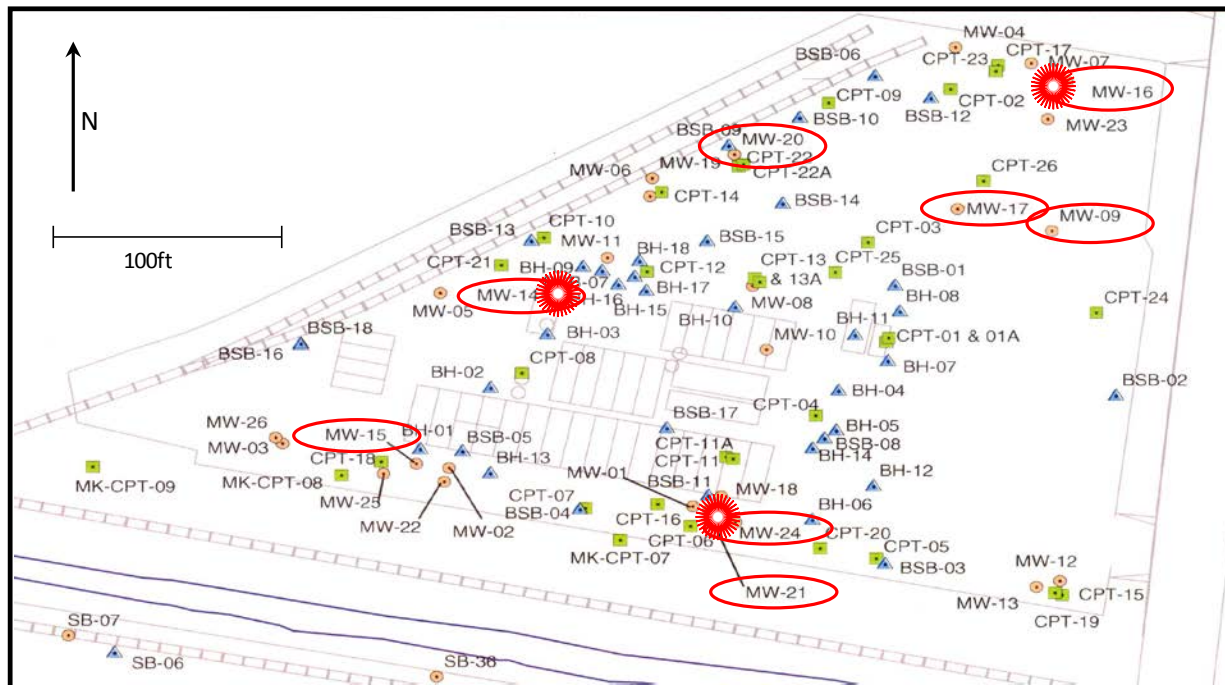


Figure 19. Locations of new wells

### 5.1.2 Purge Curve Testing Results

Using these new wells for flow-through dilution tests, purge sampling, and multilevel passive sampler/sensor deployment, multiple test scenarios were completed. These scenarios included chemical sensor data collection during a pre-sampling deployment period; pumping with multiple periodic chemical sample collection; and pre- and post-purge downhole sample capture.

Purge testing data show that pump location relative to contaminant inflow position had a sometimes dramatic effect on the shape of the purge/contaminant curve. That is, the closer or farther from the contaminant inflow position the pump was located, the more dramatic the divergence from the starting and ending inflow concentrations. Figure 20(A), shows TCE concentration drop by about a factor of 3 in early pumping, with original concentrations returning after about three well volumes pumped. In contrast, Figure 20(B) shows a smaller 50% boost in concentrations early in the purge cycle. The implication of these early purge changes is that chemical concentration changes may be a source of sampling variability that is not widely recognized. Further, only when field parameter measurements also show divergences would the field sampling practitioner know that such divergences are occurring. Additional results below illustrate that such data is not necessarily indicative of such chemical concentration divergences.

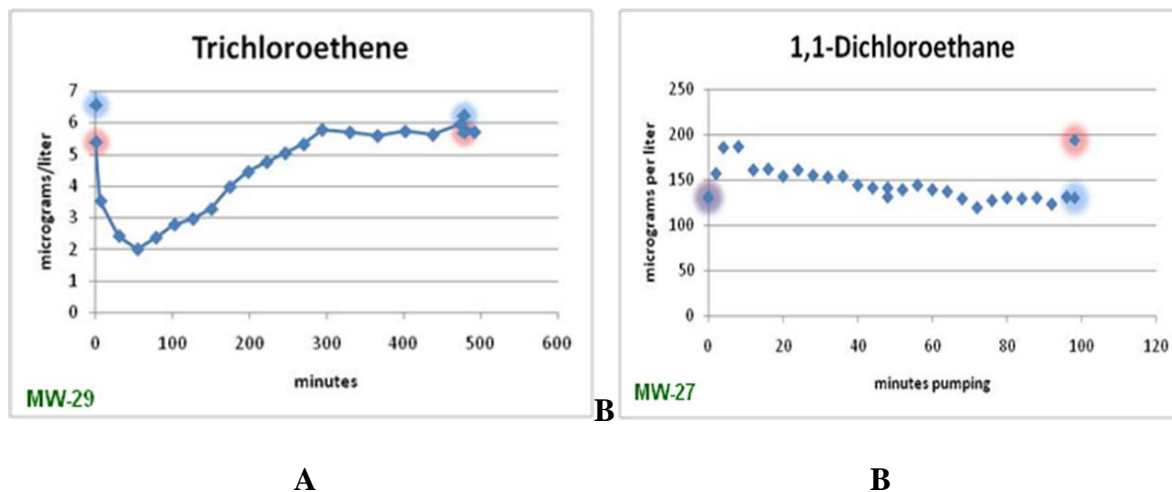


Figure 20 (A/B). Examples of purge curves for TCE in MW-29 and 1,1-DCE in MW-27. Early time divergence from flow weighted average concentrations during purging. Light blue and pink highlighted samples are Snap Samples collected *in situ* above (pink) and below (blue) the pump intake.

Figure 21(A) illustrates a case where very little change occurred in TCE concentration throughout the purge, until the very end when the purge flow rate was changed (by testing design). Figure 21(B) also shows minor slow change in *cis*-1,2-DCE concentration over the course of the purge, but a fairly rapid change in concentration when the purge rate was changed at the end of the purge cycle. Additionally, the Snap Samples above and below the pump intake collected at the beginning of the purge differ substantially from those concentrations observed after purging. Despite minimal changes in VOC concentration during the course of the purge, there are clearly different concentrations of VOC contaminants entering the well from different positions. After purging, the water collected with the Snap Samplers show undetectable VOC concentrations above the pump and approximately 25% higher than the pump discharge concentrations below the pump intake. This differential can be interpreted to mean that the pump discharge contains approximately 80% VOC-containing water entering the well from below the pump position and 20% uncontaminated water entering from above the pump.

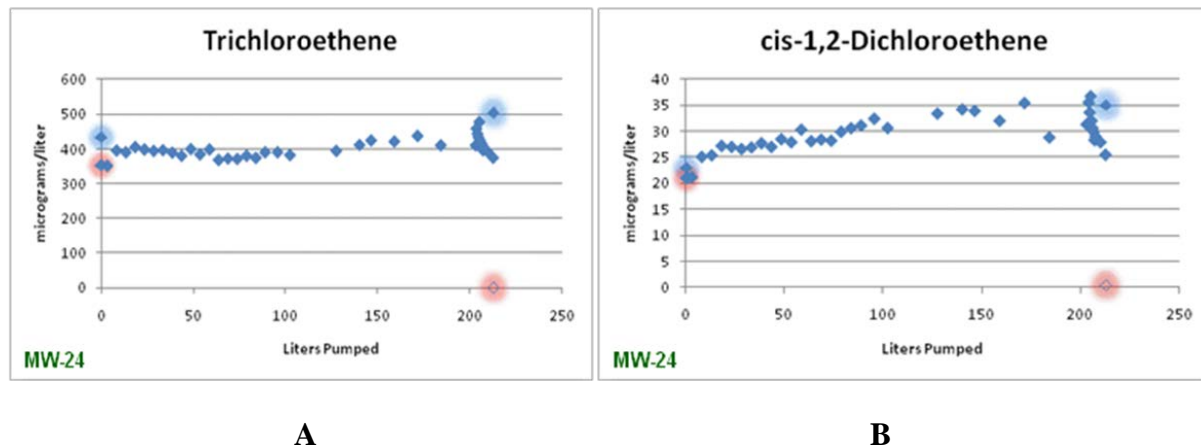


Figure 21 (A/B), Examples of purge curves for TCE cis-1,2-DCE in MW-24. Relatively stable concentrations throughout purging disrupted by changing the purge rate at the very end of purging. Light blue and pink highlighted samples are Snap Samples collected *in situ* above (pink) and below (blue) the pump intake.

Appendix A contains many additional data sheets from the several “purge curve” tests conducted during the investigation. Additional data plots are presented in the appendix for multiple chemicals provide additional illustration of the differences among test scenarios and different wells.

Another important observation from the late purge data comes from the VOC data collected in close sequence immediately after lowering the purge rate. Reducing purge rate is commonly recommended to improve VOC recovery during sample collection (USEPA 1985, USEPA 2002, ASTM 2002). When contaminants entering the well bore are stratified, changing the purge rate changes the weighting of water entering the pump intake because water level changes. When reducing flow rate, water level rises in the well. This water level change causes overweighting of water entering below the pump. In the case shown in Figure 21, this results in a temporary increase in contaminant concentration.

Lab experiments illustrate a similar effect with the opposite condition—with “contaminated” water above the pump intake. Figures 22 and 23 show the photo series of samples collected before and after changing purge rate in a pipe test. Importantly, the change in purge rate can either increase or decrease pump discharge concentrations, sometimes dramatically. In the laboratory case, the “contaminant” entering above the discharge point nearly disappeared for several minutes until water level stabilized and the flow-weighted condition returned. For field sampling, this effect will likely go unnoticed and could be a substantial source of sampling variability if sampling is conducted immediately after lowering the flow rate (the normal condition).

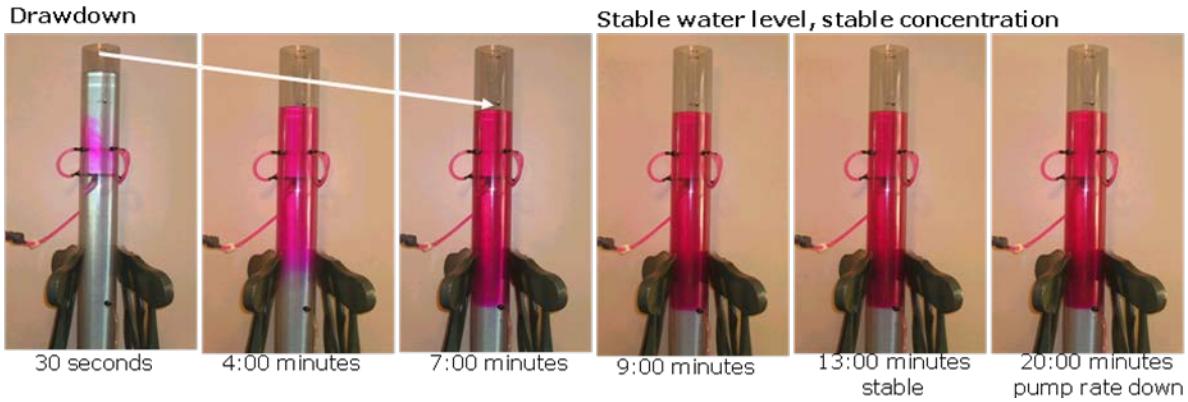


Figure 22. Simulated well with dyed water entering above pump intake, clear water entering below (out of view). Constant head reservoir tank with clear and dyed water controls equal flow into upper and lower parts of pipe. Discharge is controlled by gravity with a valve and “pump” position located equidistant from the dyed and clear water entry points. Flow rate is 1000ml per minute.

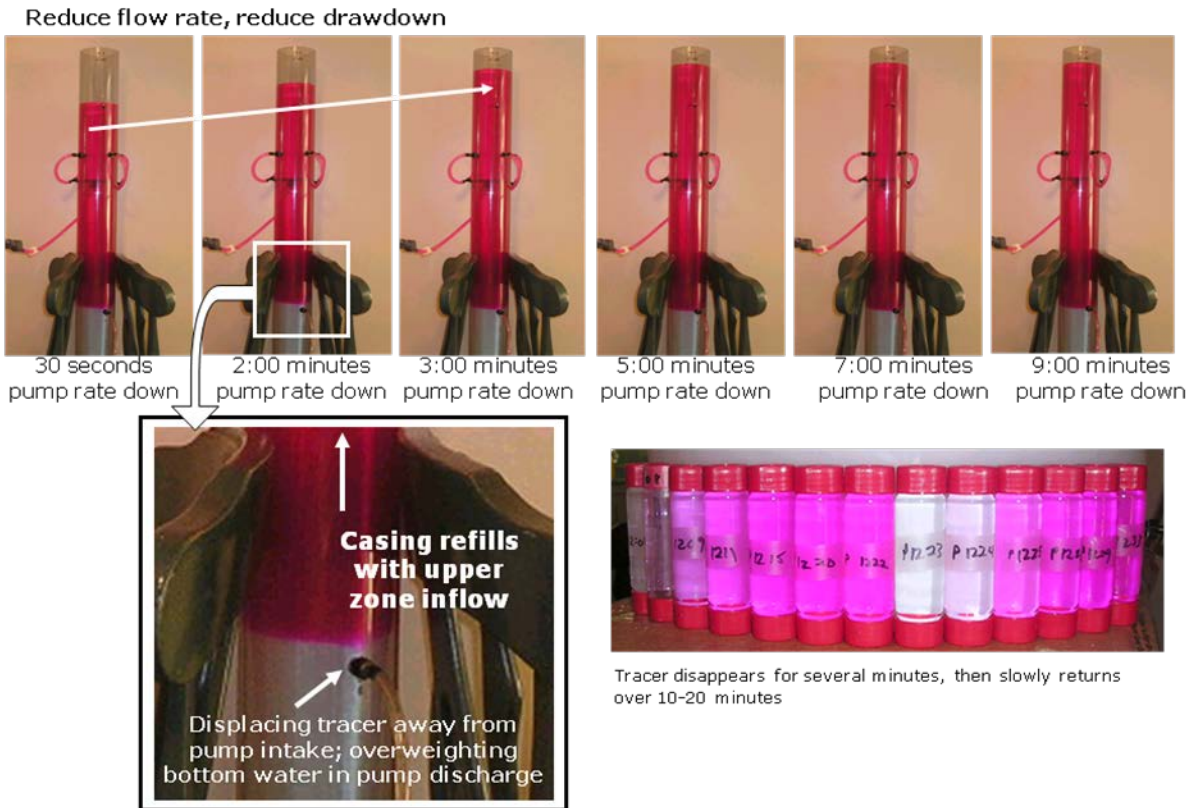


Figure 23. Flow rate reduced to 250ml per minute, causing rising water in simulated well. Rising water causes discharge to temporarily overweight water entering from the bottom half of the well.

Overall, these data show that pump position can be an important factor when it comes to rapidity of attainment of flow-weighted average concentrations during purging, and the degree to which the discharge changes concentrations throughout purging. Additionally, the data suggest that there may be times when “purge parameters” such as temperature, conductivity or oxidation

reduction potential may mislead a sampling team. As shown in Figure 24, purge parameter stabilization may appear to occur at a time when contaminant concentrations have not yet stabilized (parameter data from same purge event for MW-24 as Figure 21A/B and for MW29 as Figure 20A). Indeed, *apparent stability when observing reading-to-reading results at a purge volume of approximately one well volume pumped may actually lead the sampling team to collect samples at a time when contaminant concentrations at the furthest point from the flow-weighted average concentration during the course of the purge.*

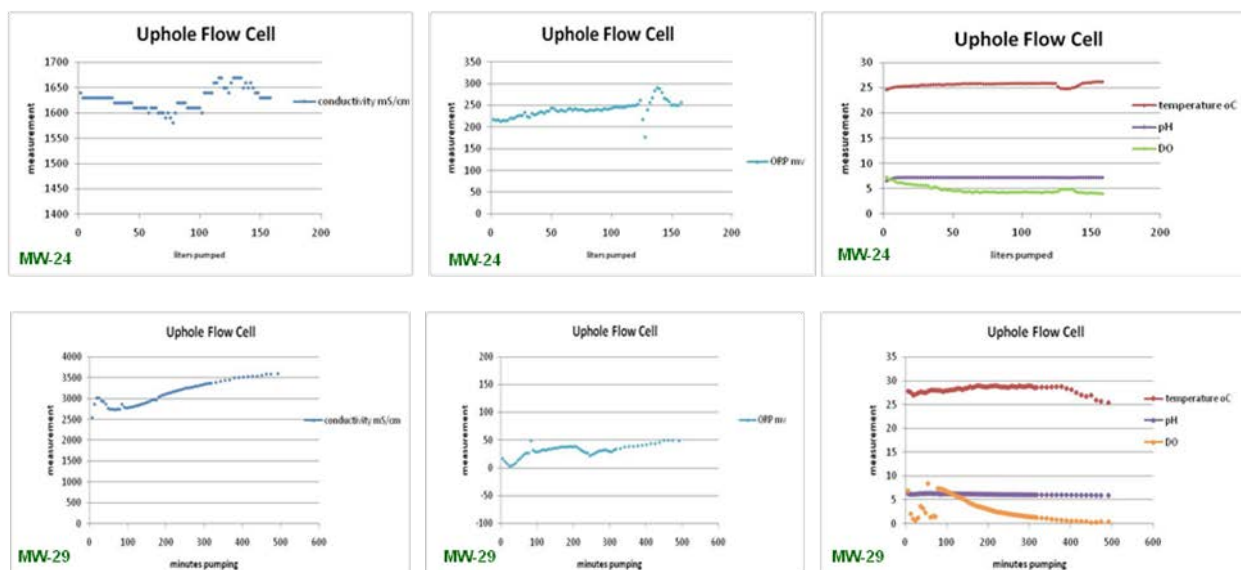


Figure 24, Purge curve data illustrate small and slow changes in parameter readings.

Alternately, for some analytes, stability of contaminant concentrations was never achieved, despite long completed parameter stability. The constituents include those that readily degrade in the presence of oxygen (*e.g.* benzene, acetone). Figure 25 illustrates examples of these compounds in the MW29 purge curve. These findings may indicate the well itself is a locus of biodegradation. In these circumstances, passive, sensor-based, and even low-flow/low-volume purge approaches may be problematic for representing formation groundwater without a thorough purge. A technical paper is in preparation that includes more detail on results and conclusions of this aspect of the study (Britt et al, in prep). These findings are not repeated in detail here to avoid rejection of the manuscript as “already published” material. Appendix A contains additional data plots of the purge/contaminant curves. Raw data lab reports are included in Appendix C.

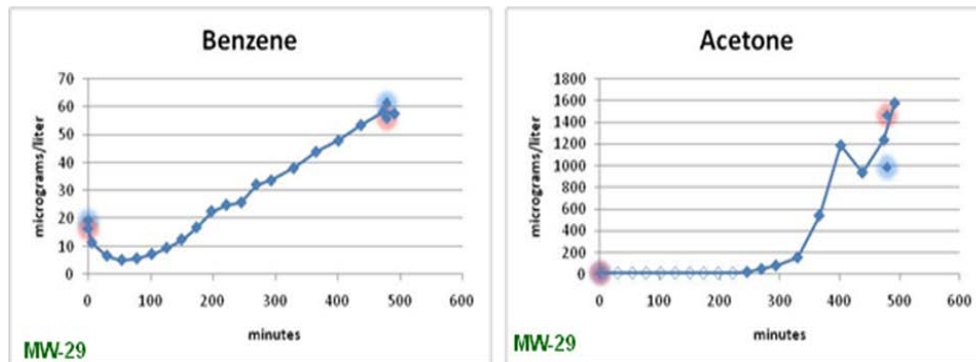


Figure 25. Continued increasing concentrations of some compounds through 5 well volumes purged.

The tube wells installed in MW-27, MW-28, and MW-29 (illustrated in Figures 15 and 16) were utilized to assess contaminant concentrations entering the well but not yet impacted by mixing and flow processes within the well. This approach was somewhat imperfect in the ambient flow regime because installation difficulties and possible flow gradient changes during the course of the study made it impossible to know for sure if the tube wells were always on the upgradient (unaffected) side of the well. Samples collected during purging were less likely to be affected by such orientation mismatch. Some of the purge curve analyses included collection of tube well samples at the end of the large volume removal actions. Similar to those interpretations allowable by collecting samples from above and below the pump intake, tube well samples provided additional information about what contaminants were entering the well at what position. Figure 26 illustrates the range of tube well samples compared to the in-well Snap Sampler results collected from above and below the pump intake, and pumped sample results. Appendix A contains many more examples of different wells and different contaminants.

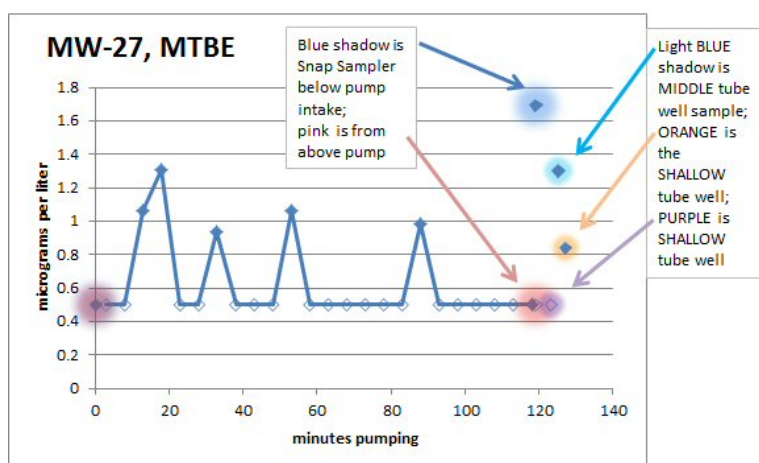


Figure 26. Purge sampling results compared to Snap Samples collected above and below pump intake (pink and medium blue) in contrast to tube well samples collected just outside the well (light blue, orange and purple highlights)

Tube wells were also used in a passive configuration with multiple-interval passive samplers. To limit the effects of in-well mixing on both the in-well passive devices, but also the indirect effect on the tube well samples, plastic baffle mixing inhibitor devices were placed between the passive samplers (Figure 13). Polyethylene Diffusion Bag (PDB) samplers were deployed at 1 foot intervals in two of the wells with tube wells. Tube well samples were collected before deployment of the PDBs and then just prior to retrieval of the PDBs. There are only 4 tube well samples, while there were 10 PDB samples in each well. The tube well samples reasonably matched the PDB samples, but there were some discrepancies. Figure 27 illustrates TCE data for MW-27 during this test. Many other examples are included in Appendix A, Tables A-14 and A-15.

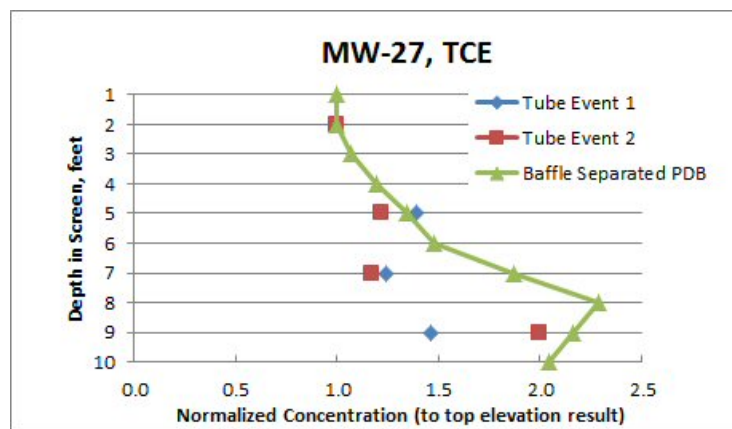


Figure 27. Tube well samples (Event 1) collected prior to insertion of the baffled PDB samples; tube well samples collected just prior to PDB removal; and PDB samples collected at 1 foot intervals within the screen zone. Stronger stratification shown in the Event 2 tube wells with zone isolation present in the well.

### 5.1.3 Sample Pour Testing Results

In addition to the passive sampling and purge curve sampling analysis, test of sample pour methods was conducted to assess the degree to which field sample handling affects analytical results. Pour tests included three different bottle fill rates and three fill methods. Fill rates for the tests were 50ml per minute, 250ml per minute and 1000 ml per minute. Fill methods included a vertical “top pour” approach where water was introduced to the VOA vial directly by free-fall from 2cm above top of the vial to the bottom; a “side pour” method where water flow was directed to the side of the bottle; and a “bottom fill” method where the discharge tube was placed to the bottom of the VOA vial and kept slightly submerged during bottle filling. Six replicates of each fill-rate and fill-method combination were collected and analyzed for VOCs.

The results for each of the pour test methods for the 50-mL/min, 250-mL/min, and 1-L/min flow rates are summarized in Table 6. The raw data can be found in Appendix A Table A-15.

Table 6. Summary of the pour-test study results.

| <b>Analyte</b>    |                    | <b>50BF</b>  | <b>50SP</b>  | <b>50TP</b>  | <b>250BF</b> | <b>250SP</b> | <b>250TP</b> | <b>1000BF</b> | <b>1000SP</b> | <b>1000TP</b> |
|-------------------|--------------------|--------------|--------------|--------------|--------------|--------------|--------------|---------------|---------------|---------------|
| <b>Benzene</b>    | <b>Mean Conc.*</b> | <b>0.88</b>  | <b>0.87</b>  | <b>0.81</b>  | <b>0.95</b>  | <b>0.88</b>  | <b>0.87</b>  | <b>0.91</b>   | <b>0.89</b>   | <b>0.88</b>   |
|                   | Std. dev.          | 0.069        | 0.029        | 0.045        | 0.074        | 0.049        | 0.057        | 0.024         | 0.19          | 0.13          |
|                   | % RSD              | 7.8          | 3.4          | 5.6          | 7.8          | 5.6          | 6.6          | 2.7           | 21.7          | 14.3          |
| <b>Chloroform</b> | <b>Mean Conc.*</b> | <b>21.7</b>  | <b>20</b>    | <b>18.6</b>  | <b>22.7</b>  | <b>20.3</b>  | <b>20.4</b>  | <b>22.9</b>   | <b>21.5</b>   | <b>22.1</b>   |
|                   | Std. dev.          | 1.28         | 0.98         | 0.61         | 0.82         | 4.34         | 0.71         | 0.48          | 3.6           | 2.02          |
|                   | % RSD              | 5.9          | 4.9          | 3.3          | 3.6          | 21.4         | 3.5          | 2.1           | 16.7          | 9.1           |
| <b>11DCA</b>      | <b>Mean Conc.*</b> | <b>99.9</b>  | <b>92</b>    | <b>85.1</b>  | <b>105</b>   | <b>93</b>    | <b>91.6</b>  | <b>106</b>    | <b>97.6</b>   | <b>100</b>    |
|                   | Std. dev.          | 5.74         | 5.36         | 2.91         | 5.91         | 20.6         | 5.7          | 3.4           | 19.1          | 10.7          |
|                   | % RSD              | 5.7          | 5.8          | 3.4          | 5.6          | 22.2         | 6.2          | 3.3           | 19.6          | 10.7          |
| <b>12DCA</b>      | <b>Mean Conc.*</b> | <b>2.35</b>  | <b>2.27</b>  | <b>2.18</b>  | <b>2.43</b>  | <b>2.34</b>  | <b>2.34</b>  | <b>2.58</b>   | <b>2.54</b>   | <b>2.58</b>   |
|                   | Std. dev.          | 0.151        | 0.063        | 0.117        | 0.39         | 0.253        | 0.136        | 0.101         | 0.292         | 0.121         |
|                   | % RSD              | 6.4          | 2.8          | 5.3          | 16.1         | 10.8         | 5.8          | 3.9           | 11.5          | 4.7           |
| <b>Toluene</b>    | <b>Mean Conc.*</b> | <b>0.83</b>  | <b>0.81</b>  | <b>0.76</b>  | <b>0.88</b>  | <b>0.83</b>  | <b>0.84</b>  | <b>0.87</b>   | <b>0.82</b>   | <b>0.84</b>   |
|                   | Std. dev.          | 0.026        | 0.045        | 0.014        | 0.036        | 0.043        | 0.022        | 0.039         | 0.123         | 0.077         |
|                   | % RSD              | 3.2          | 5.6          | 1.9          | 4.1          | 5.2          | 2.6          | 4.6           | 15            | 9.2           |
| <b>111TCA</b>     | <b>Mean Conc.*</b> | <b>1.62</b>  | <b>1.36</b>  | <b>1.44</b>  | <b>1.54</b>  | <b>1.75</b>  | <b>1.36</b>  | <b>1.79</b>   | <b>1.61</b>   | <b>1.67</b>   |
|                   | Std. dev.          | 0.104        | 0.38         | 0.085        | 0.442        | 0.102        | 0.462        | 0.126         | 0.481         | 0.261         |
|                   | % RSD              | 6.4          | 27.9         | 5.9          | 28.6         | 5.8          | 33.9         | 7             | 29.9          | 15.7          |
| <b>TCE</b>        | <b>Mean Conc.*</b> | <b>120</b>   | <b>112</b>   | <b>104</b>   | <b>123</b>   | <b>105</b>   | <b>110</b>   | <b>121</b>    | <b>113</b>    | <b>114</b>    |
|                   | Std. dev.          | 2.61         | 2.71         | 2.32         | 2.8          | 30.3         | 1.79         | 3             | 26.2          | 13.5          |
|                   | % RSD              | 2.2          | 2.4          | 2.2          | 2.3          | 28.8         | 1.6          | 2.5           | 23.2          | 11.9          |
| <b>TCFMA</b>      | <b>Mean Conc.*</b> | <b>48.2</b>  | <b>44.1</b>  | <b>40.2</b>  | <b>49</b>    | <b>40.5</b>  | <b>40.7</b>  | <b>49.7</b>   | <b>42.8</b>   | <b>44.3</b>   |
|                   | Std. dev.          | 3.36         | 2.8          | 1.37         | 5.25         | 16.75        | 5.82         | 2.35          | 15.15         | 9.71          |
|                   | % RSD              | 7            | 6.4          | 3.4          | 10.7         | 41.4         | 14.3         | 4.7           | 35.4          | 21.9          |
| <b>11DCE</b>      | <b>Mean Conc.*</b> | <b>239</b>   | <b>218</b>   | <b>198</b>   | <b>245</b>   | <b>206</b>   | <b>207</b>   | <b>242</b>    | <b>214</b>    | <b>221</b>    |
|                   | Std. dev.          | 17.3         | 16.9         | 6.9          | 22.1         | 66.9         | 10.1         | 11.1          | 63.4          | 41.1          |
|                   | % RSD              | 7.2          | 7.8          | 3.5          | 9            | 32.5         | 4.9          | 4.6           | 29.7          | 18.6          |
| <b>cDCE</b>       | <b>Mean Conc.*</b> | <b>49.7</b>  | <b>45.7</b>  | <b>42.4</b>  | <b>51.3</b>  | <b>45.8</b>  | <b>45.5</b>  | <b>51.2</b>   | <b>48.1</b>   | <b>49.2</b>   |
|                   | Std. dev.          | 3.22         | 2.83         | 1.54         | 2.48         | 8.7          | 1.71         | 1.42          | 8.27          | 4.34          |
|                   | % RSD              | 6.5          | 6.2          | 3.6          | 4.8          | 19           | 3.8          | 2.8           | 17.2          | 8.8           |
| <b>tDCE</b>       | <b>Mean Conc.*</b> | <b>BDL**</b> | <b>BDL**</b> | <b>BDL**</b> | <b>BDL**</b> | <b>BDL**</b> | <b>BDL**</b> | <b>0.72</b>   | <b>0.74</b>   | <b>0.76</b>   |
|                   | Std. dev.          |              |              |              |              |              |              | 0.202         | 0.206         | 0.155         |
|                   | % RSD              |              |              |              |              |              |              | 28.1          | 27.9          | 20.3          |
| <b>PCE</b>        | <b>Mean Conc.*</b> | <b>130</b>   | <b>123</b>   | <b>114</b>   | <b>132</b>   | <b>111</b>   | <b>119</b>   | <b>129</b>    | <b>117</b>    | <b>119</b>    |
|                   | Std. dev.          | 2.28         | 3.35         | 1.86         | 2.1          | 37.5         | 3.1          | 2.1           | 29.8          | 16.8          |
|                   | % RSD              | 1.8          | 2.7          | 1.6          | 1.6          | 33.9         | 2.6          | 1.6           | 25.4          | 14.2          |

| <b>Analyte</b>  |                    | <b>50BF</b> | <b>50SP</b> | <b>50TP</b> | <b>250BF</b> | <b>250SP</b> | <b>250TP</b> | <b>1000BF</b> | <b>1000SP</b> | <b>1000TP</b> |
|---|--------------------|-------------|-------------|-------------|--------------|--------------|--------------|---------------|---------------|---------------|
| <b>VC</b>   | <b>Mean Conc.*</b> | <b>26.1</b> | <b>25</b>   | <b>22.4</b> | <b>30</b>    | <b>23.8</b>  | <b>25.4</b>  | <b>29.4</b>   | <b>26.7</b>   | <b>26.4</b>   |
|   | Std. dev.          | 3.94        | 2.07        | 0.84        | 2.65         | 6.64         | 1.58         | 0.88          | 8.53          | 6.28          |
|   | % RSD              | 15.1        | 8.3         | 3.8         | 8.8          | 28           | 6.2          | 3             | 31.9          | 23.8          |
| <b>14Dioxane<sup>1</sup></b>  | <b>Mean Conc.*</b> | <b>1122</b> | <b>1186</b> | <b>1138</b> | <b>1172</b>  | <b>1174</b>  | <b>1111</b>  | <b>1317</b>   | <b>1310</b>   | <b>1367</b>   |
|   | Std. dev.          | 89.1        | 154.7       | 100.1       | 106          | 124          | 96           | 145           | 43.6          | 45.1          |
|   | % RSD              | 7.9         | 13          | 8.8         | 9.1          | 10.6         | 8.7          | 11            | 3.3           | 3.3           |
| * Concentration in µg/L<br>** BDL, most below detection level<br><sup>1</sup> Minus one outlier |                    |             |             |             |              |              |              |               |               |               |

The statistical analyses showed that the differences among the different fill rates and bottle-fill methods were highly significant and that the interaction of the fill rate and fill method was also significant. This significant interaction means that the effect of fill rate differed among the fill methods, and vice versa (i.e., the effect of fill method differed at different fill rates). Therefore, the impact of fill rate and fill technique were examined separately.

#### 5.1.3.1 Fill Method

There was a significant difference between the bottom-fill and side-pour methods and between the bottom-fill method and the top-pour method at all three fill rates (Table 7). For these comparisons, a number followed by two letters were used to differentiate among the methods. The number gives the vial fill rate in milliliters per minute and the letters describe the fill method. For example, 50BF means that the vial was filled at 50 mL/min using the bottom-fill method. The number 1000 is used to denote the fastest flow rate, ~1000 mL/min (~1 L/min.). The “>” symbol means that the difference in VOC recovery was greater at statistically significant level, and the “~” symbol representing no significant difference in recovery.

**Table 7. Summary of the statistical analyses comparing the different fill methods**

|                                | % Difference | Significant? | P=     |
|--------------------------------|--------------|--------------|--------|
| <b>Fill Method (BF vs. SP)</b> |              |              |        |
| 50BF > 50SP                    | 7.5          | Yes          | 0.005  |
| 250BF > 250SP                  | 14.3         | Yes          | <0.001 |
| 1000BF > 1000SP                | 8.1          | Yes          | 0.021  |
| <b>Fill Method (SP vs. TP)</b> |              |              |        |
| 50SP > 50TP                    | 6.1          | Yes          | 0.021  |
| 250SP ~ 250TP                  | 3.3          | No           | 0.199  |
| 1000SP ~ 1000TP                | 2.3          | No           | 0.358  |
| <b>Fill Method (BF vs. TP)</b> |              |              |        |
| 50BF > 50TP                    | 13.6         | Yes          | <0.001 |
| 250BF > 250TP                  | 11.4         | Yes          | <0.001 |
| 1000BF > 1000TP                | 5.7          | Yes          | 0.001  |

In both cases, recovery was best (i.e., concentrations were highest) with the bottom-fill method, and recovery was approximately 6 to 14% greater than with either the side-pour method or the top-pour method at all three fill rates. When the side-pour and top-pour methods were compared, there was no significant difference between the two methods at the two faster flow rates but there was at the slowest fill rate.

The rankings for the fill methods for each of the flow rates are summarized here:

50BF > 50SP > 50TP

250BF > 250SP ~ 250TP

1000BF > 1000 SP ~ 1000TP

These results are contrary to guidance documents that recommend a side-pour method. Also, contrary to conventional practice, this study shows that the side-pour method is no better than simply pouring straight down into the vial from the top, except when a very low fill rate is used.

### 5.1.3.2 Fill Rate

There were significant differences in the recoveries of the VOCs between the fastest and slowest fill rates for all three fill methods (Table 8). In all cases, recovery was greater (i.e., concentrations were higher) with the *faster* flow rate, and the differences in recovery ranged from ~6 to 14% for the three fill methods. When the 250-mL/min and 1-L/min flow rates were compared, there was a significant difference in the recoveries for the side-pour method and for the top-pour method, with recovery 7 to 8% greater for the faster flow rate. In contrast, when the recovery of the higher two flow rates was compared for the bottom-fill method, the percent difference in recovery was only 1.6% and this difference was not statistically significant. When the two lower flow rates were compared, there was no significant difference in the recovery for

the bottom-fill method or for the side-pour method but there was for the top-pour method. For the top-pour method, recovery was 7% greater at 250 mL/min than at 50 mL/min.

**Table 8. Summary of the statistical analyses comparing the different fill rates.**

| Fill Rate                 | % Difference | Significant? | P=     |
|---------------------------|--------------|--------------|--------|
| <b>50 vs.250 mL/min</b>   |              |              |        |
| 50BF ~ 250BF              | 4.9          | No           | 0.04   |
| 50SP ~ 250SP              | 2.2          | No           | 0.404  |
| 50TP < 250TP              | 7.1          | Yes          | 0.006  |
| <b>250 vs.1000 mL/min</b> |              |              |        |
| 250BF ~ 1000BF            | 1.6          | No           | 0.499  |
| 250SP < 1000SP            | 8.2          | Yes          | 0.002  |
| 250TP < 1000TP            | 7.3          | Yes          | 0.006  |
| <b>50 vs. 1000 mL/min</b> |              |              |        |
| 50BF < 1000BF             | 6.5          | Yes          | 0.007  |
| 50SP < 1000SP             | 6            | Yes          | 0.023  |
| 50TP < 1000TP             | 14.6         | Yes          | <0.001 |

The rankings for the recoveries for each of the pour methods at each of the flow rates are summarized below.

1000 BF ~ 250 BF; 250BF ~ 50BF; **1000BF > 50BF**

1000SP > 250SP ~ 50SP

1000TP > 250TP > 50TP

These results are contrary to conventional wisdom and guidance that recommends using slower fill rates (e.g., 100 mL/min or less) to reduce turbulence (USEPA 2002, ASTM 2002). Also, contrary to conventional wisdom, turbulence due to fast vial filling did not appear to be a factor in VOC losses as vigorous mixing was evident.

Sampling order with respect to the fill rate used was not randomized in the test (i.e., the bottles were filled first at 50-mL/min, then at ~ 250-mL/min, and finally at ~1-L/min), therefore it is possible that this affected the recovery of the analytes in some fashion. However, sampling just a few liters from a fixed position in a 55 gallon drum, a mechanism for time variation of concentration during sampling is not evident, but can't be completely ruled out. Parker and Britt (2012) contains additional details and explanation of these results and concerns.

### 5.1.3.3 Variability

There was also variability in the data for the different fill methods and flow rates. This information is summarized in Table 9, which gives the pooled Percent Relative Standard Deviation for each of the sampling methods and flow rates. The variability was generally less at

the lower fill rate. This is especially true for the side-pour and top-pour methods. Overall, the bottom-fill method had the least variability. In contrast, variability was greatest when the side-pour method was used, especially at the two higher flow rates. This finding also suggests the Bottom Fill method is an improvement over standard side pour approach.

**Table 9. Pooled %RSD values for each fill method and flow rate.**

| Flow rate  | Pooled Percent Relative Standard Deviation |      |      |
|------------|--|------|------|
|            | BF   | SP   | TP   |
| 1 L/min    | 2.14                                       | 10.4 | 6.3  |
| 250 mL/min | 4.94                                       | 10.5 | 5.04 |
| 50 mL/min  | 3.23                                       | 4.43 | 2.05 |

#### 5.1.3.4 Discussion

Contrary to conventional thought, the results of this analysis suggest that *faster* fill rates generally yield higher VOC recoveries. Also contrary to conventional thought on the subject, pouring down the side of the sample container is not substantially better than simply pouring down from the top of the vial with sample in free fall. Clearly the best pour method at the lower fill rates was the bottom fill approach. At high fill rates the fill method was less important, apparently because the sample vial was filled in just a few seconds and exposure was minimized. The results of this test strongly suggest that “turbulence” of the sample water was not a driver for VOC loss, but rather *time* of exposure and *surface area* of exposure drive VOC loss. Slow bottle fill rates such as 50ml per minute and pouring down the side of the vial or from the top yielded the lowest VOC recoveries. Bottom filling at low flow rate significant improved recovery. Bottom filling at the 250ml flow rate also significantly improved recovery over top pour and side pour methods. Based on these results, the bottom fill approach should normally be advised at low to moderate fill rates, and higher fill rates should be employed when possible and within reason. Physical constraints exist for VOA vial filling that may make rates approaching and above 1000ml/min more difficult. However, our testing showed that fill rates up to 1000ml/min using the bottom fill approach were achievable. The key point being that reduction of flow rate to accommodate vial filling is not needed at rates where the practicality of vial filling is not problematic (i.e. there is no reason to reduce flow from 250ml/minute to 50 or 100ml/min to collect samples).

**5.2 Analytical and Numerical Models of Monitoring Well Pumping**

Many of the purging curves in the field tests showed deviations similar to those predicted by the analytical models of Martin-Hayden (2000a). Those analytical models were based on several simplifying assumptions including, inviscid flow, predominantly vertical flow within the well bore, and pumps positioned at either end of the screen. In order to account for the effects of viscosity, radial flow and variable pump positions, more complex analytical and numerical models were derived for this project. Analytical and numerical models were developed to account for Poiseuille (viscous pipe) flow and investigate the influences of viscosity on flow paths, travel time and concentration distributions.

The models indicate that groundwater entering along the well screen during pumping (Figure 28a) will accumulate and velocities will accelerate as the well water approaches the pump intake (Figure 28c). The flow paths and travel times that result from this velocity distribution are used to calculate (1) the advective front of groundwater entering the well screen as a function of time, (2) the time it takes groundwater to travel from the screen to the pump intake, (3) the zone captured by the pump intake giving the position of origin of the water entering the pump intake, and (4) pumping curves giving the fraction of pumped water that is initial well water as pumping

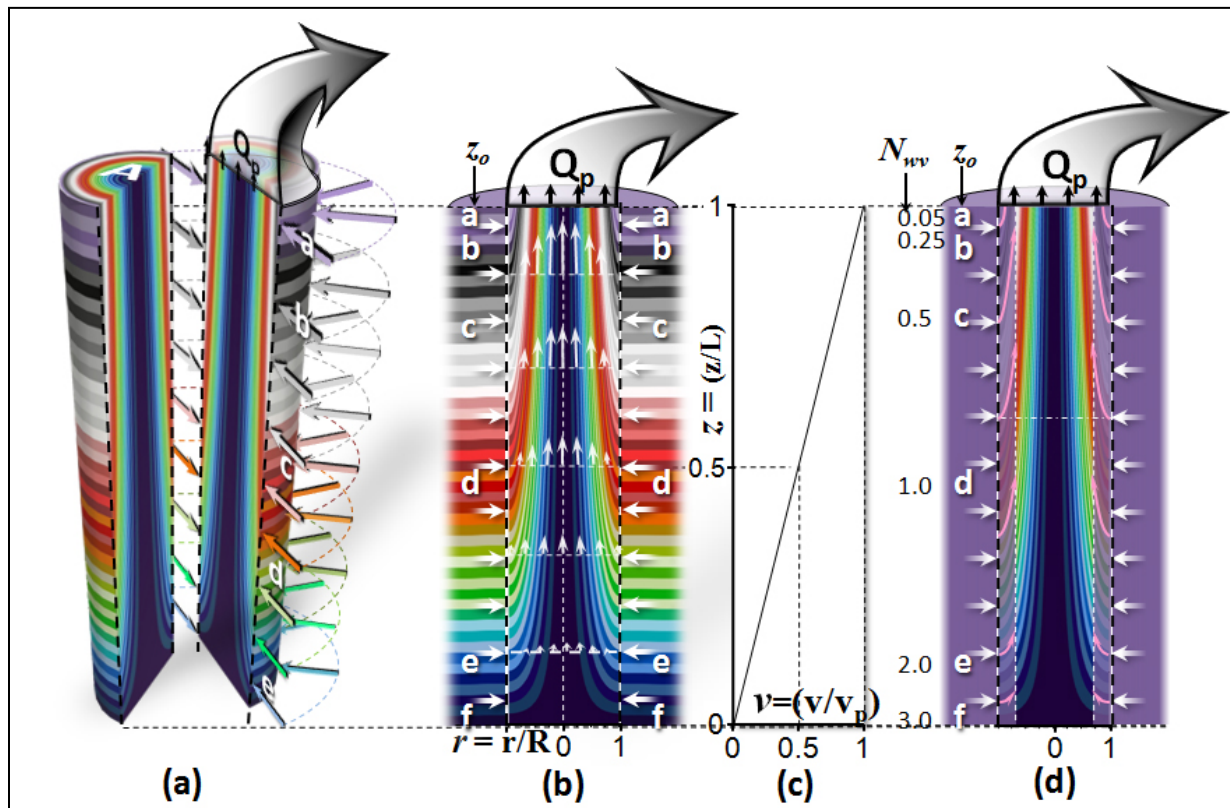


Figure 28. (a) Groundwater entering along screen, (b) Parabolic “Poiseuille” velocity distribution and stream lines, (c) Accelerating velocities approaching pump intake, (d) advancing advective front or annulus of groundwater (in violet)

proceeds. Here the volume of well water is considered the volume of water within the screen section of the well ( $V_w$ ) that is being displaced by inflowing groundwater and volume pumped ( $V_p$ ) is calculated relative to that volume, i.e.,  $N_{wv}=V_p/V_w$ .

(1) The advective front is essentially an annulus of in-flowing groundwater that is displacing pre-pumping well water of radius  $r$  (shown on Fig. 17d by the fine white dashed lines and violet zone) that advances at a rate of  $r=[(1-\tanh(N_{wv}))]^{-1/2}$ . Because the advective front is independent of the volume pumped, the remaining well water is a cylinder of uniform radius  $r$ . This characteristic of well water displacement during pumping is also demonstrated by physical and numerical models of monitoring well pumping (shown as the warm colors on Figure 29a and 29b). Here the well is pumped at the bottom and the annulus of groundwater shown as blue is replacing the cylinder of well water shown as red. Mixing is indicated by the diffuse zone between the well water and groundwater.

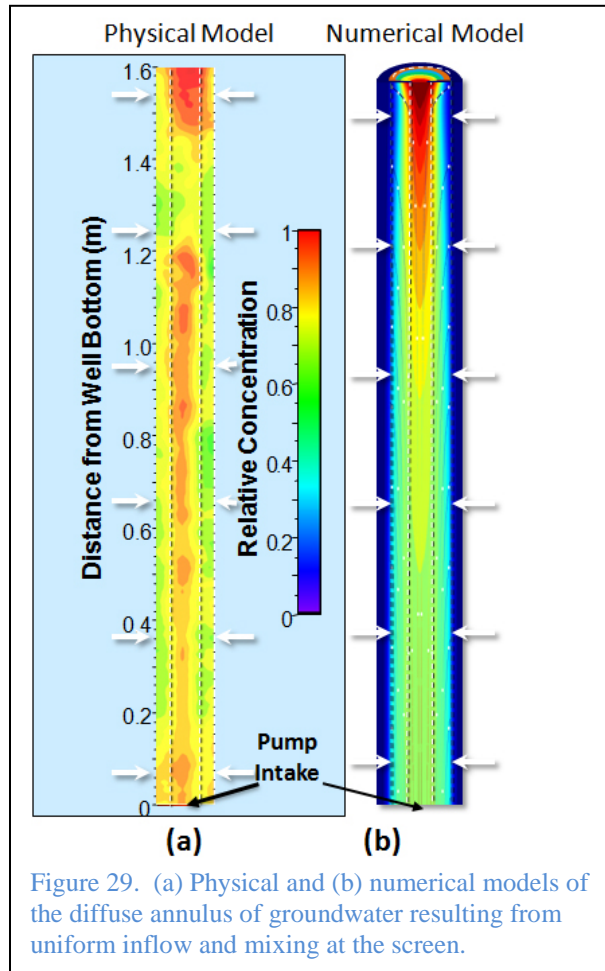


Figure 29. (a) Physical and (b) numerical models of the diffuse annulus of groundwater resulting from uniform inflow and mixing at the screen.

(2) The travel-time between a point along the screen and the pump intake is given by  $N_{wv}=\cosh^{-1}(z_0^{-1/2})$  where  $z_1$  is the entry position (e.g., labels a through f on Figure 28). Groundwater entering at position b along the screen will reach the pump intake after one quarter of a well volume is pumped ( $N_{wv}=0.25$ ) whereas groundwater entering at point d will arrive at  $N_{wv}=1$ .

(3) The travel time function is also used to calculate how the zone of groundwater and well water captured by the pump intake propagates down the well, i.e.,  $z=\text{sech}^2(N_{wv})$ . For example, if half of a well volume is pumped

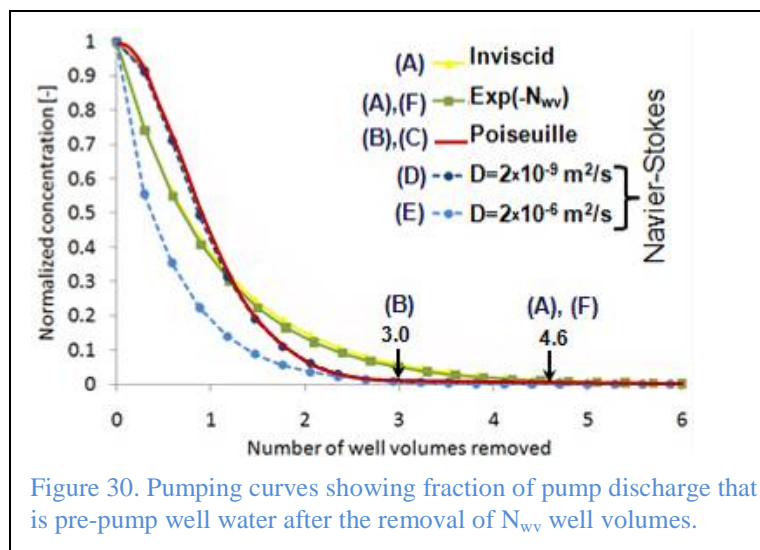


Figure 30. Pumping curves showing fraction of pump discharge that is pre-pump well water after the removal of  $N_{wv}$  well volumes.

the groundwater and well water are originated from the level that corresponds to (b). If the well water and/or the groundwater are heterogeneous, concentrations arriving at the pump intake will fluctuate as a function of this travel time (e.g., see the discussion related to Figure 30).

- (4) The volume of pre-pumping well water remaining,  $V_r$  (relative to the initial volume of well water  $V_w$ ) after a certain volume of water,  $N_{wv}$ , is pumped equals the relative contribution of well water at the pump intake. Fig. M3 shows various theoretical curves of pre-pumping well water remaining as a function of volume pumped  $N_{wv}$ . The curve labeled “(F) Exp(- $N_{wv}$ )” is calculated under the unrealistic assumption of inviscid (a.k.a., Darcian) flow within the well. This corresponds to the numerical model of inviscid flow shown as the curve labeled “(A) Inviscid” and, interestingly, purging a well with thorough mixing. Because a well is an open column of water rather than a porous (Darcian) medium, the velocity distribution has been demonstrated to be “Poiseuillian” (parabolic in lateral cross section, see

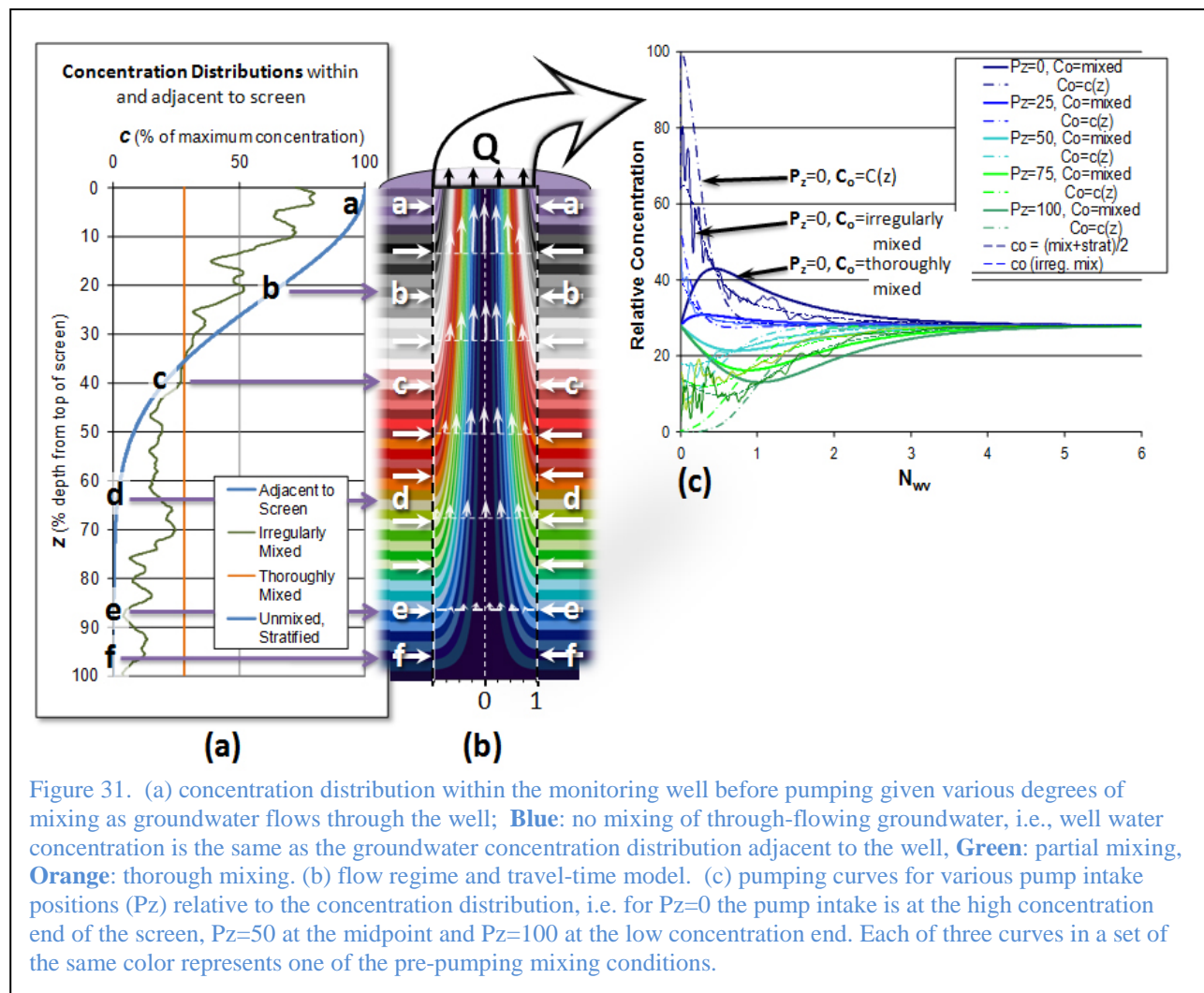
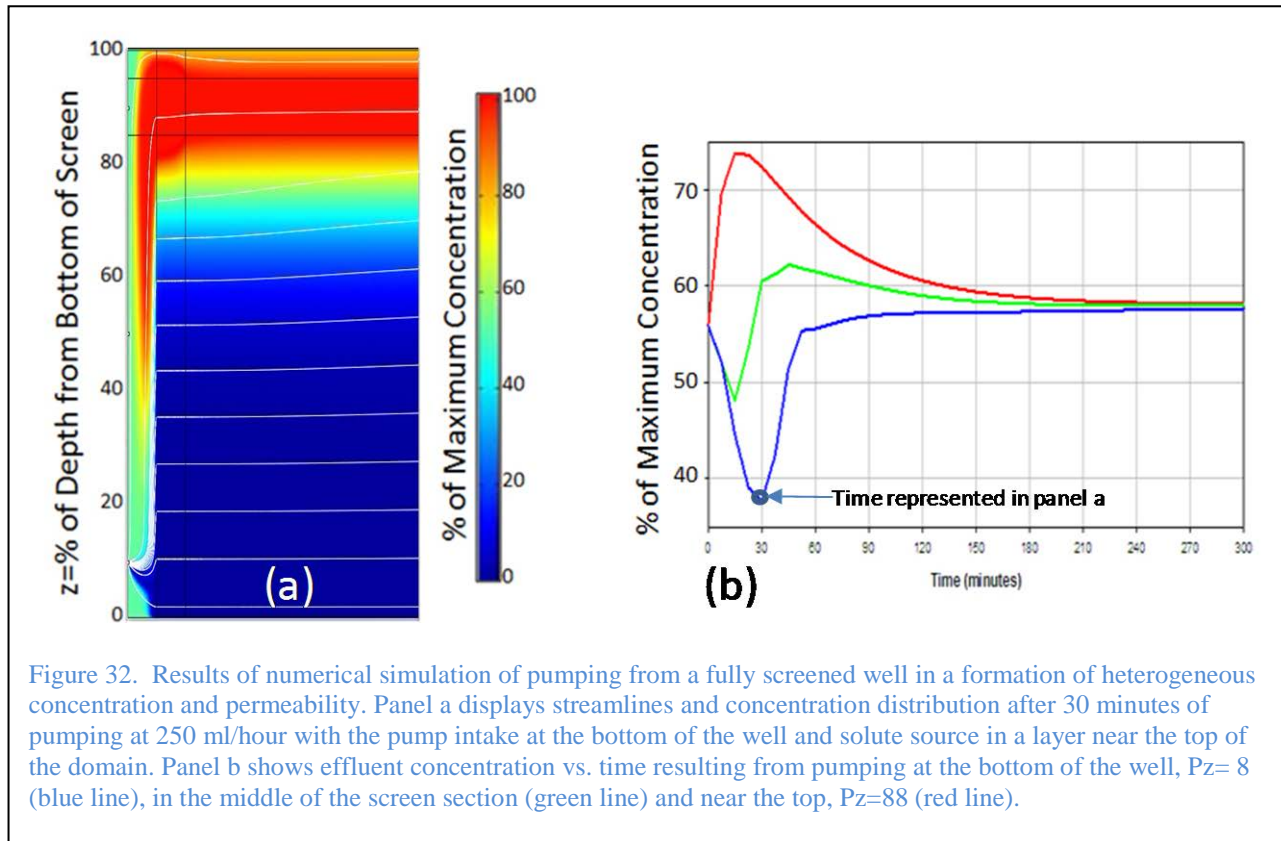


Figure 28b). Including Poiseuille flow in the analytical model gives  $C = \text{sech}^2(N_{wv})$  and the curve labeled “(C) Poiseuille.”

In the presence of a concentration gradient adjacent to the well screen (Figure 31a) the concentrations arriving at the pump intake will vary as a function of volume pumped ( $N_{wv}$ ). In Figure 31a the groundwater concentration is high at the top of the well (blue curve on Figure 31a). If the well water is thoroughly mixed before pumping begins, and the well is then pumped from the top (dark blue solid line,  $Pz=0$ ,  $C_0=\text{mixed}$ ) then the concentrations will rise rapidly early ( $N_{wv}<0.25$ ), appear to stabilize before  $N_{wv}=1$  and gradually approach the average groundwater concentration. If groundwater is flowing horizontally through the well and remains unmixed before pumping begins, the concentration distribution will mimic the groundwater concentration distribution (i.e., stratification). In this case, during early pumping the concentration at the pump intake will be high because both the well water and the approaching groundwater are high (dot-dashed dark blue line at the top of Figure 31c). The concentration will then decrease rapidly as groundwater and well water of lower concentrations arrive at the pump intake. If the well water is partially mixed, the well water concentration will be irregular and the concentrations arriving at the pump intake will fluctuate between the unmixed and thoroughly mixed condition (the irregular dark blue line on Figure 31c). These three degrees of mixing are simulated for each level of pump intake down to  $Pz=100$  (the dark green curves on Figure 31 representing pumping from the bottom of the well).

Effluent concentration during pumping is also affected by the position of the pump intake relative to contaminant sources in the surrounding formation, and by conductivity variations in the formation. Numerical modeling provides a means of examining how such variations affect effluent concentration and the time to reach a flow-weighted average concentration. Figure 32a illustrates a system with a strong variation in formation concentrations, with highest concentrations located in a zone of 10x higher hydraulic conductivity located in the upper part of the column (between dark horizontal lines at  $z=85$  to  $95$ ). The pre-pumping well water concentration is a thoroughly mixed, flow-weighted average of the concentrations adjacent to the well. During pumping from near the bottom of the screen (Figure 32,  $Pz=8$  where the stream lines converge) the concentration starts at the flow-weighted average since the first water to arrive is the thoroughly mixed pre-pumping well water. As with the analytical models (Figure 31c), the concentrations rapidly diverge from the initial concentration during early pumping (Figure 32b), with the direction of change dependent on the intake position relative to the contamination zone. With the pump intake located far from the solute source, effluent concentrations first decrease during pumping, as clean water is drawn rapidly to the intake to replace the initially well-mixed water assumed to exist in the well. Only later, when solutes have had sufficient time to advect from the more distant solute source, does the concentration revert to the flow-weighted average.

This effect is more pronounced in the presence of a hydraulic conductivity heterogeneity. Also similar to the analytical models, the concentration gradually approaches the flow weighted average concentration at late times. Major benefits of numerical models include the ability to include more complex relationships between hydraulic and concentration heterogeneities, the influences transient effects such as solutal and thermal convection, and affects of changing pumping conditions. As further field data is collected on these relationships, further complexities will be included in the numerical modeling to quantify the effects of these processes.



### 5.2.1 Flow distortions during ambient conditions

Groundwater will flow horizontally across the well only if hydraulic gradients are strictly horizontal, and no density-driven mixing occurs. Because the well presents a highly permeable conduit relative to the permeability of the surrounding formation, slight vertical hydraulic gradients will induce vertical wellbore flow. In the example shown in Figure 33 a vertical gradient that is 10% of the horizontal gradient drives a slight upward flow in the formation. When that slight upward flow encounters the highly conductive wellbore the flow lines will be refracted sharply upward (Figure 33 red, yellow and black arrows). The flow lines are shown by bands of different colors with detail at the top and bottom of the screened section where flow is most highly distorted. Inflow is focused on the high-head end of the well, the bottom of the well in this case, and attenuated at the low-head end.

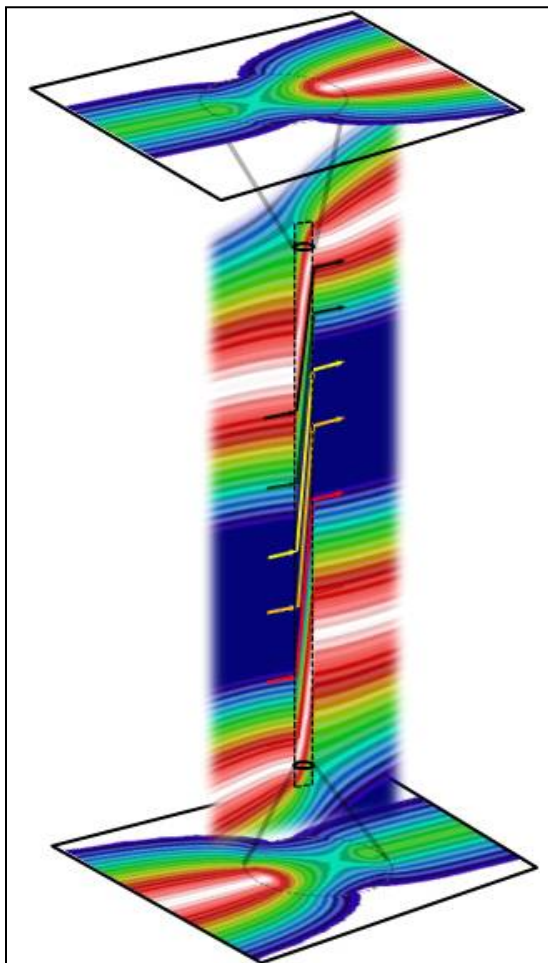


Figure 33. Ambient flow regime surrounding a well and induced vertical flow within the well due to 10% vertical gradient. Color bands represent flow tubes.

The focused flow at the high-head end of the screen will be spread over a longer segment of the screen, whereas, the distributed inflow at the low head end will be focused over a smaller length as the water leaves the well. Because groundwater inflow is focused at the high head end of the screen, flow-weighted average concentrations entering the well will also be weighted toward that end. Within the well this groundwater will be transported vertically and most likely be mixed by the many processes investigated in this study. Consequently the concentrations leaving the well down gradient will be altered and spread over a larger vertical interval, i.e., the shadow zone.

The vertical wellbore flow is proportional to the vertical gradient in the surrounding formation. In the limit, as the vertical component of the gradient exceeds the horizontal component, vertical wellbore flow will become predominantly vertical and inflow will be highly concentrated at the high-head end of the screen. In this case the groundwater will enter the high-head end of the screen and exit the low-head end. The well water will then be representative of the zone surrounding the low-head end and the shadow zone will be emanating from the high-head end.

Because vertical gradients tend to be pronounced in recharge and discharge areas where they tend to vary in time, these vertical wellbore flow effects are expected to be variable in intensity and direction. The velocity of wellbore flow will be several times that of the average linear velocity within the formation due to the focusing of flow. For example, in unconsolidated formations, e.g., silt and sand, where typical hydraulic gradients are on the order of 0.01 m/m, average linear velocities would be between millimeters and centimeters per day. Thus, wellbore flow will be in that range as well, significantly slower than solutal and thermal convection and pumping (even for pumping during low-flow sampling, e.g., 1 L/min). This would suggest that groundwater flowing through a well, regardless of the vertical or horizontal trajectory within the well, would likely mix in most cases.

### 5.3 Physical Modeling

#### 5.3.1 2D and 3D Physical Models

The physical model of monitoring wells and the surrounding environment was constructed to be flexible in terms of horizontal and vertical hydraulic gradients, thermal gradients and visibility (Figure 34). The model is essentially a rectangular tank (length  $x=90\text{cm}$ , width  $y=60\text{cm}$ , height  $z=120\text{cm}$ ) of 1 inch thick, transparent polycarbonate, filled with fine sand, with specified head reservoirs of gravel at each end ( $x=0$  and  $x=90\text{cm}$ ). The hydraulic conductivity of the gravel ( $K_G=1.2\times 10^{-1}\text{ cm/s}$ ) is approximately two orders of magnitude greater than that of the sand ( $K_S=3.8\times 10^{-3}\text{ cm/s}$ ) and acts to vertically distribute the head from the three levels of ports on each reservoir. By adjusting these heads, a vertical gradient is imposed across the model. The slight vertical trajectory of the flow lines shown on Figure 34 would result from a 10% vertical gradient equivalent to those used to produce the flow regime in Figure 33. Adjusting the vertical gradient imposed by the specified head reservoirs allows the investigation of vertical flow within the two well models, *i.e.*, the partially penetrating “Half Well” and the fully penetrating “Full 3D Well” shown in Figure 34.

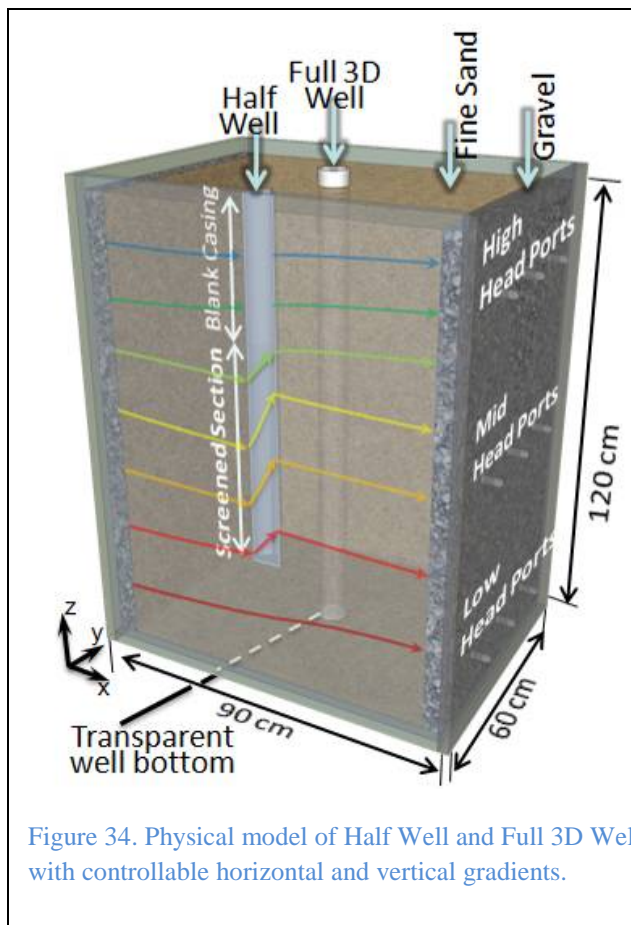


Figure 34. Physical model of Half Well and Full 3D Well with controllable horizontal and vertical gradients.

The Half Well allows the flow and mixing within the well to be directly observed using tracer dyes and recorded with time-lapse photography, *e.g.*, the method used to produce the image in Figure 29a and the images for the 2-D physical models. The image of Figure 29a was produced by equating an RGB color value with a relative concentration value stored as a matrix. This matrix of relative concentrations allows the mixing to be characterized by comparing the results to the numerical models, *e.g.*, the comparison of Figure 29a to 29b. Figure 29a was produced by introducing a uniform distribution of red dye to the wellbore before pumping and taking time-lapse photos as pumping proceeded. As the un-dyed water entered the screen it produced a diffuse annulus of groundwater as predicted by the analytical models and corroborated by the numerical models. The diffuse nature of the annulus indicates that, as shown by the numerical models of dispersive mixing (Figure 29b), there is a small scale partial mixing that occurs

adjacent to the screen that serves to partially mix the inflowing groundwater with the pre-pumping well water.

As mentioned earlier, the transparent face plate presents a no slip boundary to flow within the Half Well. The Full 3D well avoids the artifacts of that no-slip boundary and allows flow to be viewed from above or below (where the screen is sealed to the transparent bottom of the tank). It is more difficult, however, to produce detailed images of flow within the Full 3D Well. Instead, arrays of thermistors (i.e., monitoring temperature) and E.C. probes (i.e., monitoring concentrations of NaCl tracer) were installed within the well. These probes were used to plot the evolution of both temperature and concentration distributions within the well.

The thermistor string consisted of 1.5mm bead type thermistors with a response time in the range of a few seconds in order to monitor rapid changes in water temperature and minimize disturbance to flow. These thermistors were calibrated to track each other within  $0.005^{\circ}\text{C}$  in order to detect the onset of unstable thermal gradients. Figure 35 shows the temperatures

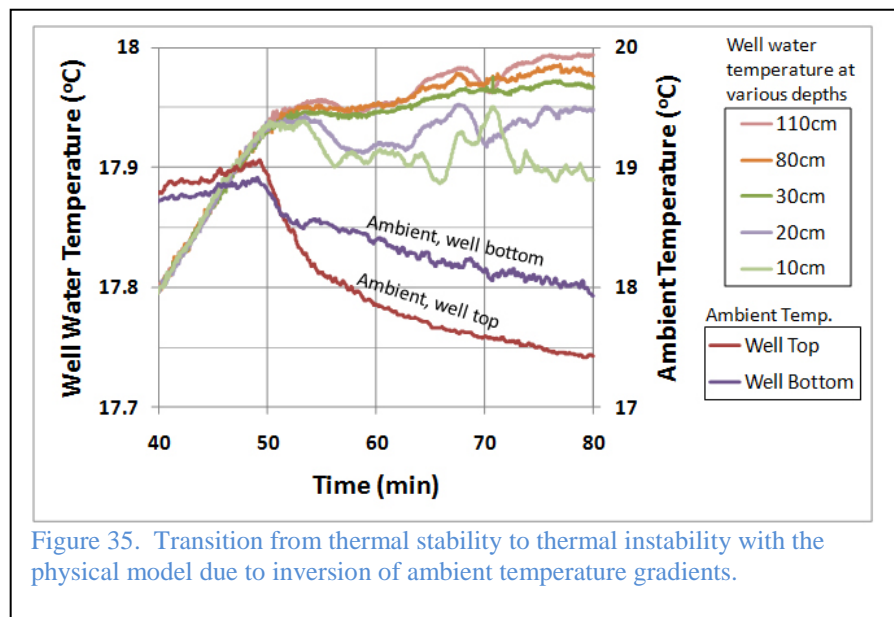


Figure 35. Transition from thermal stability to thermal instability with the physical model due to inversion of ambient temperature gradients.

within the Half Well as a function of depth. Note that the left-side y-axis relates to the wellbore temperatures and the small-scale rapid fluctuations are on the order of  $0.005^{\circ}\text{C}$ . The right-hand y-axis relates to the ambient temperatures of the transparent face plate of the Half Well. At first (before the 50 min. mark) as the ambient temperatures increased, the top of the well was warmer than the bottom, the well water temperatures were uniform and warmed simultaneously. The uniform well-water temperatures indicate a stable thermal regime, i.e., warm less dense water over cooler more dense water ( $\Delta T/\Delta z = +0.10^{\circ}\text{C}/\text{m}$ ).

Once the ambient temperatures reverse, after 51 minutes, the well water thermal gradients become unstable, i.e., cooling upward ( $\Delta T/\Delta z = -0.23^{\circ}\text{C}/\text{m}$ ). Thermal convection is indicated by the divergence of the temperatures and the fluctuation of temperature with time. The thermistor near the bottom of the well shows a periodic fluctuation observe during thermal convection. These indicate small plumes of cool water sinking past the probe from farther up the well. The magnitude and period of these fluctuations are used to estimate the rate of descent, e.g., fluctuations between 55 and 67 seconds are on the order of  $0.011^{\circ}\text{C}$  every 1.3 minutes or 0.0085

$^{\circ}\text{C}/\text{min}$ . Dividing that temperature fluctuation by the thermal gradient ( $\Delta T/\Delta z = -0.23^{\circ}\text{C}/\text{m}$ ) gives the distance that water traveled and the velocity of descent,  $(0.0085^{\circ}\text{C}/\text{min})/(-0.23^{\circ}\text{C}/\text{m})=0.037\text{m}/\text{min}=3.7\text{cm}/\text{min}$ .

When the onset of unstable thermal gradients is more gradual the transition to wellbore convection will be more gradual, however, the temperature differentials and fluctuations still occur and can be used to characterize the thermal convection. This more gradual transition is shown in Figure 36 for a thermistor 20cm from the bottom of the Full 3D Well. The vertical gradients were not recorded here but the transition from gradual

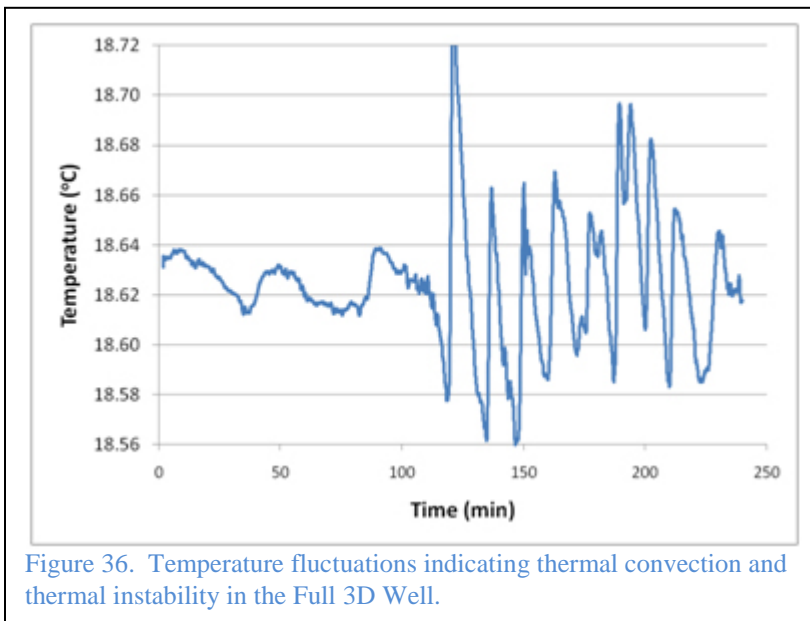


Figure 36. Temperature fluctuations indicating thermal convection and thermal instability in the Full 3D Well.

convection (before 120 min) to more rapid convection is evident. This indicates that the rates and vigor of thermal convection can be characterized in the field with inexpensive, commonly available, single thermistor probes.

The electrical conductance (EC) and relative concentration ( $C_r$ ) of NaCl tracer within the well models is measured using EC probes that consist of two parallel 8mm long stainless steel wires spaced 1mm apart. By applying a 1kHz alternating current (I), to avoid polarization, and measuring the voltage (V) the electrical conductance is calculated as  $EC=I/V$ . With a reference solution of known concentration ( $C_o$ ) and measured electrical conductance ( $EC_o$ ), the relative concentration is calculated as  $C_r=EC/EC_o$ .

The initial conditions of the test depicted by Figure 29a were reproduced in with NaCl tracer. Before pumping, the well was spiked with NaCl tracer and mixed to give a uniform  $C_r = 1.0$  throughout the well.  $C_r$  was then monitored at various levels during pumping (at 1.2 L/min) to give the change in concentration with volume pumped ( $N_{wv}$  on Figure 37) The concentration farthest from the pump intake (the top of the well) showed the slowest decrease in concentration corresponding to the zone of slow moving groundwater in the analytical and numerical models (Figure 29b). The probe at the bottom of the well (Figure 37, light green curve) most closely matched the concentrations entering the pump intake (Figure 37, dark blue curve). The pumped concentrations are somewhat lower than the dashed curve which indicates the theoretical concentrations assuming inviscid flow (Figure 30, curve A). The effect of dispersive mixing (due to small scale eddy, thermal and solutal mixing) is to cause the pre-pumping well water to

be removed more rapidly as shown by the numerical model of a pumped well (Figure 30, curve E). The rapidly decreasing concentration at the pump (Figure 37, dark blue curve) suggests that some degree of dispersive mixing is influencing the removal of well water at least early in pumping ( $N_{wv} < 2$ ).

The physical modeling suggests that natural gradient flow through (horizontal and vertical) is on the order of

millimeters to centimeters per day, while thermal convection during unstable conditions causes movement at rates on the order of centimeters to meters per hour and velocities due to low-flow pumping are on the order of centimeters per minute. Thus, *in-well transport via free convection is generally significant only in the absence of pumping or other mechanisms that force convection*. Our numerical simulations examining in-well transport behavior therefore included thermal and solutal convection effects in studies of natural gradient groundwater flow, but neglected those effects in examination of in-well transport under pumping scenarios.

### 5.3.2 Fracture Borehole Model

The physical model of a borehole within fractured rock was designed to investigate the interactions between fracture flow and borehole flow under controlled conditions. Imaging the dye passing from the fracture into the borehole allowed visualization of the mixing as the water entered the borehole and observation of mixing within the borehole (Figure 38). The zone down gradient of the borehole represented the shadow zone indicating the influence of borehole mixing on the groundwater in the fracture. The lower constant-head reservoir of the angled fracture was held at a head that was 0.24cm higher than the head of the upper constant head reservoir. This head drop resulted in a hydraulic gradient of 0.00814, a volumetric flow rate of 6.00cm<sup>3</sup>/min and an average linear velocity of 5.00cm/min toward the upper constant head reservoir. The flow field around the borehole was traced with Rhodamine dye introduced as a uniform constant source in the high head reservoir as shown at the bottom of Figure 38(a). The flow field delineated in Figure 38(a) shows convergent flow up-flow of the borehole and divergent flow down-flow of the borehole as shown in the top of Figure 38(a).

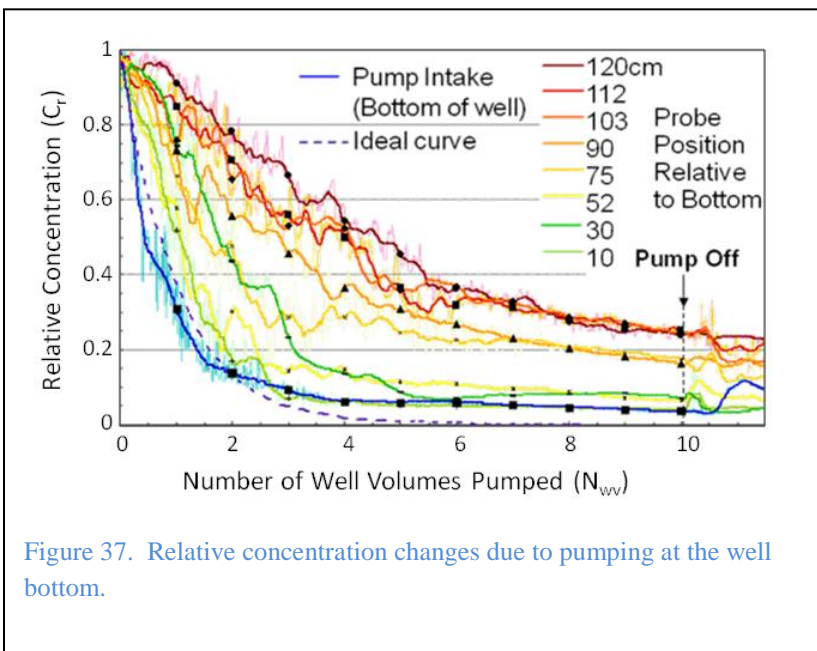


Figure 37. Relative concentration changes due to pumping at the well bottom.

The dye was carried into the borehole where it mixed with the borehole water and was carried out the down-flow side of the borehole. In this case the dye was approximately 0.01% more dense than the borehole water and mixed by convection (Figure 38(b) below angled fracture). At room temperature a 0.01% increase in density would be equivalent to a 0.5°C decrease in temperature. Since the temperature was not controlled in this experiment some of the dyed water in the fracture was

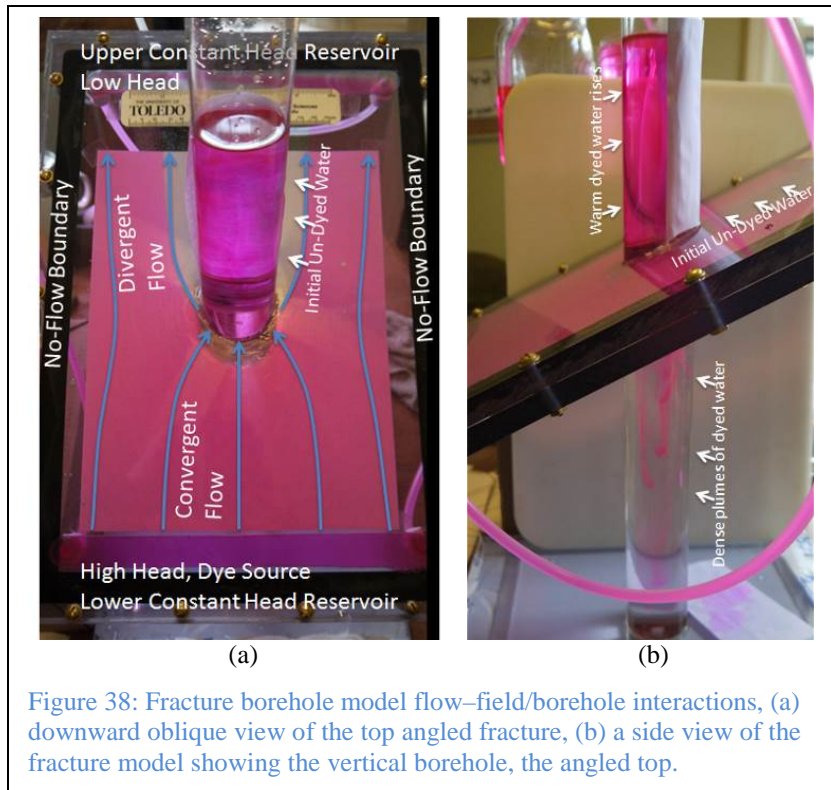


Figure 38: Fracture borehole model flow-field/borehole interactions, (a) downward oblique view of the top angled fracture, (b) a side view of the fracture model showing the vertical borehole, the angled top.

warmed enough to reduce the density below that of the borehole water and rose to the top portion of the borehole (Figure 38(b) above angled fracture). Because the dyed water mixed with the undyed borehole water and was diluted, a zone of low concentration extended down-flow of the borehole producing a “shadow zone” of borehole water as shown by the dilute water at the top of Figure 38(a).

For the next series of experiments the concentration of dye was reduced by a factor of 10 giving a density contrast of about 0.001%. This reduced density contrast reduced the sinking velocity and resulted in some of the fracture water being carried directly across the borehole before mixing with the borehole water. Because the sinking velocity in this experiment was on the order of millimeters per minute and the time water takes to traverse was less than a minute, some of the fracture water was carried across the left ¼ of the borehole as shown in Figure 39. This indicates that the degree and distribution of mixing between fracture water and borehole water depends on the balance between fracture flow velocity and density contrast. In this

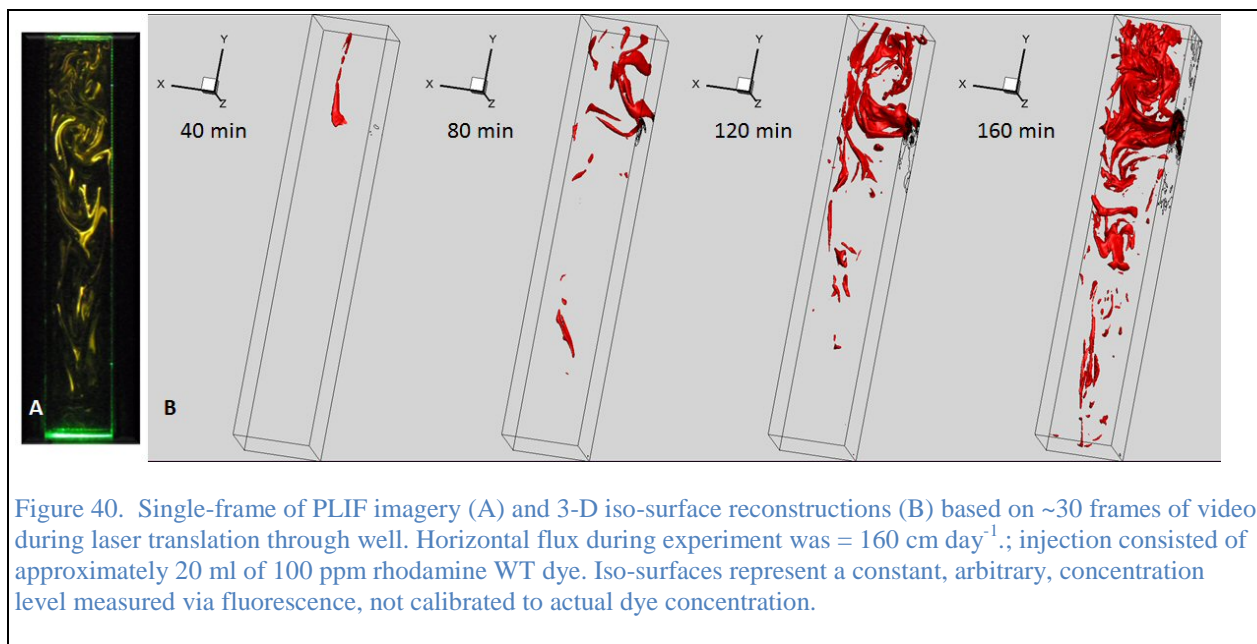


Figure 39. Lower density contrast borehole flow experiment.

case the fracture water entering the side of the borehole was carried across and exited to the fracture while the water in the center of the borehole partially mixed with the borehole water. This series of experiments indicate that fracture flow into the borehole and mixing within the borehole may result in heterogeneous concentration distributions along the borehole and a shadow zone of altered water up-gradient of the borehole.

### 5.3.3 Planar-laser-induced fluorescence (PLIF) tomographic imaging

The PLIF tomography system developed successfully demonstrated the ability to record dye movement in a pseudo 2D model well into 3D data describing concentration changes over time (Figure 40). The 2D and 3D imagery developed from that effort clearly illustrated the 3D nature of the dye transport within the well, including the initial entry point, and the increasing complexity of the dye plumes over time. However, while the imaging effort allowed development of a novel interrogation method, and a dataset that helped to illustrate the complexity of in-well flow behavior, we concluded that simpler non-physical analysis methods provided more efficient means of testing hypotheses about in-well mixing.



## 5.4 Physical and Numerical Modeling

### 5.4.1 Non-Thermal Density Driven Flow

A Rayleigh number analysis strongly suggests that natural convection should occur in the open water section of Britt's (2005) apparatus given sufficient density (including temperature) contrast. To examine free convection in that system, in which horizontal flow should act to attenuate the vertical extent of natural convective transport, we simulated flow and transport in the domain depicted schematically in Figure 41.

The 2D domain essentially reproduces Britt's experiment in dimensions, hydrostratigraphy, injection behavior and fluid flow rates. Fluid flow was controlled at the left and right boundaries of the domain, with a specified horizontal flux of  $6E-7$  m/s (5.2 cm/day) at the left-hand domain boundary and an arbitrary specified head at the right-hand boundary. The porosity of the porous media is universally defined as 30%, so that the

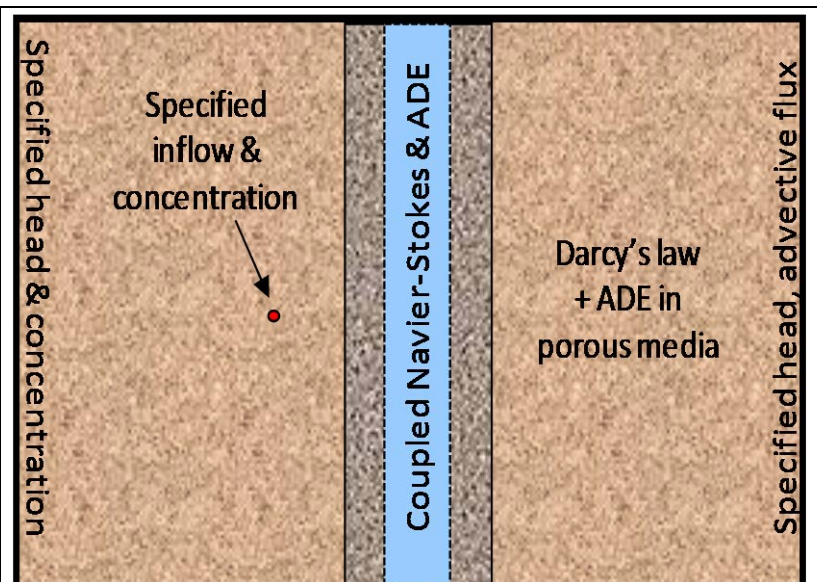


Figure 41. Schematic of the finite element model used to simulate Britt's (2005) experiment that displayed strong vertical mixing with relative density gradients less than  $1E-5$ .

seepage velocity in the Darcy's law domains of the model closely matches that described by Britt (2005). Boundary conditions for solute transport included a specified zero-concentration boundary on the left-hand side and an advective flux boundary on the right. A source point term was defined 15 cm upstream of the well, centered vertically within the domain, with tracer as in Britt's experiment – a solution injection rate equal to  $1/3$  the total inflow rate of the upstream boundary. A permeability of  $9.1E-11$  m<sup>2</sup> was specified for the aquifer and the permeability of the sand pack adjacent to the well was  $9.1E-10$  m<sup>2</sup>. With the configuration described, isopotentials diverge near the injection point but are essentially parallel when they reach the well (Figure 42). Only minor deflection of the flow lines occurs in the well section of the model.

In the initial simulation, the density of the injected solute was set to match that of the background solution and in that case the density behaves as one might intuitively expect, being transported across the well with only minor dispersive behavior due primarily to molecular diffusion (Figure 43a). The effect of solute plume density on transport through the well was then examined by repeatedly running the simulation with increasingly higher injection density. Natural convection

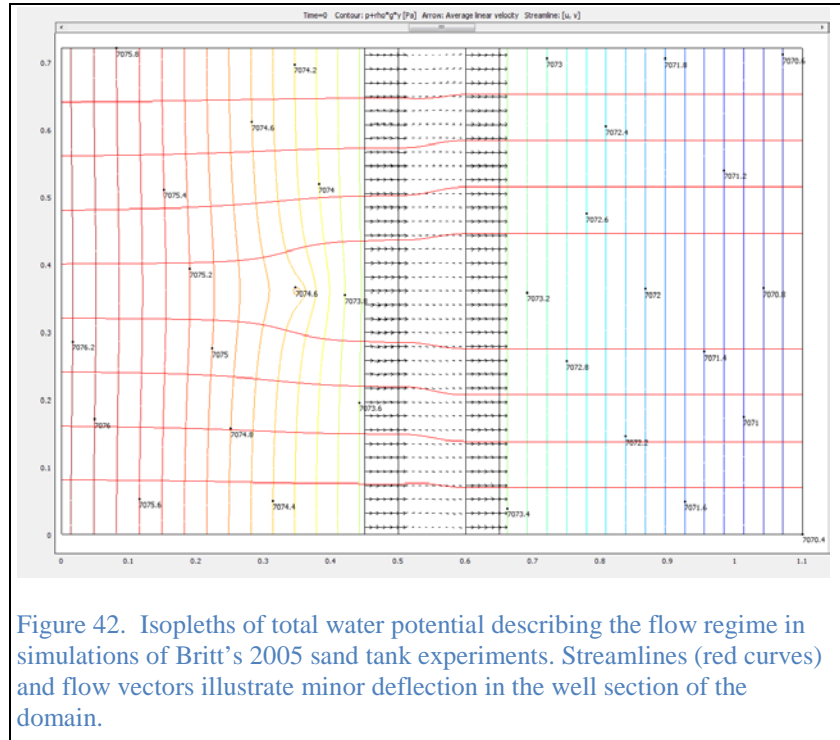


Figure 42. Isopleths of total water potential describing the flow regime in simulations of Britt's 2005 sand tank experiments. Streamlines (red curves) and flow vectors illustrate minor deflection in the well section of the domain.

began at an approximate relative density increase of  $1E-8$ . At that point, the competition between natural convection and forced convection creates extensive mixing in the well (Figure 43b), but only in the downward direction, consistent with the net buoyant force on the solution. The density driven flow evidences the characteristic finger-like projections of Rayleigh Taylor instabilities (Bird et al. 1960), with mushroom-like caps at the distal end of the downward directed plume. Lower density water entering below the solute plume also forms finger-like projections that rise upward through the solute plume, until reaching the level of clean water entering above the solute plume. The competition between the descending plume and lower density water rising through it forces the projections of each movement to change position with time, forming a sort of wagging tail in which the translation is proportional to the density contrast of the entering fluids.

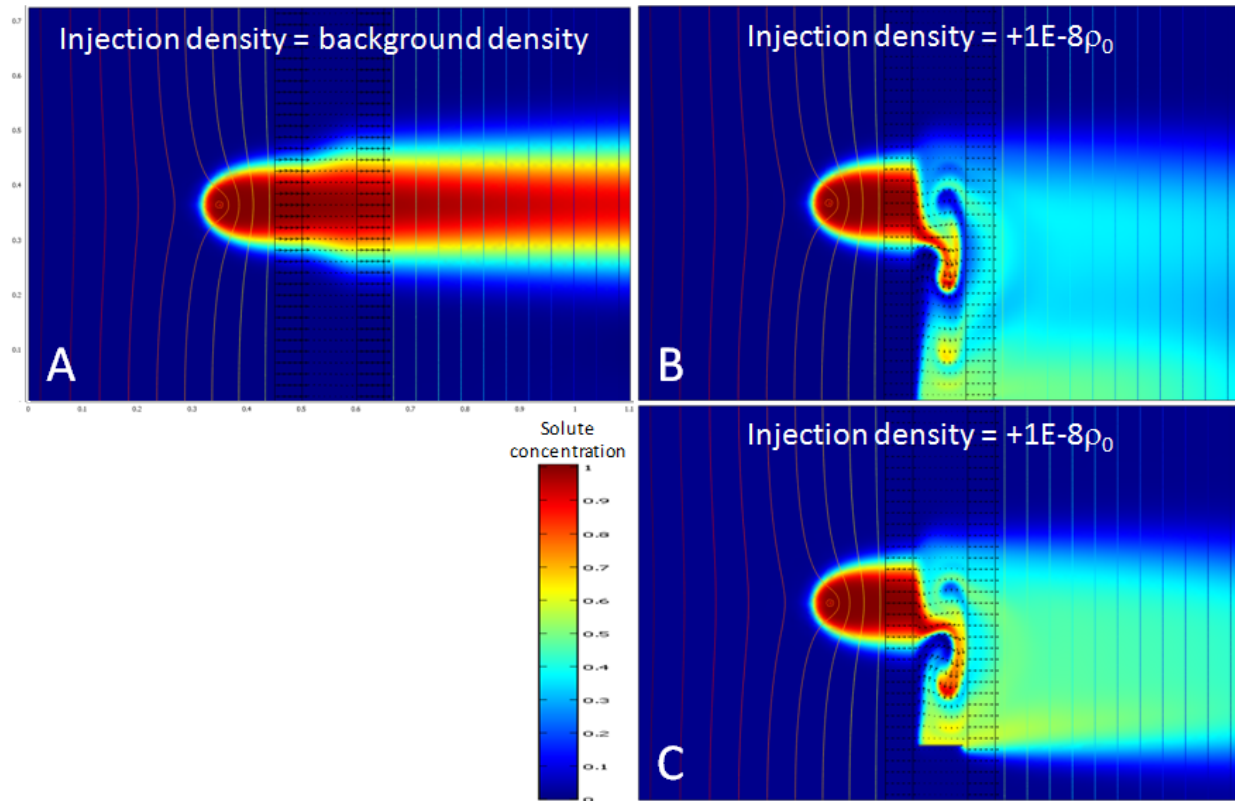


Figure 43. Simulated solute transport in a numerical replication of Britt's 2005 experiment with (A) no increase in solution density and (B) a +1E-8 increase in solution density relative to background density. Panel C illustrates the effect of adding, to the simulation shown in panel B, a partial barrier (80% of well width) in the well section of the domain. Velocity vectors (black arrows) are shown in well and sand-pack domains. Contours are total water potential.

As indicated previously, the slight increase in density producing the observed solutal convection reflects a solute density contrast of only  $\sim 10 \mu\text{g/L}$ . Consistent with the Rayleigh analysis, the simulation emphasizes that very minor solute concentrations can exert profound effects on vertical distribution of solute in a well. This implies that *in situ* monitoring devices would in many cases measure a local concentration that not reflect either the adjacent formation concentration or a flow-weighted average of well inflow concentrations. This is generally undesirable behavior if one of the goals of using *in situ* monitoring devices is to measure the vertical distribution of the formation or an average of the whole screen section. ProHydro, Inc., manufacturer of the Snap Sampler—an *in situ* sampling device that is activated remotely—has experimented with use of in-well flow inhibitors to attempt to isolate separate sampling devices in an open well screen section (Figure 44). The devices do not give complete hydrologic isolation but can provide increased stratification of concentration measurements from multi-level sampling. Because some of the vertical movement induced by natural convection reflects conservation of momentum, it is possible that even an incomplete barrier within the well could significantly inhibit vertical convection. As a test of this hypothesis, we placed a partial barrier



Figure 44. In well flow inhibitor used by ProHydro, Inc. to limit vertical solute migration in a well.

in the well section domain of our numerical model of Britt's (2005) apparatus. The width of the barrier is 80% of the width of the well section. With this partial barrier in place, the downward convective flow induced by the slightly higher density of the injected solution is largely eliminated at the location of the barrier. While this simulation represents a 2D flow regime, and cannot be considered to accurately represent 3D flow in a well, the simulation suggests that partial barriers may provide an effective means of isolating *in situ* sampling devices under certain conditions.

The simulations thus far presented demonstrate that very slight concentration differences between the injected solution and the background solution can induce significant vertical convection. In Britt's experiment however, the injected dye was observed to migrate rapidly both upward and downward in the well, whether the

injection solution density was slightly higher or lower than background density. In the course of investigating that phenomenon, INL constructed a similar sand tank and conducted several preliminary experiments using a rhodamine WT solution with density approximately 1.0001 x that of the background solution. In each experiment conducted with the tank set up similar to the arrangement of Britt's 2005 experiment, dye entering the well was observed to migrate faster in the vertical than in the horizontal direction, even at horizontal velocities up to 2.5 m/d and with a higher permeability layer arranged in the middle of the tank to attempt to reduce vertical transport within aquifer portions of the tank. A useful effect of the higher velocity experiments was greater separation of



Figure 45. Results of a dye tracer experiment conducted at INL investigating transport to a well of a negatively buoyant injection solution. The upward movement of the dye upon entry into the well is hypothesized to reflect thermal convection due inadvertent warming of the injection solution.

horizontal and vertical movement within the well. In the experiment illustrated in Figure 45, for example, the injected solution clearly rose rapidly upon entering the well and then descended after traversing a distance of approximately half the well diameter (Figure 46).

Subsequent discussions about this phenomenon indicated that nearly identical behavior had been observed in a similar experiment at the University of Toledo. Because in each case, the injected solutions were believed to be negatively buoyant based on solute concentration and density, we hypothesized that inadvertent temperature differential (warming) of the injected solution might be causing thermal convection in the well.

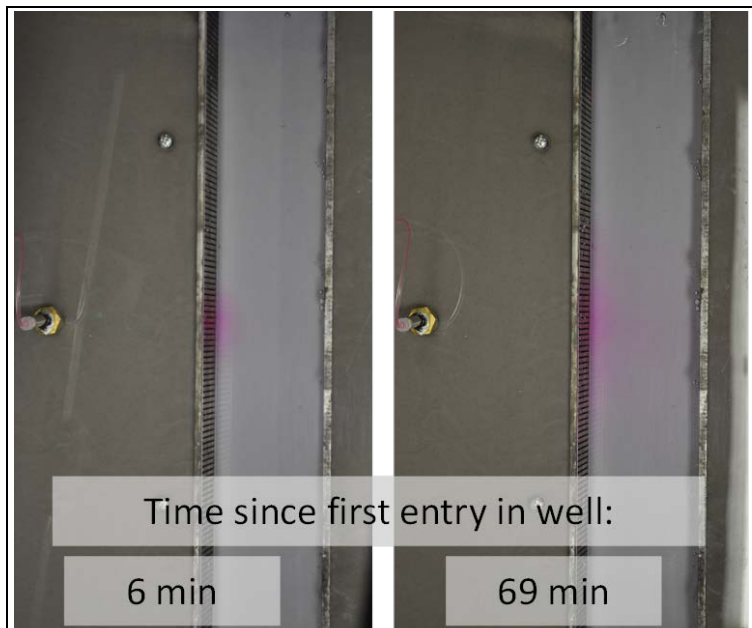


Figure 46. Results of a dye tracer experiment conducted at INL investigating transport from an aquifer to a well with buoyant effects operating in the short dimension of the tank (out of the page in figure). In this experiment, vertical dye transport was notably more diffuse and slower than in comparable experiments with the tank arranged in vertical orientation.

To test the hypothesis that rapid vertical migration of the dye within the well sections of the tank resulted from buoyant effects, we conducted a single similar experiment with the long axis of the well in the horizontal plane. With a horizontal water flux of approximately  $7E-6$  m/s (2 ft/day), the dye entering the tank behaved much more as would be expected for diffusive transport in a laminar flow regime. Unfortunately, increasing water leakage, and air entry, from the upper seals in the assembly limited our ability to continue such experiments.

To examine the potential for the combined effects of thermal and solutal convection in these sand tank experiments we added heat transport to our numerical model of Britt's 2D sand tank experiment. Results of a simulation in which the injected solution was given a constant injection temperature of  $+0.001^{\circ}\text{C}$  and a relative solutal density increase of  $1\text{E-}8$  are shown in Figure 47. Simulated solution behavior in the well section of the model is observed to have many of the characteristics displayed in our preliminary laboratory results (Figure 45). Upon entering the well, the dye immediately rises due to thermal convection and subsequently descends as the injected solution

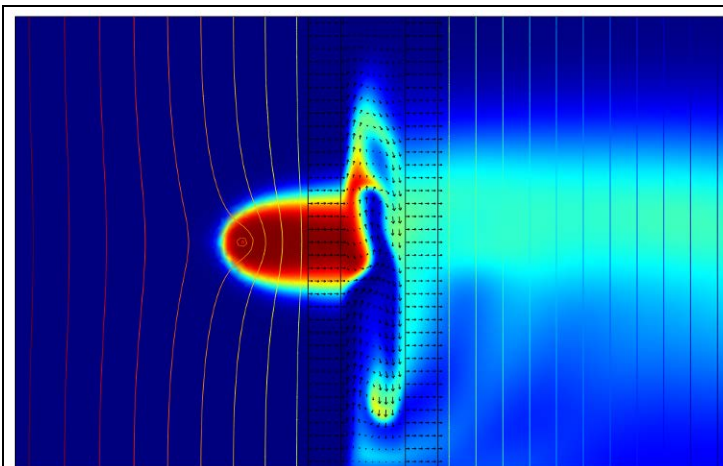


Figure 47. Results of a numerical simulation of Britt's (2005) experiment with a concentration-based relative density increase of  $1\text{E-}8$  and a temperature  $0.001^{\circ}\text{C}$  above background. Velocity vectors (black arrows) are shown in well and sand-pack domains. Contours are total water potential.

mixes with and conducts heat to the surrounding cooler water and in both simulated and observed results the height of that rise decreases over time. The simulation also appears to effectively reproduce the behavior of the injection solution below the entering plume, where the descending plume displays the characteristic fingering of Rayleigh-Taylor instabilities. While the comparison described here is preliminary and qualitative, the magnitude of the thermo-solutal convection effects are consistent with Rayleigh number analysis. We take these results as strong evidence that our simulations effectively capture the combined effects of thermal and solutal convection in these 2D representations of a well. Subsequent simulation studies will attempt to examine these effects in a 3D simulation of a well.

The vertical extent of density-induced mixing clearly depends on the density contrast, the type of convection present (thermal, solutal, or both) and the horizontal flux across the well. The interaction between horizontal flux and vertical convection is difficult to assess without detailed analysis of the flow fields. As an example, Figure 48 illustrates how a doubling of the injection density affects vertical transport in a 2D model similar to that used to reproduce Britt's (2005) experiment but extended in the vertical dimension to examine potential differences in the extent of vertical mixing. With a  $5\text{E-}9$  relative increase in density, the convective mixing effect appears to extend approximately 30 cm below where the plume enters the well. When the relative increase is doubled, to  $1\text{E-}8$ , the vertical extent of mixing is not doubled, but extends approximately another 20 cm below the former case. Doubling the relative density again (Figure 48C), however, causes the vertical mixing effect to extend to the bottom of the well, approximately 30 cm further than in Figure 48B.

In the essentially 2D flow regime of Britt's (2005) sand tank configuration, the effects of the descending solute plume extend to approximately a meter with a relative density difference of  $5E-8$  and a horizontal flow velocity of  $5.2 \text{ cm day}^{-1}$ .

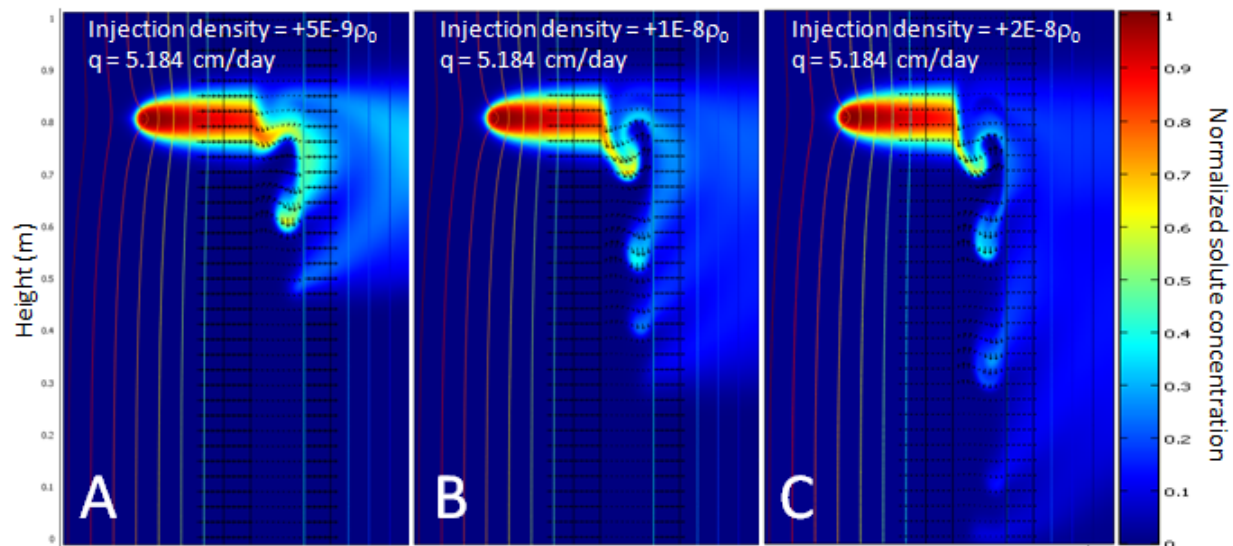


Figure 48. Simulations designed to examine how the vertical extent of convective mixing varies with density contrast. In both simulations the horizontal flux is  $6E-7 \text{ m/s}$  ( $5.2 \text{ cm/day}$ ). In panel A, the injection density is  $5E-9$  above that of the background solution. In panels B and C, the relative density increase is double (B) and quadruple (C) that of A.

#### 5.4.2 Thermal convection in a well

Although numerous studies have examined the critical Rayleigh number for thermal convection in a well (eg. Hales, 1937; Vanaparthi et al., 2003), the stability analysis does not characterize the convective movement, and a description of the magnitude and scale of the convective movement is needed to understand how it might affect concentration distribution in a well. Other studies have examined the convective processes by measuring in-well temperatures (Gretnier, 1967; Diment, 1967; Cermak et al., 2007), but those data provide information about a limited number of scenarios, and likely include other effects that complicate interpretation of the data. The thermal gradients that drive convection close to the critical Rayleigh number are also sufficiently small that the temperature variations that describe the convective movement are difficult to measure accurately. Recently, Berthold and Borner (2008) conducted transient 2D simulations of thermally convective Navier Stokes flow to compare with observations of laser sheet illuminated convection in a tube in the laboratory. Like the above simulations of mixed forced and free convection however, those simulations describe a 2D rectangular flow domain. To examine convective behavior under conditions typical in shallow wells we conducted 2D axisymmetric flow simulations designed to reproduce observations made by Martin-Hayden and Britt (2006) of thermal convection in instrumented unscreened well.

Martin-Hayden installed three strings of high-resolution thermistors in and adjacent to an initially empty 2"-diameter PVC well with a bottom depth of 5.7 meters. One thermistor string monitored the vertical temperature profile just outside the well, another monitored temperature along the inside wall of the well and another monitored temperature along the axis of the well. After filling the tube with water to a depth of 2.2 meters, temperatures were monitored to observe behavior while and following equilibration with the background temperature gradient. Our numerical simulation reproduced that experiment by incorporating a non-flowing (thermal transport by diffusion, no advection) domain around a 2D axisymmetric well section (Figure 49A) in which Navier-Stokes equations are solved. Dimensions, temperatures applied at top and bottom boundaries, and temperature gradient applied at the right-hand boundary of the model ( $\sim 1^\circ\text{C}/\text{m}$ ) were defined to reproduce the field experiment of Martin-Hayden (Martin-Hayden and Britt, 2006). Results of this simulation demonstrate a toroidal convection pattern in the well with two separate cells, with upward convection (Figure 49B) deformation of that gradient close to the well because of the toroidal convection pattern in the well. Colors and arrows in the well show intensity and direction of convection in the well, with a maximum velocity of  $-8\text{ cm}/\text{min}$ . The results reproduce many of the features of Martin-Hayden's experiment, including the apparent number of convection cells, estimated vertical velocity, and the effect of convection on

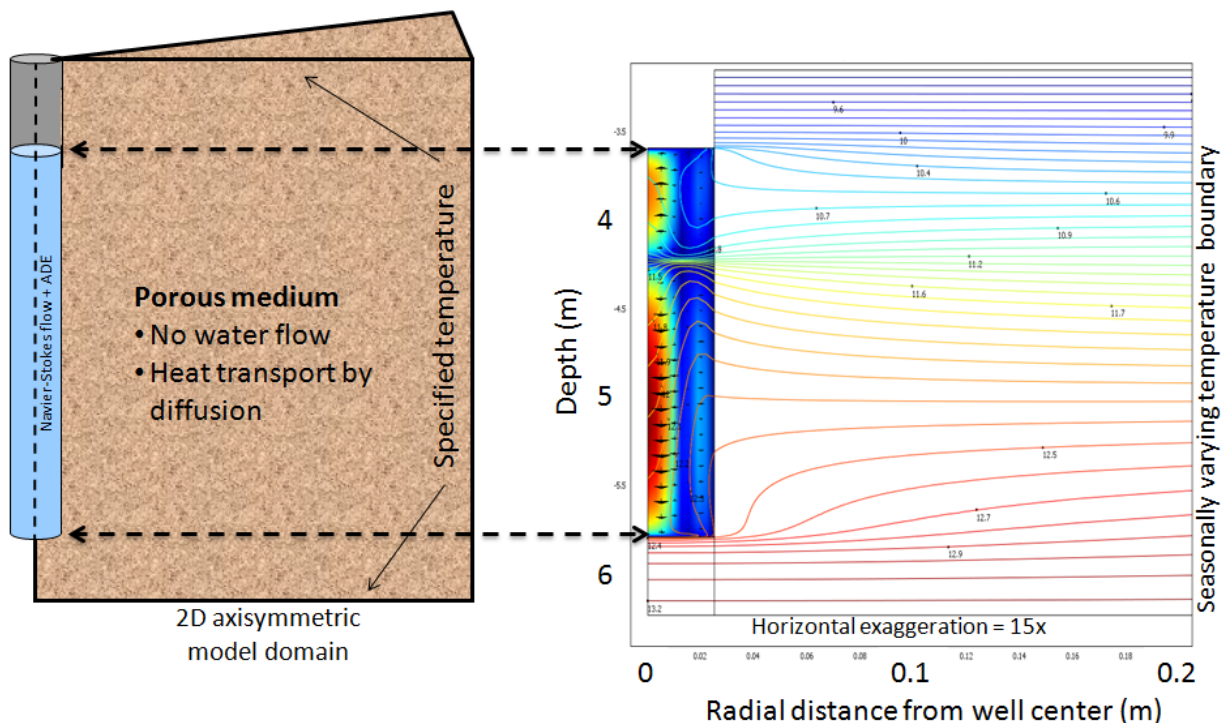


Figure 49. Schematic diagram (A) and results (B) of a 2D axisymmetric model of thermally convective flow in a well in the shallow subsurface. Dimensions, temperatures applied at top and bottom boundaries, and temperature gradient applied at right-hand boundary were designed to reproduce the field experiment of Martin-Hayden and Britt (2006). Isotherms (B) show background gradient of approximately  $1^\circ\text{C}/\text{m}$  and deformation of that gradient close to the well because of the toroidal convection pattern in the well. Colors and arrows in well show intensity and direction of convection in the well.

vertical temperature profiles (Figure 50) in the well. Simulated temperature profiles domain demonstrate crossover between the inner and outer profiles that is similar, though greater, to the crossover observed between the inner and outer thermistor strings. Differences between simulated and observed temperature distribution may be due the representation of thermal conductivity immediately adjacent to the well, as the simulated temperatures adjacent to the well clearly demonstrate stronger connection to in-well temperatures than Martin-Hayden observed.

To our knowledge, this is the first study of thermal convection in a shallow well that combines numerical simulation with precise temperature monitoring at several radial positions in and around the well, and for which simulation results appear to provide a reasonable characterization of the observed convective effects. Additional simulation experiments are currently being performed to examine several related processes, including (1) the rate of vertical mixing induced by thermal gradients with and without solutal convective effects, (2) the likely mechanisms that produce in-well temperature oscillations that are frequently observed in in-well convection

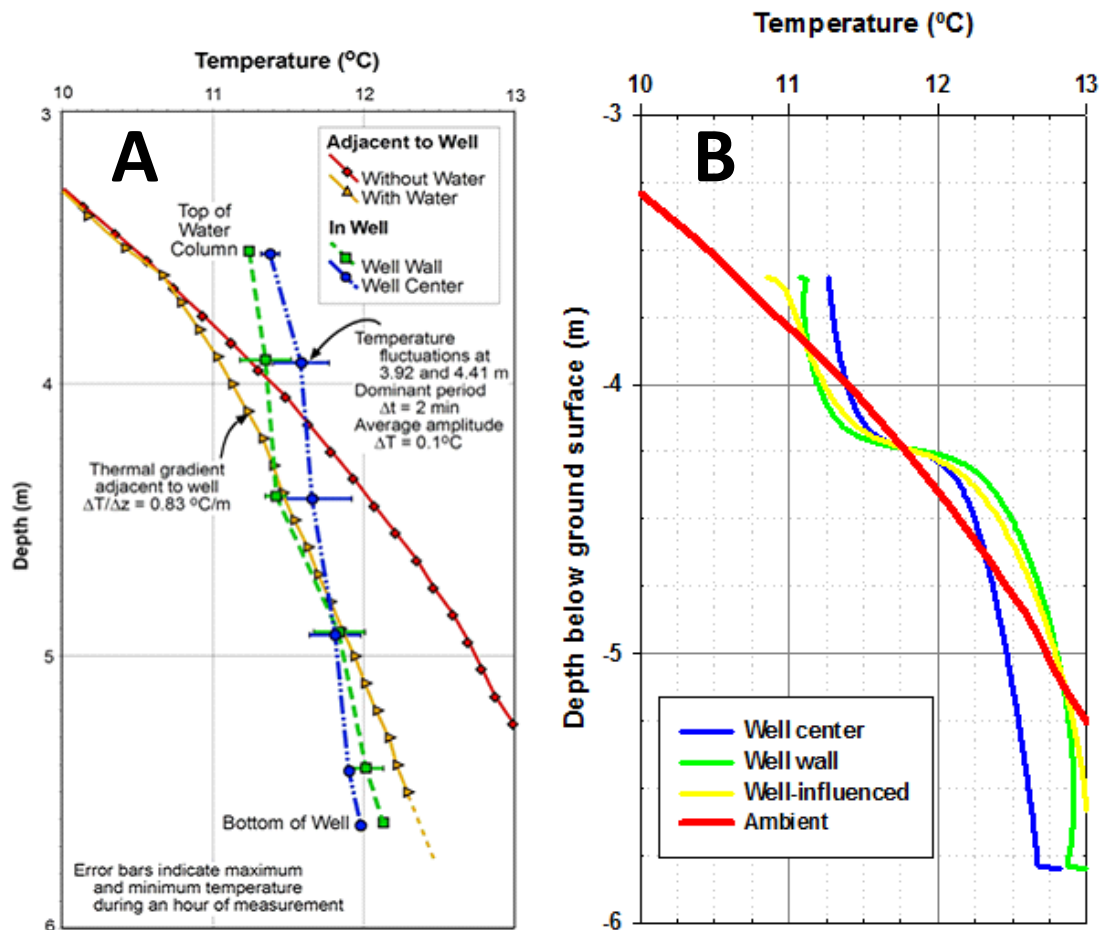


Figure 50. Temperatures measured in a shallow unscreened well (Martin-Hayden 2001) and calculated temperatures (B) in a numerical simulation designed to reproduce that experiment.

studies and (3) convective effects in multilayered formations with varying concentration, permeability and total water potential.

Numerical simulations have thus far been used to investigate the mechanisms causing the counter intuitive in-well solute behavior described by Britt (2005), examine the character of solutal and thermal convection with and without competing forced convection perpendicular to the free convection gradient, and to examine in-well solute concentration during low-flow pumping. In each of these studies, good matches between observed and simulated behavior appears to confirm that solution of the Navier-Stokes equations for in-well flow is critical for accurate representation and prediction of in-well mixing effects under ambient flow and, in some cases, low-flow pumping conditions. Results further demonstrate that solutal and thermal convective effects can produce substantial vertical mixing under ambient flow conditions in a well and that these effects must be considered in well design where non-purge sampling/monitoring methods are employed. Finally, simulations of low-flow pumping in a well are consistent with analytical solutions describing temporal changes in effluent concentration during pumping. Those calculations demonstrate that (1) the volume that must be purged from a well to ensure a flow-weighted average of the surrounding formation concentrations should be based on hydraulic considerations rather than purge parameters that may suggest stability before the proper average concentration is reached and (2) while the necessary purged volume may vary with the degree of in-well mixing induced by irregularities or other perturbations from the ideal well systems considered here, under ideal conditions removal of three well volumes is sufficient to reach the desired flow-weighted average of the concentration distribution outside the well.

## **6.0 Conclusions and Implications**

Physical and numerical modeling efforts were completed to examine the relationship between solute distribution in a well and that in the adjacent formation. Physical mixing processes that occur during ambient flow in aquifers and during active pumping activities were explored to show how potentially stratified contaminants may manifest in open well screens. Complex flow patterns driven by flow velocity changes, very small density contrasts, and temperature contrasts were identified as possible sources of in-well convection and mixing.

These varied drivers for contaminant redistribution work together to alter in-well concentration distributions from that in the adjacent formation. These effects may lead to virtually complete mixing within the well screen. This is not to say that all wells are homogenized with respect to aquifer stratification, but they do reflect some degree of redistribution that is nearly always present. Thus, while stratification can be found in wells, it is unlikely that such stratification is equivalent to that found in the adjacent aquifer. When little or no stratification is found in a monitoring well, it is likely the concentration identified throughout the well represents an aquifer with little stratification in the target interval, a specific interval that is weighted due to hydraulic effects, or an averaging of the screen interval exposed to the aquifer. Rather than a problem, this could be viewed as an advantageous condition where purging wells probably adds no significant benefit for data utility. This investigation did not attempt to quantify how frequent that condition exists, but others have found that it is quite common (ITRC 2007). Therefore, given the variety of drivers toward strong redistributive effects, the default assumption should be that a given well is probably mixed unless shown otherwise. In the case where pumped and passive samples do not reasonably match, detailed investigation may be helpful for determining the cause. However, determining such root cause must be weighed against cost, and may not be worthwhile unless critical decisions are being made on a well-specific basis. There are conditions that can cause concentration dependence on vertical position, including positive vertical temperature gradients, but these conditions are transient and also do not necessarily maintain an aquifer/well concentration elevation parity.

The major conclusions developed from the work include the following:

### **I. Field Setting**

A. Identification of contaminant stratification in the aquifer using longer screen wells (>5 ft) is dependent on multiple factors including contaminant inflow position, sampling method, and degree of zone isolation.

1. Contaminant position in the aquifer relative to the passive sampling device position in the well is usually not known, and understanding of that geometry may not be substantially improved by passive sampling in an open bore.

2. Similarly, aquifer contaminant position relative to the pump intake position is rarely known, but may be discerned with multiple samples collected during purging.
  3. *Isolated* zone sampling can improve determination of aquifer contaminant stratification, using packers or other mixing inhibition devices installed in-between passive samplers.
- B. Representation of the adjacent aquifer through pump sampling is dependent on several factors including contaminant inflow position, volume of the purge, and contaminant of interest.
1. Contaminant position in the aquifer adjacent to the well relative to the pump position drives the speed to which contaminant concentration stability is achieved.
  2. Volume of water removed from the well is a more reliable predictor of contaminant concentration stability than measurement of traditional “purge parameters” such as temperature pH, EC, ORP and DO; however, even large volumes removed do not always assure contaminant concentration stability.
  3. Some contaminants of interest stabilize faster than others, depending on conditions at the individual well, suggesting that contaminant distribution heterogeneity or chemical-specific biological activity can influence the stability of contaminant concentrations during purging.
- C. Sample handling at surface can impart substantial artifacts to measured concentrations:
1. Pouring samples for VOC analysis in the open air results in differential losses dependent on the properties of the chemical of concern.
  2. Conventional thought that pouring sample “smoothly” with little agitation is an important aspect to VOC recovery is largely incorrect—rather, surface area of exposure is the apparent driver of agitation-based losses.
  3. Conventional thought that pouring a sample slowly is an important aspect of VOC recovery is also largely incorrect—rapid bottle filling with short exposure time appears to limit VOC losses.
  4. Pouring and sealing sample quickly (at 250ml/min or greater—10 seconds or less to fill a vial) and filling with the discharge tube submerged (very little surface area exposed) yielded up to a combined nearly 20% higher average

VOC recoveries compared to pouring slowly (50ml/min) and down the side of the container.

## II. Laboratory Experimentation

- A. Physical model experiments confirm previous work by Britt (2005) that small heterogeneities exert strong influence on flow in the open bore of a model well.
1. Horizontal flow of near neutrally buoyant tracer *in porous media*, including both simulated aquifer and filter pack, is confirmed, given a horizontal flow field.
  2. Horizontal flow is not maintained in the open well bore upon tracer incidence into the non-porous media, for all densities tested.
  3. Similar lack of horizontal flow and in-well mixing phenomena were observed in simulated fractured media.
- B. Horizontal laminar flow across the model bore could not be produced (water entering one side of the model well exiting at the same vertical interval with limited mixing).
1. No configuration of velocity or lithologic heterogeneity could reproduce horizontal flow in the open bore.
  2. Density could not be controlled sufficiently to test all possible scenarios—perfect neutral buoyancy was the most difficult to approach, and given that difficulty, we conclude that it is equally or perhaps even more unlikely to occur in natural environments.
- C. Slight vertical hydraulic gradients in a model aquifer apparatus yield flow in the well with similar trajectories predicted by analytical approaches; namely, very small vertical gradients in porous media are amplified by the high hydraulic conductivity of the well bore resulting in substantial vertical redistribution.
1. An upward vertical gradient of 0.005 m/m (10% of the 0.05 m/m horizontal gradient) in the U Toledo tank yielded a vertical redistribution of dye in the well.
  2. The same gradient caused dye to be distributed over an approximately 20-cm vertical distance down-gradient of the model well.
- D. Slight density and/or temperature contrasts are effective causes of tracer redistribution in the aquifer/well models.

1. All tracer density contrasts yielded redistribution in the well models
2. In examples where temperature contrast was also suspected, compound behaviors changing density of the tracer were observed.

### III. Modeling of Field and Laboratory Experiments

- A. A series of numerical modeling experiments were completed in which solute transport is tied to solution of the Navier-Stokes equations in the well and to Darcy's law only outside the well. Good matches between simulation results, experimental data, and theoretical analysis of flow and transport support our hypotheses of homogenization effects.
- B. Numerical modeling experiments confirm our conceptual model of in-well flow and transport behavior that flow is best represented by a Poseuille flow model.
  - i. Simulations of well effluent concentrations during pumping indicate that purging three well volumes effectively brings the well back to a flow-weighted average of concentrations in the surrounding formation.
  - ii. Simulations of well effluent concentrations during pumping, using Darcy's law to describe in-well flow, indicate that approximately five well volumes would be required to reach the desired flow-weighted average.
- C. Numerical modeling experiments demonstrate that very slight density differences in an open well, due to solutal or thermal effects, can induce significant vertical convection and, therefore, much greater vertical mixing than would otherwise be anticipated.
  - i. Density contrasts equivalent to as little as 10 parts per billion of dissolved solids are enough to cause near complete vertical redistribution of solute in the short well section incorporated in Britt's (2005) apparatus.
  - ii. Zone isolation within the bore using an 80% impermeable barrier was sufficient to effectively stop the vertical density-driven flow.
  - iii. Convection rates during mild unstable gradients, e.g., 1°C/m, can drive convection with velocities on the order of 10 cm/min.
  - iv. While typical geothermal gradients are sufficient to produce convection in the wells of diameter typical of observation wells, much stronger temperature gradients near the ground surface where the seasonal temperature signal penetrates to a depth of approximately 20 meters. Simulation of experimental data from a near surface well in this study

demonstrates that we can reasonably accurately describe convective effects that likely exert significant control on measured concentrations in near-surface monitoring wells. Further efforts will attempt to characterize convective behavior and its effects at lower and higher temperature gradients than described in this report.

- v. Examples of additional effects to be considered include the differences in convective behavior induced by seasonal thermal changes, which redistribute solutes in a well differently at different times of the year.
  1. During winter the cool surface temperatures lead to unstable thermal gradients within monitoring wells, i.e., cooler denser water over warmer less dense water leads to thermal convection.
  2. As surface temperatures warm, stable thermal gradients will propagate downward at a rate determined by the rate of warming, the thermal diffusivity of the formation and groundwater recharge.
  3. Deeper regions where geothermal gradients persist (i.e., increasing temperature with depth) will be continually thermally unstable.

**Overall Conclusions and Technical Transfer.** Contaminant redistribution effects in wells are nearly always present. Complete mixing appears to be very common; however, it is not universal. There is a continual balance between inflowing contaminant stratification (where present) and factors driving in-well mixing. Findings here imply common and very small drivers are responsible for slow but vigorous mixing relative to the residence time of water flowing through a typical well screen. Therefore, a tendency toward homogenization is anticipated to be common in field conditions. Most wells should experience strong redistribution effects, but some wells may maintain stratification or perhaps re-stratify differently from the surrounding formation. Variations in chemical concentrations during purge sampling indicate that the same well/aquifer flow dynamics are at play while purging. Passive sampling does not alternative mixing phenomena, while purging tries to overcome these unknowns through well clearing. Both are imperfect in providing proof-positive of “representativeness” of collected samples. However, this research shows that under common conditions the mechanics of averaging by both approaches is similar in its end result. Ongoing technical transfer of these findings will promote better understanding in the environmental community that wells often represent a mixed flow-weighted average of the adjacent formation chemistry. This better understanding will yield cost savings in both short-term and long-term timeframes by accelerating the approval process for non-purge alternative sampling strategies, including passive sampling and *in situ* sensor technologies.

## Literature Cited

- Anderson, M.R., R.L. Johnson, and J. F. Pankow. 1992. Dissolution of Dense Chlorinated Solvents into Groundwater: Modeling Contaminant Plumes from Fingers and Pools of Solvent. *Environmental Science and Technology* 26, no 5: 901-908.
- American Society of Testing Materials (ASTM). 2002. Standard Practice for Low-Flow Purging and Sampling for Wells and Devices Used for Ground-Water Quality Investigations. *ASTM Subcommittee D18.21*: Designation D 6771-02.
- Berthold, S. and F. Borner, 2008, Detection of free vertical convection and double-diffusion in groundwater monitoring wells with geophysical borehole measurements, *Environmental Geology* 54: 1547-1566
- Bird, R.B., W.E. Stewart and E.N. Lightfoot. 1960. Transport phenomena, John Wiley & Sons, Inc. ISBN 0-471-07392-X.
- Britt, S.L., 2005, Testing the In-Well Horizontal Laminar Flow Assumption with a Sand-Tank Well Model, *Ground Water Monitoring and Remediation* 25(3): 73-81.
- Britt, S.L. 2006, Multilevel Sampling in Traditional Monitoring Wells, Proceedings of the Ground Water Resources Association of California 2<sup>nd</sup> Symposium on Tools and Technologies: High Resolution Site Characterization and Monitoring. Long Beach, California, November 14-15, 2006.
- Britt, S.L. 2008, Simple In-Well Baffles May Allow Multilevel Sampling in Traditional Monitoring Wells, *Proceedings of the North American Field Conference and Exposition*, Tampa Florida, January 2008.
- Britt, S.L. and Calabria, M., 2008, Baffles may Allow Effective Multilevel Sampling in Traditional Monitoring Wells, *Proceedings of the Battelle Conference on Chlorinated and Recalcitrant Compounds*, Monterey, California, May 2008.
- Cermak V., L. Bodri, J. Safanda. 2007. Precise temperature monitoring in boreholes: Evidence for oscillatory convection? Part II. Theory and interpretation. *Int J Earth Sci.* doi: 10.1007/s00531-007-0237-4.
- Chiang, C., G. Raven and C. Dawson. 1995. The Relationship between Monitoring Well and Aquifer Solute Concentrations. *Ground Water* 33, no. 5: 718-726.
- Church, P.E. and G.E. Granato. 1996. Bias in Ground-Water Data Caused by Well-Bore Flow in Long-Screen Wells. *Ground Water* 34, no. 2: 262-273.
- Conant, B., Jr., F.F. Akindunni, and R.W. Gillham. 1995. Effect of Well-Screen Placement on Recovery of Vertically Stratified Contaminants. *Ground Water* 33, no. 3: 445-457.

- Cussler, E.L., Diffusion, Cambridge University Press, second edition, 1997.
- Diment, W.H. 1967. Thermal regime of a large diameter borehole: Instability of the water column and comparison of air- and water-filled conditions. *Geophysics* 32, no. 4: 720–726.
- Donaldson, I.G. 1961. Free convection in a vertical tube with a linear wall temperature-gradient. *Austral. J. Phys.* 14, 529-539.
- Einarson, M.D. and J.A. Cherry. 2002. A New Multilevel Ground Water Monitoring System Using Multichannel Tubing. *Ground Water Monitoring and Remediation* 22, no.4: 52-65.
- Elci, A., F.J. Molz III, and W.R. Waldrop. 2001. Implications of Observed and Simulated Ambient Flow in Monitoring Wells. *Ground Water* 39, no. 6: 853-862.
- Elci, A., G.P. Flach, and F.J. Molz. 2003. Detrimental Effects of Natural Vertical Head Gradients on Chemical and Water Level Measurements in Observation Wells: Identification and Control. *Journal of Hydrology* 281: 70-81
- Gibs, J. and T.E. Imbrigiotta. 1990. Well-Purging Criteria for Sampling Purgeable Organic Compounds, *Ground Water* 28, no 1: 68-78.
- Gibs, J., G.A. Brown, K.S. Turner, C.L. MacLeod, J.C. Jelinski, and S.A. Koehnlein. 1993. Effects of Small-Scale Vertical Variations in Well-Screen Inflow Rates and Concentrations of Organic Compounds on the Collection of Representative Ground-Water-Quality Samples. *Ground Water* 31, no. 2: 201-208.
- Gibs, J., Z. Szabo, T. Ivahnenko, and F.D. Wilde. 2000. Change in Field Turbidity and Trace Element Concentration During Well Purging. *Ground Water* 38, no. 4: 577-588.
- Gretener, P.E. 1967. On the thermal instability of large diameter wells—An observational report. *Geophysics* 32, no. 4: 727–738.
- Hales A.L. 1937. Convection currents in geysers. *Mon Not Roy Ast Soc Geophys Suppl* 4:122–131.
- Hutchins, S.R. and S.D. Acree. 2000. Ground Water Sampling Bias Observed in Shallow, Conventional Wells. *Ground Water Monitoring and Remediation* 20, no. 1:86-93
- Interstate Technology and Regulatory Council (ITRC). 2004. Technical and Regulatory Guidance for Using Polyethylene Diffusion Bag Samplers to Monitor Volatile Organic Compounds in Groundwater. *ITRC Technical/Regulatory Guidelines*, Document DSP3.
- ITRC. 2006. Technology Overview of Passive Sampler Technologies. *Interstate Technology and Regulatory Council*, Document DSP4.

- ITRC, 2007, Protocol for Use of Five Passive Samplers to Sample for a Variety of Contaminants in Groundwater, *Interstate Technology and Regulatory Council*, Document DSP5.
- Kram, M, D. Lorenzana, J. Michaelson, E. Lory. 2001. Performance Comparison: Direct-Push Wells Versus Drilled Wells. *NFESC Technical Report TR-2120-ENV*, 55p.
- Martin-Hayden, J.M. and G.A. Robbins. 1997. Plume Distortion and Apparent Attenuation Due to Concentration Averaging in Monitoring Wells. *Ground Water* 35, no. 2: 339-346.
- Martin-Hayden, J.M. and N.B. Wolfe, 2000, A novel view of well-bore flow and partial mixing: digital image analysis. *Ground Water Monitoring and Remediation* v.20, n.4, p. 96-103, Fall Issue.
- Martin-Hayden, J.M. 2000a. Sample Concentration Response to Laminar Wellbore Flow: Implications to Ground Water Data Variability. *Ground Water* 38, no. 1: 12-19.
- Martin-Hayden, J.M. 2000b. Controlled Laboratory Investigations of Wellbore Concentration Response to Pumping. *Ground Water* 38, no.1: 121-128.
- Martin-Hayden, J.M. and S.L. Britt, 2006, Revealing the Black Box of Groundwater Sampling: Effects of Well Bore Flow and Mixing During Purging, *North American Field Conference and Exposition*, Tampa Florida, January 2006.
- Newell, C.J., R.S. Lee, A.H. Spexet, Groundwater Services Inc. 2000. No-Purge Groundwater Sampling: an Approach for Long-Term Monitoring. *American Petroleum Institute Summary of Research Results* no. 12: October 2000.
- Parker, L.V. and C.H. Clark. 2002. Study of Five Discrete Interval-Type Groundwater Sampling Devices. *U.S. Army Corps of Engineers ERDC/CRREL*: TR-02-12, August 2002, 49 p.
- Parker, Louise, and Nathan Mulherin. 2007. Evaluation of the Snap Sampler for sampling ground water monitoring wells for VOCs and explosives, *US Army Engineer Research and Development Center, Cold Regions Research and Engineering Laboratory Report TR-07-14*, Hanover, NH, ERDC/CRREL TR-07-14.
- Parker, L.V. and T.A. Ranney. 1997. Sampling Trace-Level Organics with Polymeric Tubing: Part I. Static Studies. *Ground Water Monitoring and Remediation*, XVII (4): 115-124.
- Parker, L.V. and T.A. Ranney. 1998. Sampling Trace-Level Organics with Polymeric Tubing: Part 2. Dynamic Studies. *Ground Water Monitoring and Remediation*, XVIII (1): 148-155.

- Parker, L.V. and T.A. Ranney. 2000. Decontaminating Materials Used in Ground Water Sampling Devices: Organic Contaminants. *Ground Water Monitoring and Remediation*, XIX (1): 56-68.
- Parker, L.V. and T.A. Ranney. 2003. An Environmentally Friendly Decontamination Protocol for Ground Water Sampling Devices. *Ground Water Monitoring and Remediation* XIII (2): 84-91.
- Parsons Engineering Science. 2003. Final Technical Report for the Evaluation of Groundwater Diffusion Samplers. *Air Force Center for Environmental Excellence*.
- Powell, R.M., and R.W. Puls. 1993. Passive Sampling of Groundwater Monitoring Wells Without Purging: Multilevel Well Chemistry and Tracer Disappearance. *Journal of Contaminant Hydrology* 12: 51-77.
- Puls, R.W. and M.J. Barcelona. 1996. Low-Flow (Minimal Drawdown) Ground-Water Sampling Procedures. *USEPA Office of Research and Development*, EPA/540/S-95/504.
- Puls, R.W. and C.J. Paul. 1997. Multi-Layer Sampling in Conventional Monitoring Wells for Improved Estimation of Vertical Contaminant Distributions and Mass. *Journal of Contaminant Hydrology* 25: 85-111.
- Reilly, T.E. and J. Gibs. 1993. Effects of Physical and Chemical Heterogeneity on Water-Quality Samples Obtained from Wells. *Ground Water* 31 no. 5:805-813.
- Reilly, T.E. and D.R. LeBlanc. 1998. Experimental Evaluation of Factors Affecting Temporal Variability of Water Samples Obtained From Long-Screened Wells. *Ground Water* 36, no. 4: 566-576.
- Reilly, T.E., O.L. Franke, and G.D. Bennett. 1989. Bias in Groundwater Samples Caused by Wellbore Flow. *Journal of Hydraulic Engineering* 115, no. 2: 270-276.
- Robin, M.J.L. and R.W. Gillham. 1987. Field Evaluation of Well Purging Procedures. *Ground Water Monitoring Review* 7, no. 4: 85-93.
- Robbins, G.A. 1989. Influence of Using Purged and Partially Penetrating Monitoring Wells on Contaminant Detection, Mapping and Modeling. *Ground Water* 27, no. 2: 155-162.
- Taylor, G. I. 1954. Diffusion and mass transport in tubes. *Proc. Phys. Soc. B* 67, 857.
- United States Environmental Protection Agency (USEPA). 1977. Procedures Manual for Ground Water Monitoring at Solid Waste Facilities. *USEPA*, EPA 530/SW-611.616, 284p.
- U.S. Environmental Protection Agency, 1995, Ground Water Sampling - A Workshop Summary. Texas, November 30-December 2, 1993, *EPA/600/R-94/205*, 146 pp.

- U.S. Environmental Protection Agency, 2002, Ground-Water Sampling Guidelines for Superfund and RCRA Project Managers. Ground Water Forum Issue Paper by D. Yeskis and B. Zevala. *EPA 542-S-02-001*, 53 pp.
- U.S. Environmental Protection Agency, 1985, Practical Guide for Ground-Water Sampling, *EPA 600/2-85/104*
- United States Geological Survey (USGS). 1980. National Handbook of Recommended Methods for Water Data Acquisition, *USGS*.
- Vanaparthi, S.H., E. Meiburg and D. Wilhelm. 2003. Density driven instabilities of miscible fluids in a capillary tube: Linear stability analysis”, *Journal of Fluid Mechanics*, 497, p. 99-121.
- Varljen, M.D., M.J. Barcelona, J. Obereiner, and D. Kaminski, 2006, Numerical Simulations to Assess the Monitoring Zone Achieved during Low-Flow Purging and Sampling. *Ground Water Monitoring and Remediation 26:1*, p 44-52.
- Vroblesky, D.A. 2001. User’s Guide for Polyethylene-Based Passive Diffusion Bag Samplers to Obtain Volatile Organic Compound Concentrations in Wells, Parts 1 and 2, *U. S. Geological Survey Water Resources Investigations Reports 01-4060 and 01-4061*.
- Vroblesky, D.A. and B.C. Peters. 2000. Diffusion Sampler Testing at Naval Air Station North Island, San Diego County, California, November 1999 to January 2000. *U.S. Geological Survey Water Resources Investigation 00-4182*.
- Vroblesky, D.A., C.C. Casey, and M.A. Lowery, 2007, Influence of Dissolved Oxygen Convection on Well Sampling. *Ground Water Monitoring and Remediation 27:3*, p 49-58.
- Zhukhovitskii, E.M. and G.Z. Gershuni. 1976. Convective Stability of Incompressible Fluids, *Keter Publishing House Jerusalem Ltd*. 336 pp.

**APPENDIX A. SUPPORTING DATA**

Table A-1: 2 June 2009 Sampling Event Lab Data, Zone Sampling with Baffles

Table A-2: 17 June 2009 Sampling Event Lab Data, Zone Sampling without Baffles

Table A-3: 24 August 2009 Sampling Event Lab Data, MW-24 Purge Event Complex

Table A-4: 25 August 2009 Sampling Event Lab Data, MW-28 Purge Event Complex

Table A-5: 1 September 2009 Sampling Event Lab Data, MW-29 Purge Event Complex

Table A-6: 2 September 2009 Sampling Event Lab Data, MW-27 Purge Event Complex

Table A-7: 16 March 2010 Sampling Event Lab Data, MW-15 Purge Event Complex

Table A-8: 16 March 2010 Sampling Event Lab Data, MW-27 Purge Event Complex

Table A-9: 17 March 2010 Sampling Event Lab Data, MW-16 Purge Event Complex

Table A-10: 17 March 2010 Sampling Event Lab Data, MW-28 Purge Event Complex

Table A-11: 16 August 2010 Sampling Event Lab Data, MW-24 Purge Event Complex

Table A-12: 20 July 2011 Sampling Event Lab Data, MW-27 and MW-28 Tube Wells

Table A-13: 9 August 2011 Sampling Event Lab Data, MW-27 and MW-28 Tube Wells and Baffled PDB Sampling

Table A-14: MW-27 Tube Well/ Baffled PDB Data Reduction and Plots

Table A-15: MW-28 Tube Well/ Baffled PDB Data Reduction and Plots

Table A-16: Vial Filling Pour Tests

---

## Appendix B. List of Scientific/Technical Publications

### Journal Publications

Britt, Sanford L., Louise Parker, James Martin-Hayden, and Mitchell Plummer, (in prep) *Concentration Variation During Well Purging in Contaminant-Stratified Aquifers*. Manuscript in development for submittal to *Groundwater or Groundwater Monitoring and Remediation*, 2014.

Britt, Sanford L. and Louise Parker, (in prep), *The Effect of Changing Pump Discharge Rate During Purging*, Manuscript in development for submittal to *Groundwater or Groundwater Monitoring and Remediation*.

Parker, Louise, and Sanford Britt, (2012), *The Effect of Bottle Fill Rate and Pour Technique on the Recovery of Volatile Organics*. *Ground Water Monitoring and Remediation*, 32 (4): 78-86.

Martin-Hayden, James, Mitchell Plummer, and Sanford L. Britt, (2012), *Controls of Wellbore Flow Regimes on Pump Effluent Composition*. *Groundwater*, v 52, p. 96-104

Martin-Hayden, James, Mitchell Plummer, and Sanford L. Britt, (in prep), *Characteristics of Thermal Convection Within Groundwater Monitoring Wells*. Manuscript in development for submittal to *Groundwater*, 2014.

### Conference Presentations & Abstracts

Britt, Sanford L., (2009), *Downhole Sensor Measurements Before and During Low Flow Purging: Dynamics of Flow-Weighted Averaging*, Wednesday Poster #207, SERDP/ESTCP Partners Symposium, Washington, DC, December 1-3, 2009.

Britt, Sanford L., and Louise Parker, (2010), *Low Flow Purging and Sampling in a Stratified Aquifer: Purge Stability and Attainment of Flow-Weighted Averages*, Abstract A-086, Proceedings of the 7<sup>th</sup> International Conference on Remediation of Chlorinated and Recalcitrant Compounds, Monterey, California, May 24-27, 2012.

Britt, Sanford L., James Martin-Hayden, Mitchell Plummer, Louise Parker, Jacob Gibs, (2010), *Well Purging, Travel Times, and Discharge Concentrations: Where the Water Comes From and When it Arrives*, North American Environmental Field Conference and Exhibition, Tampa, Florida, January 12-15, 2010.

Britt, Sanford L., James Martin-Hayden, Mitchell Plummer, (2010), *Groundwater Sampling Results may Differ when Sampling Methods Differ: Methods and Mechanisms*, North American Environmental Field Conference and Exhibition, San Diego, California, January 10-13, 2010.

Britt, Sanford L., and Louise Parker, (2011), *Testing VOA Vial Pour Methods and Fill Rates-- "Slow and Smooth" Convention is All Wrong*, Tuesday Poster #159, SERDP/ESTCP Partners Symposium, Washington, DC, November 28 – December 1, 2011.

Parker, Louise and Sanford Britt. (2012), *Effect of flow rate and fill method on the recovery of VOCs*. North American Environmental Field Conference and Exposition, February 7-10 in San Diego, CA and March 13-16 in Tampa, FL.

Britt, Sanford L., James Martin-Hayden, Mitchell Plummer, Louise Parker, (2012), *Sources of Field Variability During Purging*, North American Environmental Field Conference and Exposition, February 7-10 in San Diego, California and March 13-16 in Tampa, Florida.

Martin-Hayden, JM, MA Plummer, SL Britt, (2010), *Modeling Hydrodynamics of Well-Bore Flow During Pumping: The Black Box of Groundwater Sampling Revealed*. SERDP/ESTCP Partners in Environmental Technology Conference, Nov.-Dec. 2010, Washington DC.

Martin-Hayden, JM, (2011), *The Effects of Ambient Flow Regimes Adjacent to and Within Screened Monitoring Wells*. North American Field Conference, San Diego, CA, January, 2011.

Martin-Hayden, JM, (2011), *Revealing the Black Box of Groundwater Sampling: Effects of Bore-Hole Flow and Mixing During Purging*. University of Kansas, Department of Geology Colloquium, May, 2011.

Martin-Hayden, JM, (2011), *Analytical Modeling of Flow Regimes Within and Surrounding Screened Monitoring Wells Under Ambient and Pumped Conditions*. Geological Society of America Annual Meeting, Minneapolis, MN, October, 2011.

Martin-Hayden, JM, MA Plummer, SL Britt, (2011), *Flow Regimes Within and Surrounding Screened Monitoring Wells Under Ambient and Pumped Conditions*. SERDP/ESTCP Partners in Environmental Technology Conference, Nov.-Dec. 2011, Washington DC.

## Appendix C. Laboratory Reports

| <b>AETL</b>          |               |             |              |   |
|----------------------|---------------|-------------|--------------|---|
| <b>Job</b>           |               |             |              |   |
|                      | <b>Number</b> | <b>Date</b> | <b>pages</b> | <b>Content</b>                            |
| Lab Report Number 1  | 52918         | 5/28/2009   | 5            | EB/TB                                     |
| Lab Report Number 2  | 53071         | 6/15/2009   | 37           | Multilevel GW                             |
| Lab Report Number 3  | 53071a        | 8/3/2009    | 8            | additional compounds reported             |
| Lab Report Number 4  | 53235         | 7/7/2009    | 54           | Multilevel GW                             |
| Lab Report Number 5  | 53235a        | 7/22/2009   | 10           | additional compounds reported             |
| Lab Report Number 6  | 53389         | 7/10/2009   | 12           | Soil for disposal                         |
| Lab Report Number 7  | 53871         | 9/10/2009   | 34           | MW24 complex                              |
| Lab Report Number 8  | 53871R        | 10/1/2009   | 5            | includes reruns                           |
| Lab Report Number 9  | 53872         | 9/11/2009   | 27           | MW24 complex                              |
| Lab Report Number 10 | 53873         | 9/11/2009   | 21           | MW24 complex                              |
| Lab Report Number 11 | 53873R        | 10/1/2009   | 5            | includes reruns                           |
| Lab Report Number 12 | 53966         | 9/17/2009   | 31           | Pour tests + MW29 Complex                 |
| Lab Report Number 13 | 53967         | 9/18/2009   | 34           | Pour tests<br>Pour tests + MW28 Complex + |
| Lab Report Number 14 | 53968         | 9/18/2009   | 34           | MW29 Complex                              |
| Lab Report Number 15 | 53969         | 9/21/2009   | 15           | MW28 Complex                              |
| Lab Report Number 16 | 53970         | 9/21/2009   | 22           | MW28 Complex + MW27 Complex               |
| Lab Report Number 17 | 53970R        | 10/1/2009   | 5            | includes reruns<br>MW27 Complex and MW29  |
| Lab Report Number 18 | 53971         | 9/21/2009   | 28           | Complex                                   |
| Lab Report Number 19 | 56231         | 3/19/2010   | 5            | MW15 MW16 prelim                          |
| Lab Report Number 20 | 56232         | 3/19/2010   | 5            | MW27 S/D                                  |
| Lab Report Number 21 | 56345         | 3/30/2010   | 27           | MW16 Complex                              |
| Lab Report Number 22 | 56346         | 3/30/2010   | 24           | MW27 Complex                              |
| Lab Report Number 23 | 56347         | 3/30/2010   | 31           | MW28 Complex                              |
| Lab Report Number 24 | 56348         | 3/30/2010   | 28           | MW15 Complex                              |
| Lab Report Number 25 | 57830         | 9/3/2010    | 35           | MW24 complex                              |
| Lab Report Number 26 | 62195         | 8/2/2011    | 17           | T zone MW27                               |
| Lab Report Number 27 | 62558         | 8/31/2011   | 44           | T-Zone MW27, MW28, MW29                   |
| Lab Report Number 28 | 62810         | 9/7/2011    | 5            | MW29 bubbler                              |
| Lab Report Number 29 | 63181         | 10/7/2011   | 5            | MW29 bubbler                              |
| Lab Report Number 30 | 63664         | 11/29/2011  | 15           | MW29 bubbler, MW24 complex                |
| Lab Report Number 31 | 64084         | 12/14/2012  | 15           | Soil for disposal                         |